

Analysis of two exceptional chromosome-types in plants

Dissertation

zur Erlangung des Doktorgrades der Naturwissenschaften

doctor rerum naturalium (Dr. rer. nat.)

der Naturwissenschaftlichen Fakultät III- Agrar- und Ernährungswissenschaften,
Geowissenschaften und Informatik

der Martin-Luther-Universität Halle-Wittenberg

vorgelegt von Wei Ma

Geb. am 10.02.1988 in Pingluo, Ningxia province, China

Gutachter /in:

1. Dr. Andreas Houben
2. Prof. Dr. Klaus Pillen
3. Prof. Dr. Zhukuan Cheng

Halle (Saale): 30.05.2016

Verteidigungsdatum: 23.01.2017

Acknowledgements

This work was funded by the China Scholarship Council (CSC) scholarship and was carried out in the research group of 'Chromosome Structure and Function (CSF)' at the Leibniz Institute of Plant Genetics and Crop Plant Research (Leibniz-Institut für Pflanzengenetik und Kulturpflanzenforschung, IPK), Gatersleben, Germany from October 2012.

First of all I would like to express my greatest thanks to Dr. habil. Andreas Houben, the group leader of CSF group, for providing me the opportunity to join his team, for continuous guidance, permanent encouragement as well as fruitful discussions. Also, I would like to thank the former postdoc of CSF group Dr. Ali Mohammad Banaei Moghaddam, for supervising and discussing with me on the B chromosome project.

I wish to thank all present and former members especially Maja Jankowska who really helped me a lot, as well as visitors of the CSF group. Also great thanks to the technical support from Katrin Kumke, Oda Weiss and Karla Meier. All of them made our group an enjoyable place to work.

I would like to thank all the co-authors for their input into the publications and make the story better, especially Dr. Veit Schubert for his discussion.

I would also like to thank Prof. Dr. Zhukuan Cheng for the opportunity to work in his lab and to Dr. Yi Shen and Wenqing Shi from his lab for the excellent collaboration as well as the group members for warm welcoming.

Particularly, I would like to thank to all friends, especially Zhaojun Liu who supported me a lot and made my life easier during my stay in Gatersleben, to “噶村吃货团” members Rongfan Wang, Ying Liu, Yinjun Sheng, Wenjie Xu, Guozheng Liu and Fanghua Ye for sharing the nice food and spending a lot of free time together. You made the life abroad as home.

Finally, my gratitude belongs to my whole family who all supported me from the beginning until now. 老爸老妈，想对你们说健康快乐最重要，希望你们身体健康，能保持好的心态，同时非常感谢你们这么多年来对我的支持。也特别感谢我的家人们在我人生道路上的陪伴，尤其是年迈的姥姥，希望您健康快乐。

Contents

About the thesis	i
Abbreviations.....	ii
1. The distribution of α-kleisin during meiosis in the holocentromeric plant	
<i>Luzula elegans</i>.....	- 1 -
1.1 Introduction	- 1 -
1.1.1 Centromere and the centromere-specific histone H3 variant CENH3..	- 1 -
1.1.2 <i>Luzula elegans</i> and holocentric centromeres	- 2 -
1.1.3 Meiosis in holocentric species	- 3 -
1.1.4 Cohesin complex	- 5 -
1.1.5 Synaptonemal complex	- 7 -
1.2 Open questions and aims of the PhD work.....	- 9 -
1.3 Materials and Methods	- 10 -
1.3.1 Plant material and plant cultivation	- 10 -
1.3.2 RNA extraction, RT-PCR and qRT-PCR	- 10 -
1.3.3 Sequence analysis	- 11 -
1.3.4 Total protein extraction and Western blot analysis	- 12 -
1.3.5 Antibody production	- 13 -
1.3.6 Indirect immunostaining and light microscopy	- 13 -
1.3.7 Electron microscopy	- 14 -
1.3.8 Accession numbers	- 14 -
1.4 Results	- 16 -
1.4.1 Identification of the centromere-specific histone H3 variant CENH3 in <i>L. elegans</i>	- 17 -
1.4.2 Identification of the <i>L. elegans</i> α -kleisins.....	- 20 -
1.4.3 Identification of SGO1 in <i>L. elegans</i>	- 23 -
1.4.4 Prophase I is conventional in <i>L. elegans</i>	- 24 -
1.4.5 $\text{Le}\alpha$ -kleisin colocalizes with the centromeres of condensed chromosomes	- 26 -
1.5 Discussion.....	- 29 -
1.5.1 The CENH3 of <i>L. elegans</i>	- 29 -
1.5.2 α -kleisins colocalize with the centromere	- 29 -

1.5.3 The meiotic prophase I is conventional in <i>L. elegans</i>	- 30 -
1.6 Summary	- 33 -
1.7 Outlook	- 34 -
2. Rye B chromosomes encode a functional Argonaute-like protein with <i>in vitro</i> slicer activities similar to its A chromosome paralog	- 35 -
2.1 Introduction.....	- 35 -
2.1.1 B chromosomes.....	- 35 -
2.1.2 The origin of B chromosomes.....	- 35 -
2.1.3 B chromosome composition in general	- 37 -
2.1.4 The DNA composition of the rye B chromosome	- 38 -
2.1.5 Introduction of candidate genes	- 39 -
2.2 Open questions and aims of the PhD work.....	- 41 -
2.3 Materials and methods.....	- 42 -
2.3.1 Plant material and cultivation.....	- 42 -
2.3.2 Probe preparation, indirect immunostaining and fluorescence in situ hybridization	- 42 -
2.3.3 Genomic DNA and RNA extraction, PCR and RT-PCR	- 44 -
2.3.4 Sequence analysis	- 45 -
2.3.5 Molecular phylogenetic analyses.....	- 48 -
2.3.6 Genotyping of <i>ScKIF4A</i> and <i>ScSHOC1</i> fragments by CAPS.....	- 48 -
2.3.7 <i>In vitro</i> transcription	- 48 -
2.3.8 siRNAs.....	- 49 -
2.3.9 Cell culture and preparation of cytoplasmic BY-2 cell extract	- 49 -
2.3.10 Target cleavage assay	- 49 -
2.3.11 Accession Number	- 49 -
2.4 Results	- 51 -
2.4.1 Active RNAPII enzymes are closely associated to rye B chromatin... -	52 -
2.4.2 The B chromosome-located genes <i>ScKIF4A</i> , <i>ScSHOC1</i> and <i>ScAGO4B</i> are transcribed.....	- 52 -
2.4.3 Amplification increased the copy number of the B chromosome-located genic sequences.....	- 60 -
2.4.4 The number of Bs affects the gene expression pattern.....	- 60 -

2.4.5 A and B chromosome-encoded ScAGO4B-like proteins show similar <i>in vitro</i> RNA slicer activities	- 66 -
2.5 Discussion	- 70 -
2.5.1 B chromosomes of rye are transcriptionally active	- 70 -
2.5.2 Rye B chromosomes undergo pseudogenization.....	- 71 -
2.6 Summary	- 74 -
2.7 Outlook	- 75 -
3. References	- 76 -
List of publications related to this thesis	- 88 -
Curriculum Vitae	- 89 -
Eide sstattliche Erklärung / Declaration under Oath	- 92 -
Erklärung über bestehende Vorstrafen und anhängige Ermittlungsverfahren / Declaration concerning Criminal Record and Pending Investigations	- 93 -

About the thesis

In frame of my PhD work two exceptional plant chromosomes-types were analyzed. The first project is focused on the meiotic process of the holocentric plant species *Luzula elegans*. In the second project I answered the question whether supernumerary B chromosomes of rye (*Secale cereale*) carry functionally active protein-coding genes.

Therefore this thesis is arranged basically in two major separate parts based on two different topics. For each part, it is arranged under the headings Introduction, Open Questions and Aims, Materials and Methods, Results, Discussion, Summary and Outlook.

Abbreviations

As	A chromosomes
Bs	B chromosomes
BLAST	Basic Local Alignment Search Tool
bp	base pair
kbp	kilo base pair
Mbp	Mega base pair
gDNA	genomic deoxyribonucleic acid
cDNA	complementary deoxyribonucleic acid
DNA	deoxyribonucleic acid
dNTP	deoxy-ribonucleotide triphosphate
GAPDH	glyceraldehyde 3-phosphate dehydrogenase
RNA	ribonucleic acid
µm	Micrometer
nm	Nanometer
C-terminus	Carboxy-terminus
N-Terminus	Amino-terminus
kDa	Kilodaltons
min	Minute
h	Hour
mg	Milligrams
wt/vol	weight/volume

1. The distribution of α -kleisin during meiosis in the holocentromeric plant *Luzula elegans*

1.1 Introduction

1.1.1 Centromere and the centromere-specific histone H3 variant CENH3

The centromere has been described as the region where spindle microtubules attach to the chromatids to enable their movement to the daughter cells during cell divisions in eukaryotes. According to the localization of the centromere, chromosomes can be classified into two types: monocentric and holocentric chromosomes (Figure 1).

During mitotic metaphase, in monocentric species the kinetochore protein complex assembles at the single centromere region named primary constriction (Figure 1A). In contrast, holocentric chromosomes are characterized by the lack of this localized centromeric region. Consequently, the kinetochore protein complex assembles almost along the whole length of the chromosomes (Figure 1B).

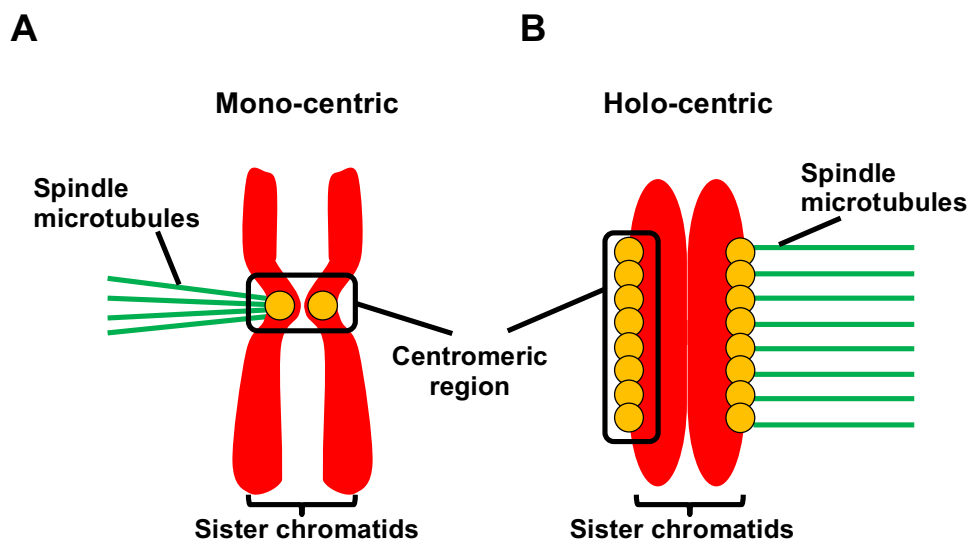


Figure 1. The organization of mitotic monocentric and holocentric chromosomes.

The centromere (in yellow) of a monocentric chromosome (A) is characterized by a primary constriction. In contrast, a holocentric chromosome (B) does not form a constriction, instead the centromere is distributed almost the entire length of the sister chromatid. Spindle microtubules are indicated as green lines.

Active centromeres where the kinetochore complex assembles are marked by the centromere-specific histone H3 variant CENH3, also known as “CENP-A” (Figure 2)

(Palmer et al. 1987). CENH3 replaces histone H3 in centromeric nucleosomes and thus marks centromeres epigenetically initiating the kinetochore formation (Kalitsis and Choo 2012). However, not all histone H3s are replaced in the centromere, more likely blocks of CENH3- and H3-associated nucleosomes are interspersed which can be observed on extended centromere fibers after immunostaining with corresponding antibodies (Blower et al. 2002). Unlike conventional histone H3s, CENH3 evolved rapidly, particularly in its N-terminus tail domain. It has a rather conserved C-terminus domain, while the N-terminus is more variable in size and amino acid composition between species (Figure 2A) (Henikoff and Dalal 2005). Absence of CENH3's N-terminus allows its targeting, recruitment of kinetochore proteins, and does not affect severely the mitosis in *Arabidopsis thaliana* (Lermontova et al. 2006). However, the N-terminal part is essential for meiotic CENH3 loading in plants (Lermontova et al. 2011). The conserved C-terminal part is required for CENH3 centromere targeting or loading (Lermontova et al. 2006).

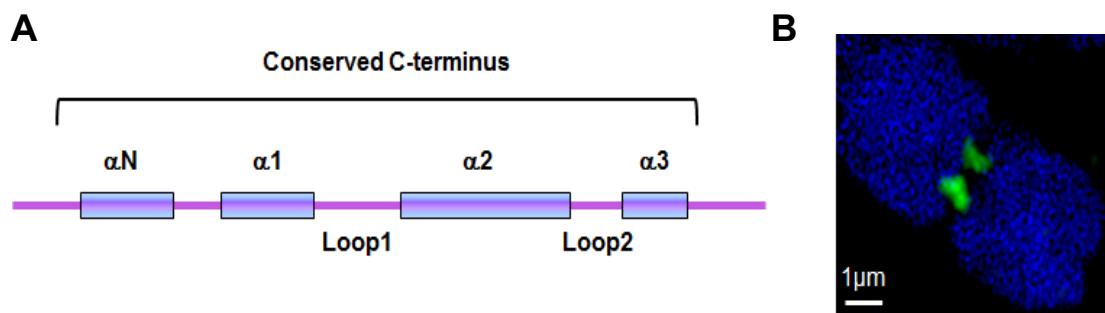


Figure 2. The centromere-specific histone H3 variant CENH3.

The C-terminus of CENH3 is highly conserved among eukaryotes, in contrast to the N-terminal. Schematic structure of the conserved C-terminus (A). Immunolocalization of CENH3 (green) at one mitotic metaphase chromosome of *Hordeum vulgare* (B).

1.1.2 *Luzula elegans* and holocentric centromeres

Holocentric chromosomes can be found throughout the plant and animal kingdoms, with the most well-studied example being the nematode *Caenorhabditis elegans* (Dernburg 2001). In flowering plants, holocentric chromosomes could be found in the monocots *Juncaceae*, *Cyperaceae* (Malheiros and de Castro 1947; Hakansson 1958) and *Chionographis* (Tanaka and Tanaka 1977) families, the dicots *Drosera* (Sheikh et al. 1995) family and *Cuscuta* (the subgenus of *Cuscuta*)(Pazy and Plitmann 1995).

The woodrush species *Luzula elegans* ($2n=6$, 3.81 Gbp/1C), like the other members in the *Juncaceae* family have holocentric chromosomes. Light and scanning electron microscopy observations provided evidence for the existence of a longitudinal groove along each sister chromatid (Figure 3) (Heckmann et al. 2011). The centromeric-specific histone H3 variant, CENH3, colocalizes with this groove and with microtubule attachment sites in both mitosis and meiosis (Heckmann et al. 2011; Heckmann et al. 2014a).

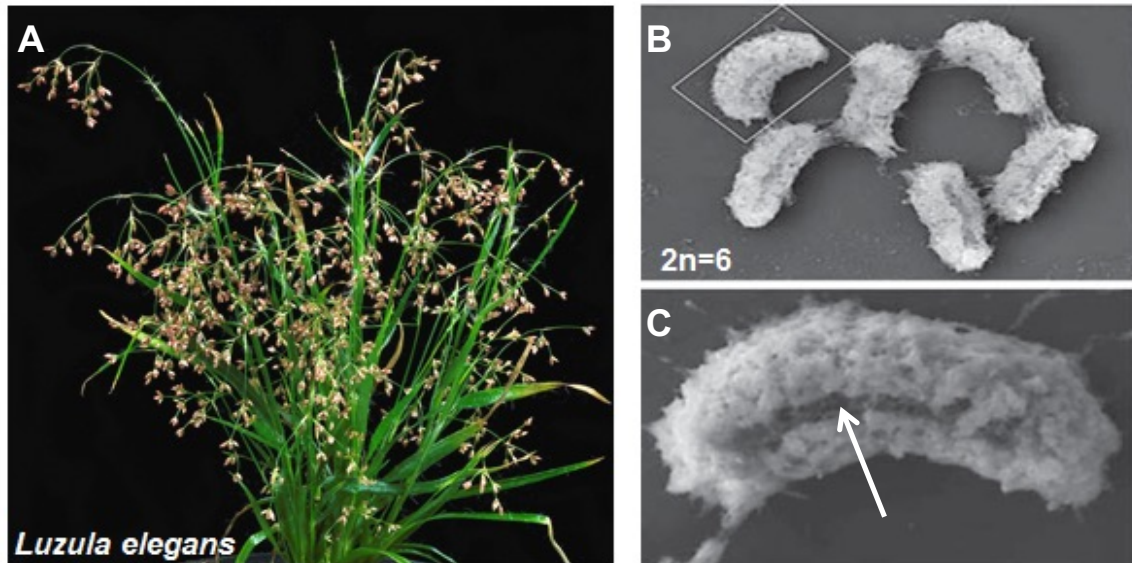


Figure 3. The existence of a longitudinal groove along each sister chromatid in *L. elegans*.

(A) A picture of flowering plant *L. elegans*. (B) Scanning electron micrographs of isolated metaphase chromosomes of *L. elegans*. (C) Selected chromosome shows the existence of a longitudinal groove (indicated as an arrow) (Figures from Heckmann et al. (2011)).

1.1.3 Meiosis in holocentric species

In meiosis two rounds of chromosome segregation follow a single replication step to generate haploid gametes. Thus, sister chromatid cohesion must be released in two steps during meiosis in monocentric species (Figure 4a). i) Loss of chromatid arm cohesion between both homologues to release chiasmata and to enable the reductional segregation at anaphase I (Kudo et al. 2006; Kudo et al. 2009), ii) loss of sister centromere cohesion to allow sister chromatid segregation at anaphase II (Llano et al. 2008). However, the process of meiosis in organisms with holocentric chromosomes illustrates that our knowledge of meiotic chromosome arrangement and control based on observations of monocentric chromosomes may not apply to all organisms (Cabral et al. 2014; Heckmann et al. 2014a).

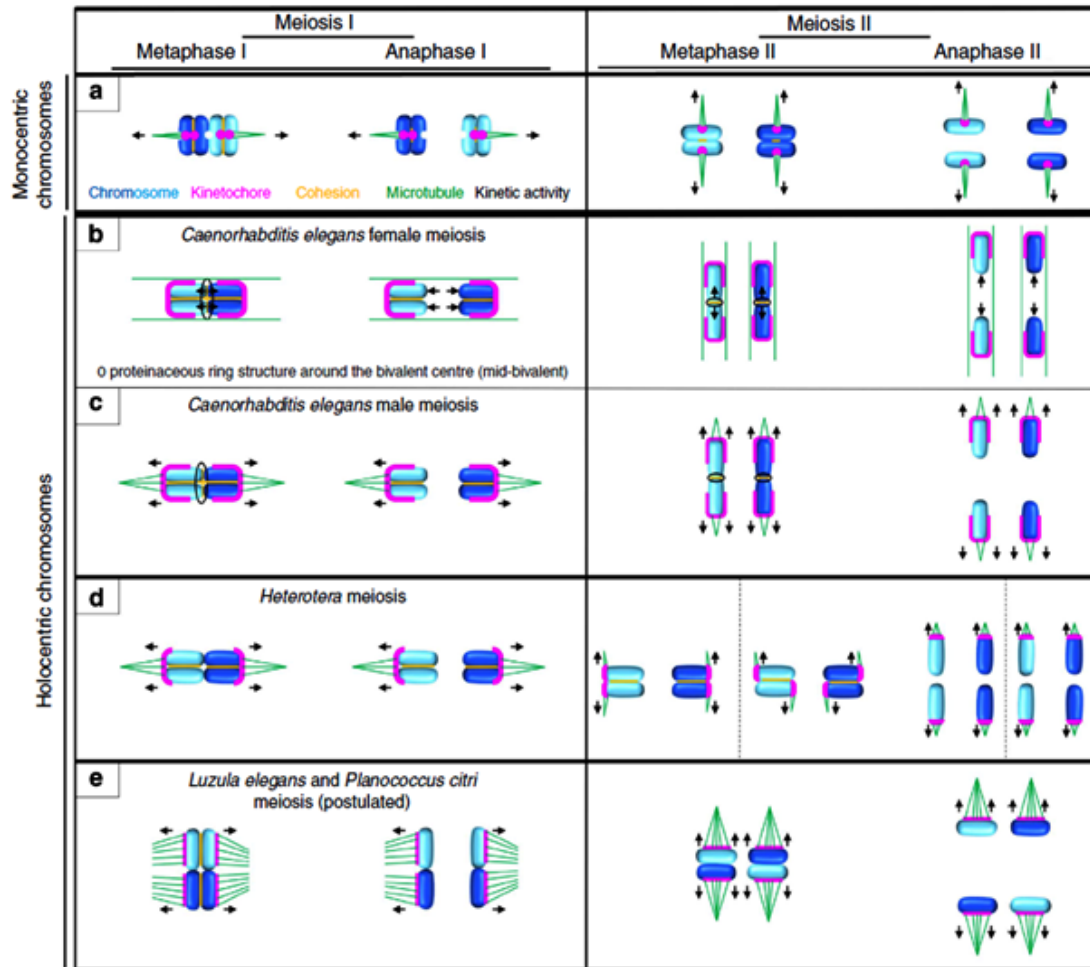


Figure 4. Schematic model of meiosis in species with monocentric chromosomes and of meiotic adaptations in species with holocentric chromosomes (Figure from Heckmann et al. (2014a)).

(a) “Classical” meiosis in monocentric species: kinetochores of sister chromatids are fused at metaphase I allowing homologous chromosome segregation, whereas kinetochores of sister chromatids behave as separate units allowing the separation of sister chromatids at anaphase II. (b–e) Holocentric chromosomes: Several options exist to deal with a holocentric chromosome architecture and meiosis: (b–d) The sequence of meiosis is similar as monocentric chromosomes, but with different kinds of chromosome remodeling. (b–c) A rod-shaped bivalent is shown with short and long arms. At anaphase I the cohesion at short arms is released and enabling the separation of homologous chromosomes. And the cohesion in the short arms is released and the sister chromatids separated. (d) Holocentric chromosomes become functional monocentric (‘telokinetic’), because microtubules attached to the restricted terminal chromosomal region and enable the separation of homologues during meiosis I. Active sister kinetochores can form at opposite metaphase II chromosome termini and enable the separation of sister chromatids. (e) ‘Inverted meiosis’. Microtubules attached to the centromeres along the entire homologous sister chromatids, and enable the separation of homologous chromosomes at anaphase I. Homologous non-sister chromatids are connected and separated at anaphase II.

It is expected that the degradation of cohesins during holocentric meiosis may deviate from that of monocentric species. In principle there are two options to release cohesins during holocentric meiosis (Figure 4b-e): (i) like in the nematode *C. elegans*, at a cruciform bivalent with a short (mid-bivalent) and a long arm, spindle fibers attach to a restricted terminal chromosome region during metaphase I allowing the degradation of cohesins in the short arm region and to the opposite one during metaphase II allowing the degradation of cohesins between long arms (Albertson and Thomson 1993; Kaitna et al. 2002; Nabeshima et al. 2005); (ii) in other holocentric species like *L. elegans*, a holocentric chromosome architecture and behavior occur throughout meiosis. In contrast to the cohesive monopolar sister centromeres, the unfused holokinetic sister centromeres behave as two distinct functional units during meiosis I, resulting in sister chromatid separation already during the first meiotic division (Heckmann et al. 2014a). Homologous non-sister chromatids remain linked after metaphase I at their termini by satellite DNA enriched chromatin threads, until metaphase II. Then they separate at anaphase II. Thus, an inverted sequence of meiotic sister chromatid segregation occurs, it is suggested that cohesins are released only once during meiosis I (Cabral et al. 2014; Heckmann et al. 2014a).

1.1.4 Cohesin complex

The cohesin complex consists of different subunits: namely the SMC1 and SMC3 (Structural Maintenance of Chromosomes) proteins, the α -kleisin SCC1 (also named RAD21 or MCD1) and the SCC3 protein (Nasmyth 2011). These subunits have been extensively studied in yeast, animals and human, but also homologs in plants have been characterized. Biochemical and structural studies demonstrated that SCC1 simultaneously binds to SMC1 and SMC3 to form a tripartite ring proposed to mediate sister chromatid cohesion by encircling sister chromatids (Figure 5) (Haering and Nasmyth 2003). In almost all eukaryotes SCC1 is present in the mitotic cohesin complex and is mostly replaced during meiosis by REC8 (Anderson et al. 2002; Cai et al. 2003; Golubovskaya et al. 2006; Pasierbek et al. 2001).

In mitosis, most of the cohesins are degraded from the chromosome arms via phosphorylation of the SCC3 subunit by PLK1 before metaphase (Losada et al. 2002; Sumara et al. 2002). However, the centromeric cohesins remained until the anaphase onset when SCC1 are cleaved by the separase (Haering and Nasmyth 2003).

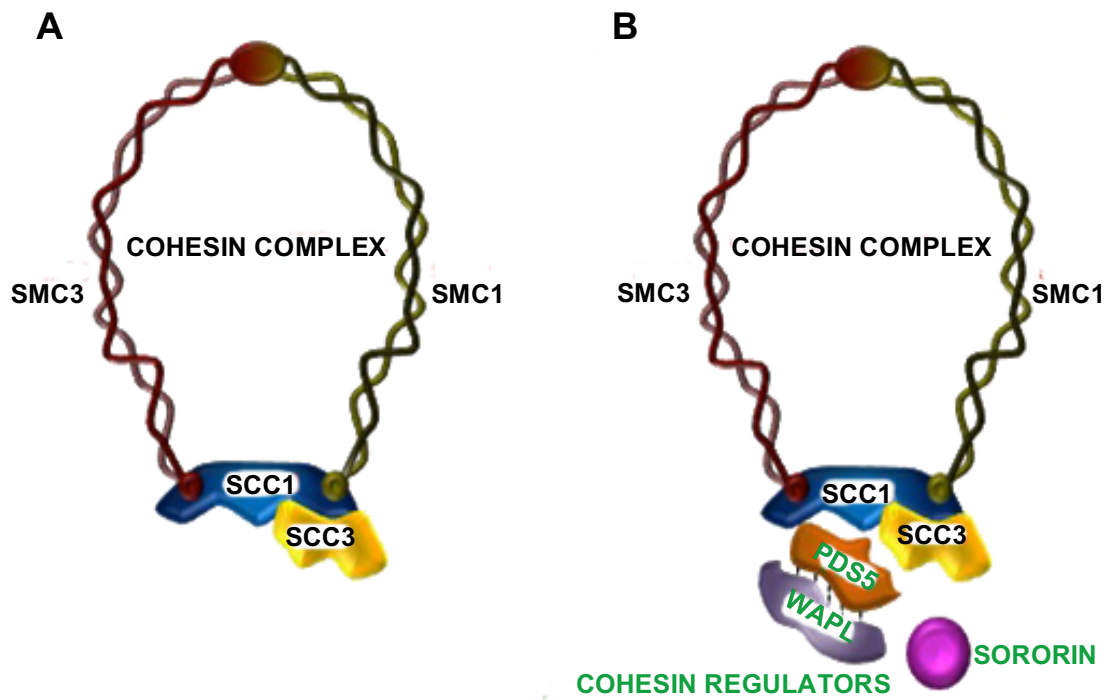


Figure 5. Cohesin complex and cohesin regulators (Figure from <http://atlasgeneticsoncology.org/Deep/CohesinsID20100.html>).

(A) A tripartite ring model of a cohesin complex which composed of four subunits SMC1, SMC3, SCC1/RAD21/ α -kleisin and SCC3/STAG. (B) The cohesin complex with different regulators (indicated in green characters).

In contrast to mitosis, sister chromatid cohesins must be released in two steps during meiosis in monocentric species as mentioned above (Figure 6A). To make sure that homologous chromosomes separate first, it is necessary to prevent premature separation sister chromatids before meiosis I. In 2004, the protein family shugoshin: SGO1 and SGO2 were identified for protecting centromere cohesins in many species (Kitajima et al. 2004). As also mentioned above, there are two options to release the cohesins during meiosis for holocentric species. (i) in *C. elegans*, the cohesin Rec8 was phosphorylated in between homologous chromosomes (also called short arm) during meiosis I. However, Rec8 in the long arm region are protected by LAB-1 (long arm of the bivalent) but not Sgo1 till meiosis II (Figure 6B) (Albertson and Thomson 1993; Kaitna et al. 2002; Nabeshima et al. 2005). (ii) In the case of *L. elegans* which performed inverted meiosis, it is suggested that cohesion is released once only at meiosis I (Heckmann et al. 2014a). However, the dynamics and function of cohesin is not yet known. Besides realising sister chromatid cohesion, cohesin complexes also participate in the assembly of the synaptonemal complex (SC) in prophase I (Hartsuiker et al. 2001; Klein et al. 1999).

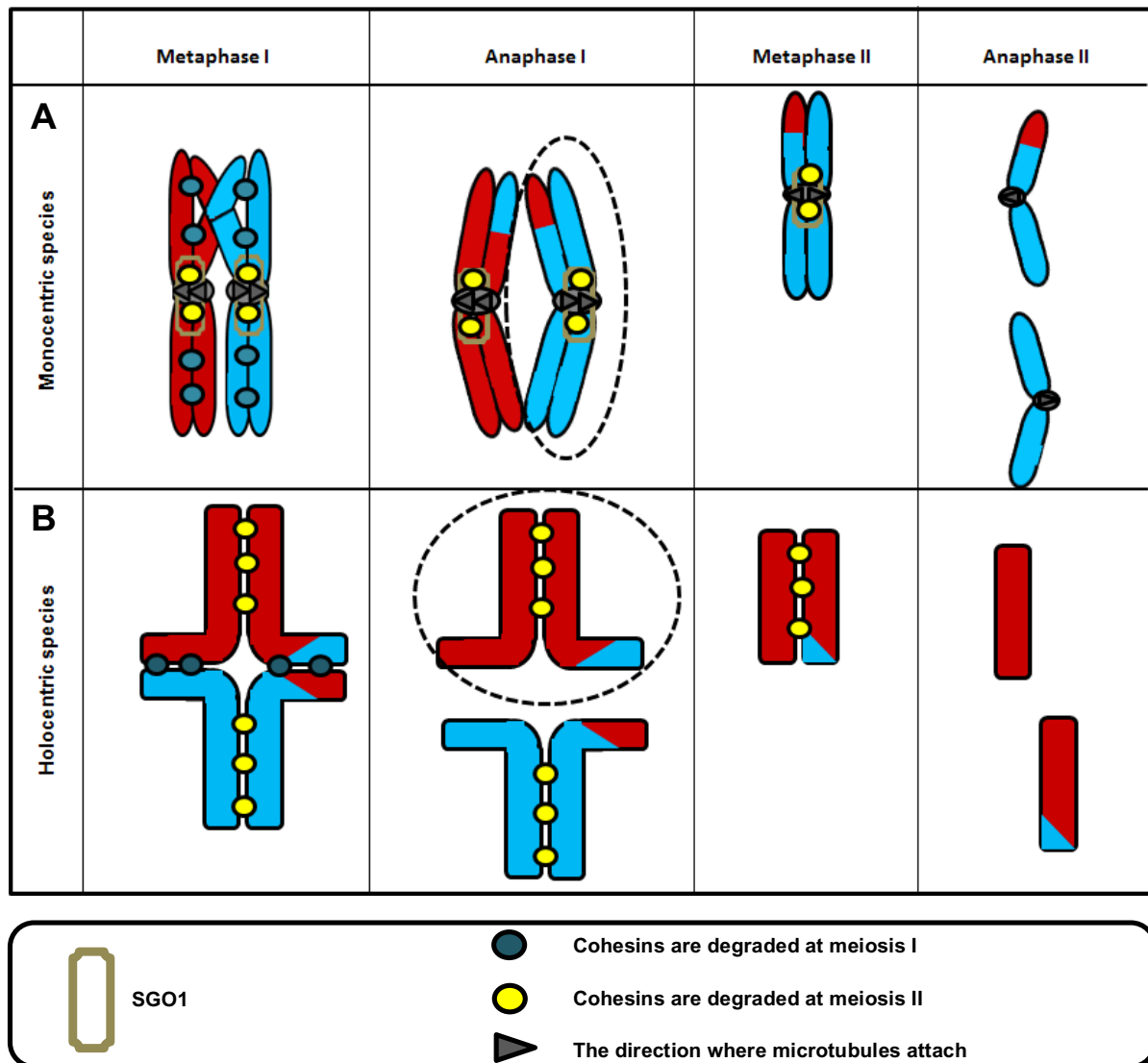


Figure 6. Cohesin complex and cohesin regulators.

In monocentric species (A), SGO1 recruits PP2A to centromeres to counteract the phosphorylation of Rec8 (the meiosis homolog of Rad21/SCC1) which prevents the degradation of centromere cohesion till meiosis metaphase II. In holocentric species *C. elegans* (B), the phosphorylation of Rec8 at the short arm region (between homologous chromosomes) allows the degradation of cohesin first at this region. But the Rec8 in the long arm region is protected by nematode unique protein LAB-1 (long arm of the bivalent) (de Carvalho et al. 2008) instead of SGO1 till the onset of anaphase II.

1.1.5 Synaptonemal complex

Pairing and synapsis are unique processes which occur only in meiosis. In this process, the synaptonemal complex (SC) plays an important role. The SC complex consists of a proteinaceous structure, two electron dense lateral elements (LE/AE) and a dense central region (CE) traversed by thin filaments (Figure 7). Surrounded

by chromatin, the synaptonemal complex lies “zipper-like” along the central axis of the bivalent.

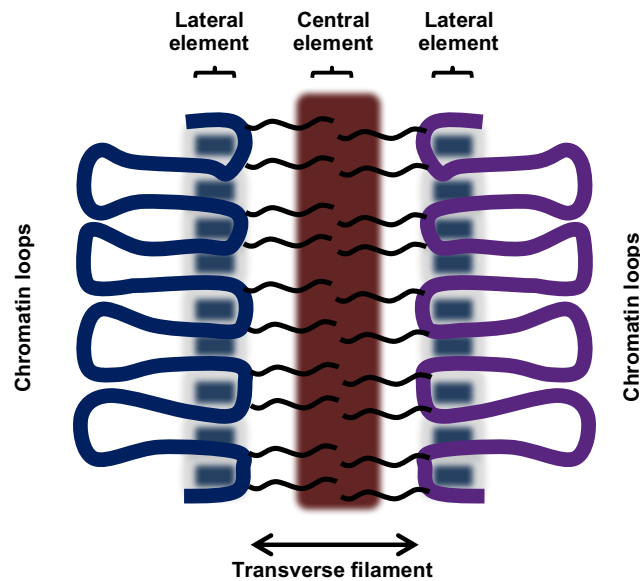


Figure 7. Schematic model of the synaptonemal complex (SC).

A schemata of the tripartite structure of the SC showing locations of central element (in brown), lateral element (in blue) and chromatin loops.

At leptotene, a lateral component is organized between the non-sister chromatids and the telomeres attach to the nuclear envelope. At early zygotene, the attachment sites aggregate and a chromosome bouquet is formed. The axial elements become associated by transverse filaments to the central element to establish the tripartite SCs. The SC provides the structural framework for synapsis, double strand-break repair and exchange between homologues (Henderson and Keeney 2005). Until now, this process seems quite conserved in all studied organisms. However, unknown is whether the SC complex structure conserved in the holocentric species *L. elegans*.

1.2 Open questions and aims of the PhD work

We have indication that in the holocentric plant species *Luzula elegans* the sequence of meiotic chromosome segregation events is inverted (Heckmann et al. 2014a). Homologous non-sister chromatids remain linked after metaphase I at their termini by chromatin threads, until metaphase II. To decipher the organization of the end-to-end connection between non-sister chromatids during meiosis I and II, the cohesin related genes α -kleisin and SGO1 were identified and analyzed in *L. elegans*. In addition we aimed to determine whether the meiotic process during prophase I differs between holo- and monocentric species.

1.3 Materials and Methods

1.3.1 Plant material and plant cultivation

Luzula elegans Lowe (2n=6) (Vouchers at the Herbarium Gatersleben: GAT 7,852–7,856) plants were cultivated for 4 weeks under short-day conditions (8 h light/16 h dark, 20°C /18°C) and then vernalized (10 h light/14 h dark, 4°C) for at least 4 weeks. The plants were finally grown under the long-day conditions (16 h light, 22°C day/16°C night) and all experimental materials from different tissues were collected during this period.

1.3.2 RNA extraction, RT-PCR and qRT-PCR

Total RNA was extracted from leaves, stems and flower buds by the TRIzol method (Life Technologies). The RNA samples were treated with RNA-free DNase I (Ambion TURBO DNase; Invitrogen) before cDNA synthesis. The absence of genomic DNA was confirmed by PCR with *LeGAPDH*-specific primers G1F and G1R (Table 1). All cDNAs (20 µl) were generated from 1 µg DNase I-treated RNA, using the Reverse Aid H Minus First Strand cDNA Synthesis Kit (Fermentas). cDNA used for 5'- and 3'- RACE PCR were synthesized from mRNA of flower buds according to the SMART RACE cDNA Amplification Kit (Clontech, Palo Alto, CA) manual protocol.

25 µl PCR reaction mixtures contained: 1 µl cDNA, 10 µM of each forward and reverse primers (Table 1), 5 mM of each deoxynucleotide triphosphates, 2.5 µl 10xPCR reaction buffer and 1 unit of *Taq* polymerase (Qiagen). The cycling protocol was: 94°C for 3 min, 35 cycles at (94°C for 40s, 58°C for 40 s, 1 min/kb elongation at 72°C), 72°C final elongation for 10 min. 25 cycles PCR were run with *LeGAPDH*-specific primers (G1F and G1R, Table 1) to quantify the abundance of transcripts. 5'- and 3'- RACE PCR were performed according to the SMART RACE cDNA Amplification Kit (Clontech, Palo Alto, CA) manual protocol.

qRT-PCR was performed using the SYBR Green Master (Applied Biosystems) on the 7900HT Fast Real-Time PCR System (Applied Biosystems). 10 µl of PCR mixture contained 0.2 µl of cDNA template, 5 µl of 2× Power SYBR Green PCR Master Mix (Applied Biosystems), and 0.33 mM of the forward and reverse primers (Table 1) for each gene. The amplification conditions were one cycle at 95°C for 10 min, 40 cycles of two consecutive steps at 95°C for 15 s and at 60°C for 60s. *LeGAPDH*-specific primers G2F and G2R (Table 1) were used as endogenous control.

Table 1 List of primer sequences for PCR, RT-PCR and FISH

Primer Name	Primer seq (5'-3')
<i>LeCENH3</i>	
C1F	CCGCAAGTTCAGAGATCCACCGA
C1R	GAGAGCTTCCGCTTGCCAGCGATTAAC
C2F	AGCAAACCTCCCGCAAATTT
C3F	AGCAAACCTCCCGCTACGGAG
C2R	AGTCTTTCGGGCTGAGGATT
C4F	GGTTCGCGTGTCTCTCTTGA
C4R	TGCCCACTTATCCGCCTAGCAAGCT
<i>LeGAPDH</i>	
G1F	GTTTGTGGTTGGTGTGAACG
G1R	CCTCCTTGATAGCAGCCTTG
G2F	TTCACTCGATCACTGCCACC
G2R	CGGTGCTGCTTGGAATGATG
<i>Leα-kleisin-1</i>	
R1F	atccgGAATTCTCACAGTTTATACTAGCG
R1R	tatcaaatGCGGCCGCAGAAGGAGAAGCGTCATTATC
R2F	ACTTCCAGATTCCGGCTTGGA
R2R	CTCGCCTTGCTCAAATTCGT

1.3.3 Sequence analysis

DNA fragments were sequenced by the service facility of the IPK (Gatersleben, Germany). Sequences were analyzed by Sequencher 5.2.4 (Gene Codes Corporation Inc), assembled using Seqman pro 12.0.0 (DNASTAR, Inc) and processed by EditSeq and MegAlign Lasergene 8 (DNASTAR, Inc). Reference IDs for the phylogenetic analysis of the α -kleisin sequences used in this study are available in Table 2, CENH3 sequences used for comparison are described in (Marques et al. 2015). Phylogenetic trees were constructed by the software Geneious (version 7.0.6; <http://www.geneious.com>).

Table 2. List of sequence identifiers and description of α -kleisin sequences used for phylogenetic tree construction.

Sequence Name	Species	Accession Number
Le α -kleisin-1	<i>Luzula elegans</i>	KT932948
Le α -kleisin-2	<i>Luzula elegans</i>	KT932949
Le α -kleisin-3	<i>Luzula elegans</i>	KT932950
Le α -kleisin-4	<i>Luzula elegans</i>	KT932951
AtSYN1	<i>Arabidopsis thaliana</i>	AED90880.1
AtSYN2	<i>Arabidopsis thaliana</i>	AAG44842.1
AtSYN3	<i>Arabidopsis thaliana</i>	AAG44843.1
AtSYN4	<i>Arabidopsis thaliana</i>	NP_197131.2
OsRad21-1	<i>Oryza sativa</i>	AAQ21081.1
OsRad21-2	<i>Oryza sativa</i>	AAQ75093.2
OsRad21-3	<i>Oryza sativa</i>	AAQ75094.1
OsRad21-4	<i>Oryza sativa</i>	AAQ75095.1
ZmRad21-1	<i>Zea mays</i>	ACN33882.1
ZmRad21-2	<i>Zea mays</i>	AFW58674.1
ZmRad21-3	<i>Zea mays</i>	ACN33677.1
ZmREC8	<i>Zea mays</i>	NP_001105829.1
RcRad21-1	<i>Ricinus communis</i>	XP_002514774.1
RcRad21-2	<i>Ricinus communis</i>	XP_002509552.1
RcRad21-3	<i>Ricinus communis</i>	XP_002513194.1
RcRad21-4	<i>Ricinus communis</i>	XP_002520771.1
PtRad21-1	<i>Populus trichocarpa</i>	XP_002312205.1
PtRad21-2	<i>Populus trichocarpa</i>	XP_002331697.1
PtRad21-3	<i>Populus trichocarpa</i>	XP_002299652.1
PtRad21-4	<i>Populus trichocarpa</i>	XP_002312177.1
CsRad21-1	<i>Camelina sativa</i>	XP_010453785.1
CsRad21-2	<i>Camelina sativa</i>	XP_010441244.1
CsRad21-3	<i>Camelina sativa</i>	XP_010413676.1
CsRad21-4	<i>Camelina sativa</i>	XP_010423466.1

1.3.4 Total protein extraction and Western blot analysis

For isolation of total *L. elegans* proteins 200 mg of grinded flower buds were suspended in 250 μ l extraction buffer (112 mM Na₂CO₃, 112 mM DTT, 4% SDS, 24% sucrose, 4 mM EDTA and 1 mg 3,3,5,5-tetrabromophenolsulfonephthalein) and kept at 65°C for 20 minutes. After centrifugation at 14,000 rpm for 5 min at 4°C the supernatant contained the total soluble proteins.

The proteins were separated by 10% (wt/vol) polyacrylamide gels according to Schägger and Von Jagow (1987), then the gels were blotted on Immobilon PVDF membranes (Millipore). These membranes were incubated first with primary antibodies (1:1,000 rabbit anti-LeCENH3, 1:5,000 rabbit anti-histone H3 (Sino Biological Inc., 100005-MM01-50) and 1:5,000 mouse anti- α tubulin (clone DM 1A, Sigma) and then with the corresponding secondary antibodies [1:5,000 anti-rabbit IgG IRDye800CW (LI-COR, 925-32213) or 1:5,000 anti-mouse IgG IRDye 680RD (LI-COR, 926-32222)]. The immunoblots were imaged using a LI-COR Odyssey Imager. Histone H3 and α -tubulin signals were used as controls.

1.3.5 Antibody production

To generate antibodies against Le α -kleisin, a 1017-bp fragment of Le α -kleisin (primers R1F and R1R, Table 1) was amplified from flower bud cDNA. The fragments were cloned into the vector pSC-A-amp/kan using the StrataClone PCR cloning kit (Stratagene), sequenced and then sub-cloned into the expression vector pET-23a-d(+) (Novagen). The resulting pET-23a-Le α -kleisin construct was transformed into *Escherichia coli* BL21 (DE3) and the expression of proteins was induced by 1 mM isopropylthio-beta-D-galactoside (IPTG). The Le α -kleisin recombinant proteins were purified under native condition on Ni-NTA agaroses (Qiagen), then confirmed by Western blot using mouse monoclonal anti-His-tag (1:1,000, Millipore, 05-949) and 1:5,000 anti-mouse IgG IRDye 680RD (LI-COR, 926-32222) antibodies. A polyclonal rabbit anti-Le α -kleisin antibody was produced by Pineda (Antikörper-Service, Berlin, Germany). The specificity of anti-Le α -kleisin antibody (1:1,000) was checked on a Western blot with recombinant proteins. The method for Western blot was discussed above.

For the generation of LeCENH3-specific antibodies an epitope corresponding to the N-terminal end of LeCENH3 (3-RTKHFSNRKSIPPKKQTPAK-23) was identified. Peptide synthesis, immunization of rabbits, and peptide affinity purification of antisera were performed by LifeTein LLC (South Plainfield, NJ, USA).

1.3.6 Indirect immunostaining and light microscopy

Indirect immunostaining of *L. elegans* was performed as described by Heckmann et al. (2014a), of *Hordeum vulgare* and *Vicia faba* as described by Schubert et al. (1993). The following primary antibodies were used: rabbit anti-Le α -kleisin (1:100),

mouse anti-OsSgo1 (1:200) (Wang et al. 2011), guinea pig anti-ZmZYP1 (1:100) (Golubovskaya et al. 2011), rabbit anti-grass CENH3 (1:300) (Sanei et al. 2011) and rabbit anti-LeCENH3 (1:100). Texas red-conjugated anti-rabbit antibodies (1:400) (Molecular Probes), fluorescein isothiocyanate-conjugated anti-mouse antibodies (1:300) (Molecular Probes) and Alexa 488 conjugated anti-guinea pig (1:300) (Dianova) antibodies were used as secondary antibodies. Anti-LeCENH3 and anti-grass CENH3 antibodies were directly labelled by the Fluorescein Labeling Kit-NH2 (Dojindo, LK01-10).

Images were collected in gray scale using an Olympus BX61 microscope (Olympus; <http://www.olympus.com>) and an ORCA-ER CCD camera (Hamamatsu; <http://www.hamamatsu.com>), then pseudocoloured and merged with Adobe Photoshop CS5 (Adobe). To achieve a lateral optical resolution of ~120 nm (super-resolution, obtained with a 488 nm laser), we applied structured illumination microscopy (SIM) using a 63x/1.4 Oil Plan-Apochromat objective of an Elyra PS.1 microscope system and the software ZEN (Carl Zeiss GmbH). Images were captured separately for each fluorochrome using the 561 nm, 488 nm and 405 nm laser lines for excitation and appropriate emission filters (Weisshart et al. 2016).

1.3.7 Electron microscopy

For transmission electron microscopy cut-opened anthers undergoing prophase I were fixed for 4 h in 3% glutaraldehyde (Sigma, Taufkirchen, Germany) in 0.1 M sodium cacodylate buffer pH 7.2 (SCB), washed, postfixed for 1 hour with 1% osmiumtetroxide (Carl Roth, Karlsruhe, Germany) in SCB, dehydrated in a graded series of ethanol and embedded in epoxy resin according to Spurr (1969). Ultrathin sections (70 nm) were transferred to formvar coated grids and poststained with uranyl acetate and lead citrate. Subsequently the grids were observed with an EM 900 (Carl Zeiss Microscopy, Oberkochen, Germany) transmission electron microscope (acceleration voltage 80 kV). Electron micrographs were taken with a slow scan camera (Variospeed SSCCD camera SM-1k-120, TRS, Moorenweis, Germany) using the iTEM software from Olympus SIS (Münster, Germany).

1.3.8 Accession numbers

Sequences information from this project can be found in the GenBank/EMBL data libraries under accession numbers *LeCENH3* gDNA (KT932953), *LeCENH3.1* mRNA

(KT932953), *LeCENH3.2* mRNA (KT932954) *Le α -kleisin-1* mRNA (KT932948), *Le α -kleisin-2* mRNA (KT932949), *Le α -kleisin-3* mRNA (KT932950) and *Le α -kleisin-4* mRNA (KT932951).

1.4 Results

We have indications that in the holocentric species *L. elegans* the sequence of meiotic chromosome segregation events is inverted. Sister chromatids separate at anaphase I, homologous separate at anaphase II, and the homolog non-sister chromatids are linked at the termini from metaphase I to metaphase (Heckmann et al. 2014a). However, the following questions still remain (Figure 8): The workflow below represents the questions we asked and how we answered the questions in this study.

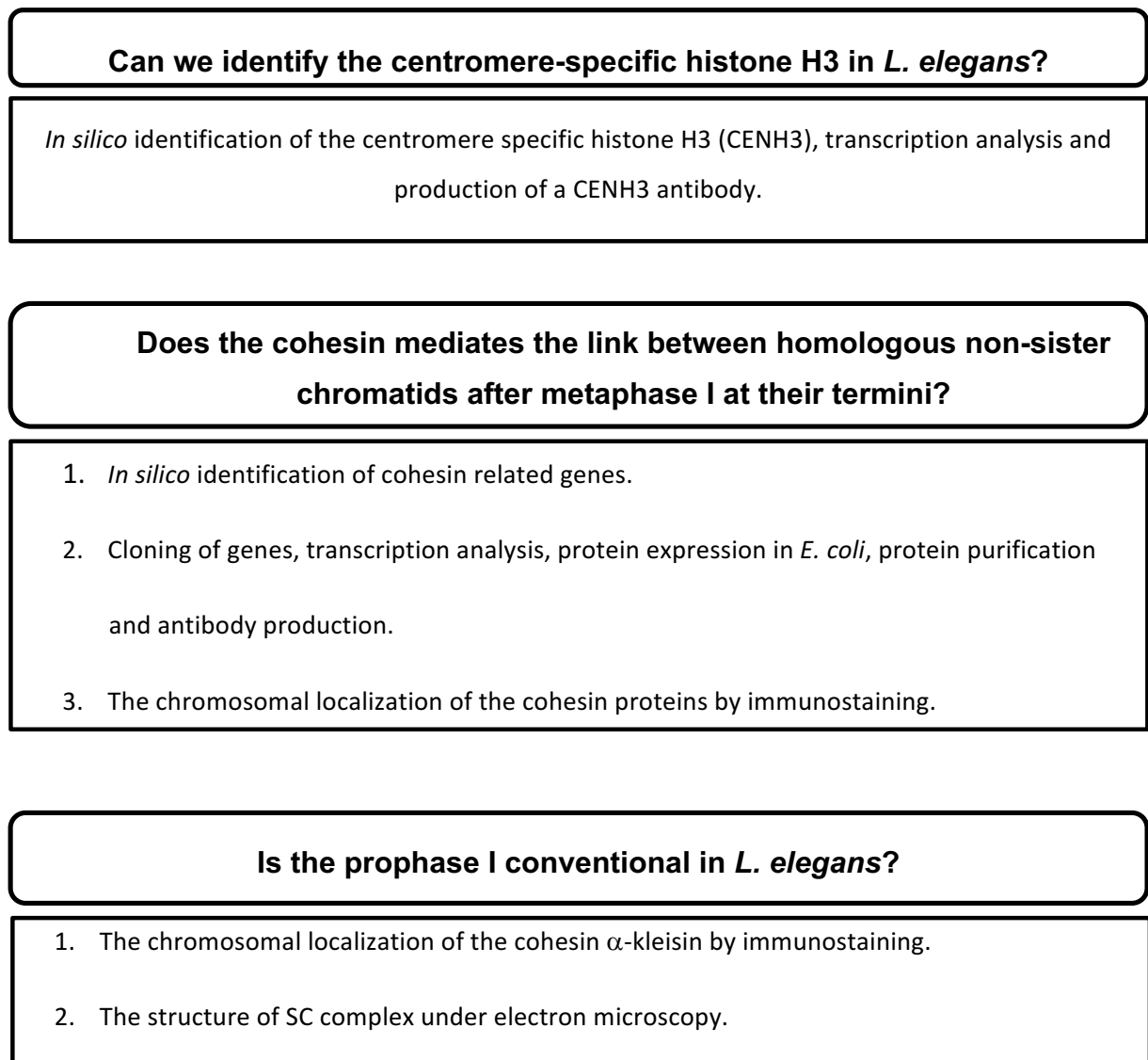


Figure 8. A workflow describing the steps of the study.

The questions asked in each step are indicated in bold. The methods we used to answer the questions are listed below the questions.

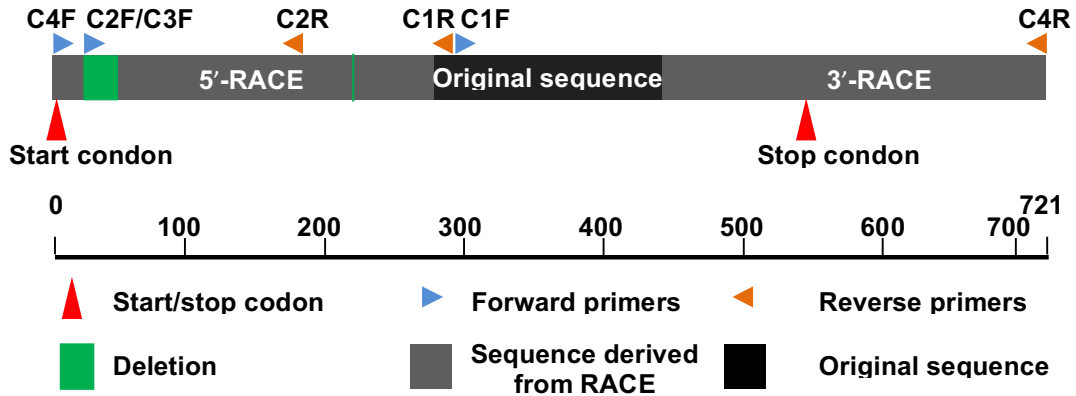
1.4.1 Identification of the centromere-specific histone H3 variant CENH3 in *L. elegans*

First a *L. elegans*-specific centromere antibody recognizing the centromere-specific histone H3 (CENH3) was established. Both CENH3 variants of *Luzula nivea* (GenBank BAE026 and ADM18965) (Nagaki et al. 2005; Moraes et al. 2011) were used as query to identify the corresponding gene in the established RNAseq database of *L. elegans* pollen mother cells (<http://webblast.ipk-gatersleben.de/luzula/>). To determine the start and end of the *LeCENH3* transcript, 3'-RACE and 5'-RACE experiments were performed based on a 55 amino acids fragment showing high similarity to the C-terminal part of *L. nivea* CENH3 (Figure 9A, 9B). Cloning of the 5'-RACE products revealed two gene splicing variants (called *LeCENH3.1* and *LeCENH3.2*). *LeCENH3.2* differs from *LeCENH3.1* by having 21 bp- and 3 bp-long deletions near the 5'-terminal part (Figure 9A). The full sequences of *LeCENH3.1* and *LeCENH3.2* were confirmed after PCR and RT-PCR using the primer pair C4F/C4R (Figure 9A).

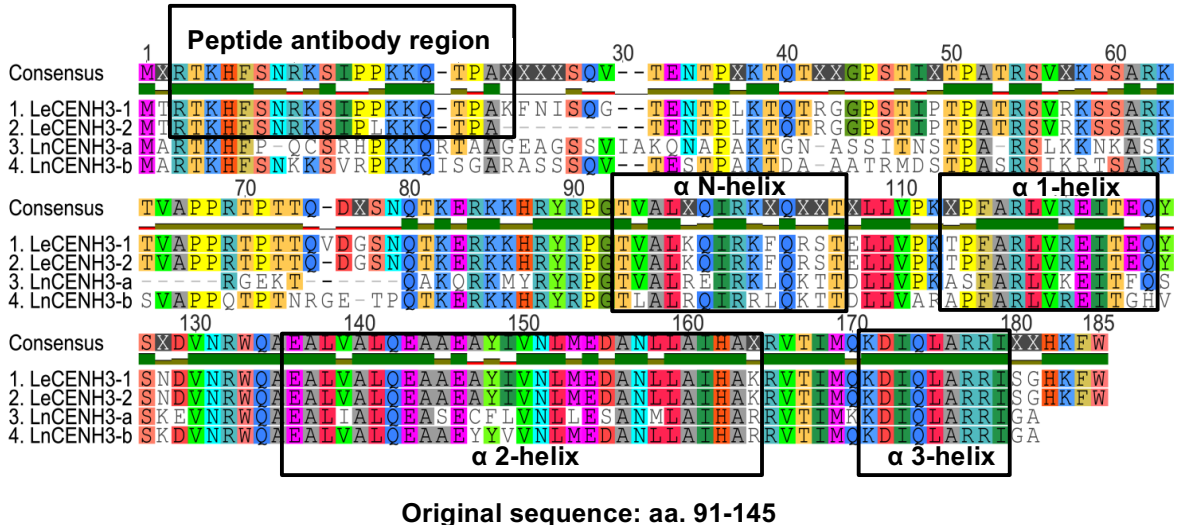
Both *LeCENH3* splicing variants show a higher expression in flower buds than in stems and leaves as revealed by quantitative RT-PCR using the primer combinations (C2F/C2R and C3F/C2R). *LeCENH3.1* exhibited a higher expression than *LeCENH3.2* in flower buds and stems. In leaves the activity of both was almost identical (Figure 9C). But a diverging expression was found in anthers by sequencing the cloned 5'-RACE products. 74% and only 26% of the products (n=38) originated from *LeCENH3.1* and *LeCENH3.2*, respectively.

Next, a rabbit anti-*LeCENH3* antibody was raised against a synthetic peptide containing the N-terminal 20 amino acid residues of both CENH3s (Figure 9B). To determine the antibody specificity, immunostaining was performed on *Luzula* chromosomes, the result also confirmed the specificity of the *LeCENH3* antibody (Figure 9D). Afterwards, a Western blot assay was performed using the affinity purified antibodies as probe on total protein extracts from flower buds of *L. elegans*. The major band identified fitted to the expected size of 20 kD (Figure 9E). Our phylogenetic analysis also grouped both *LeCENH3* variants together with CENH3s of other *Juncaceae* species in a sister branch of monocots (Figure 9F).

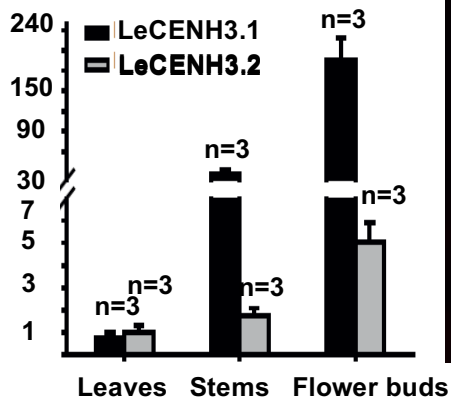
A



B



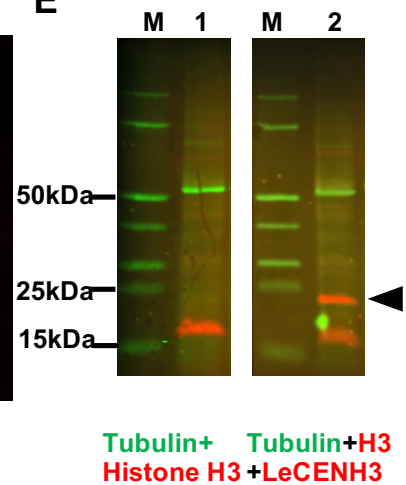
C



D



E



F

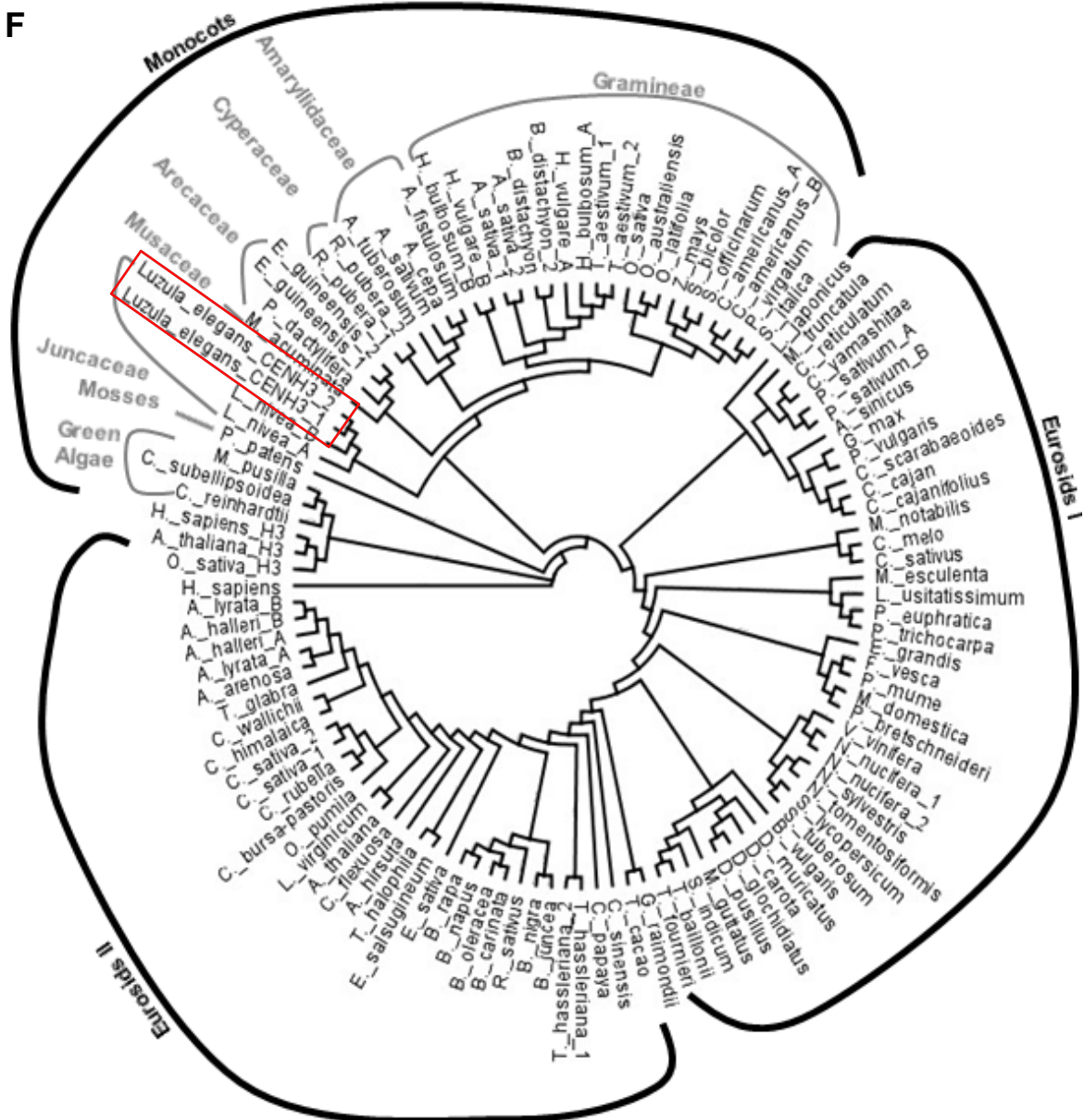


Figure 9. CENH3 of *L. elegans*.

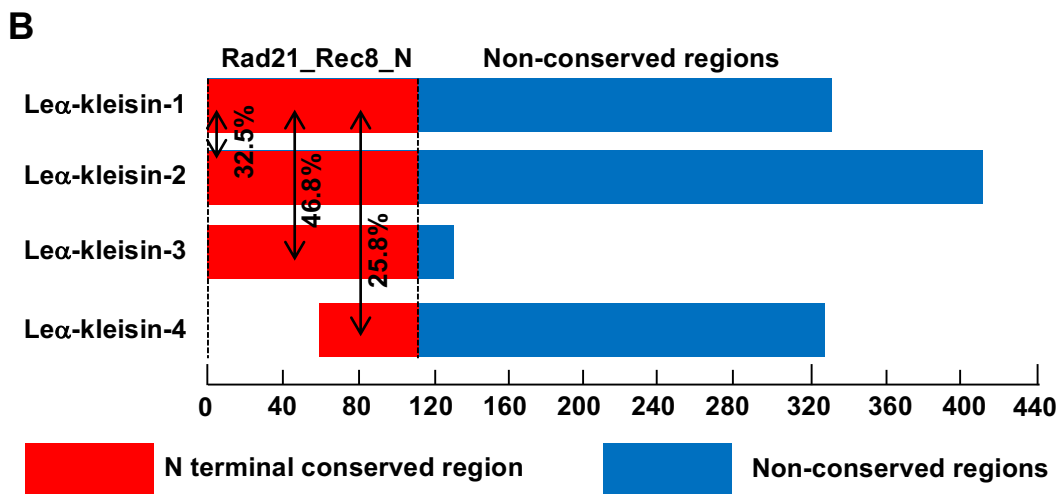
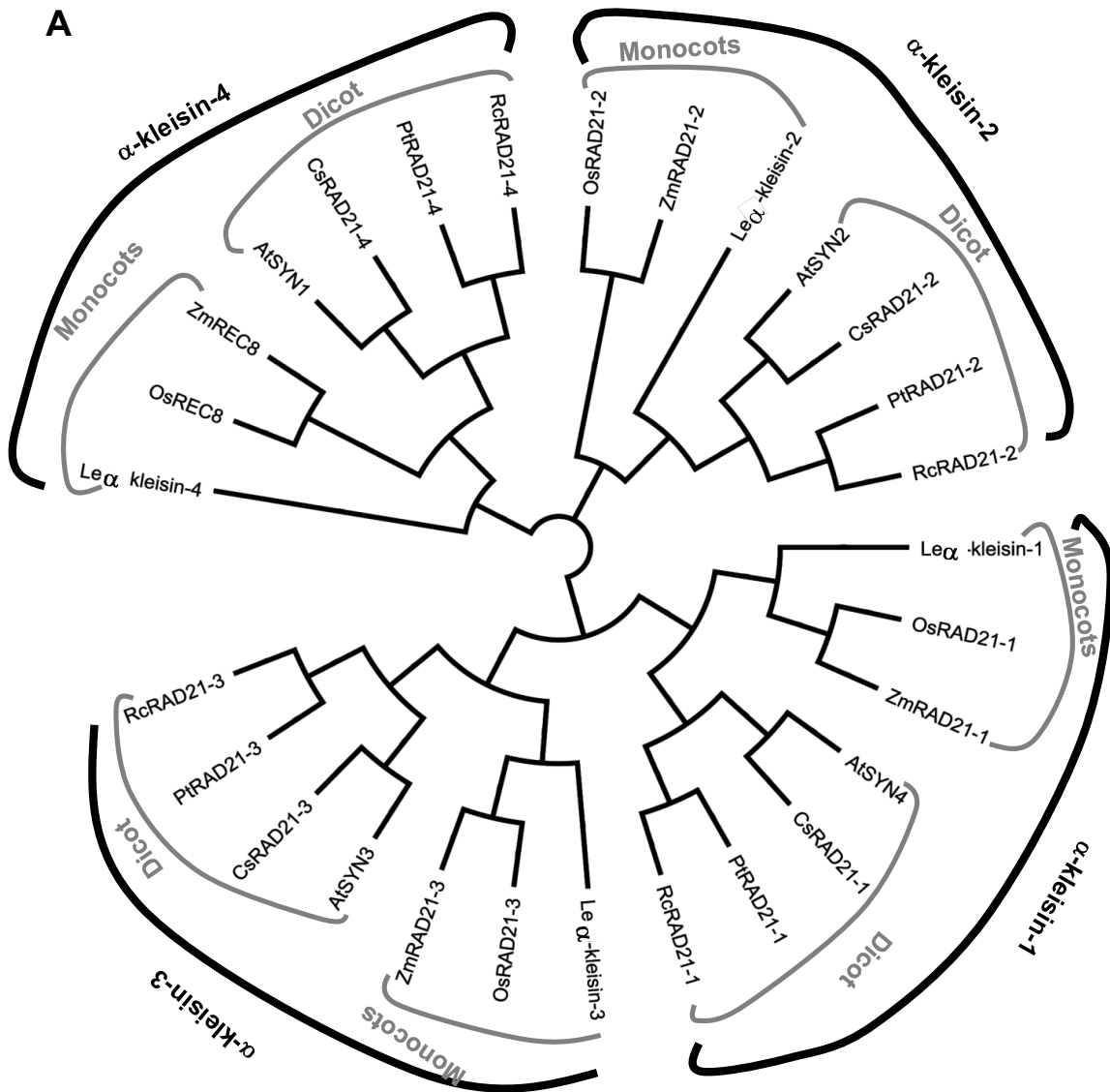
(A) Gene structure model of LeCENH3, the positions of start/stop codons, and the *in silico* identified sequence. The obtained 5' and 3' RACE sequences and primer sites are indicated. (B) Alignment of CENH3 sequences from two *Luzula* species. The conserved domains of CENH3 are indicated by rectangle frames. (C) The relative transcription level of *LeCENH3.1* and *LeCENH3.2* was measured by qRT-PCR. (D) Immunostaining of anti-LeCENH3 (red) on metaphase II chromosomes. Bar=10 μ m. (E) Western blot analysis using anti-LeCENH3, anti-histone H3 and anti- α -tubulin (as control) antibodies. The triangle indicates the band observed corresponding to the LeCENH3 protein. The total protein was extracted from *L. elegans* flower buds. (F) Phylogenetic analysis of CENH3 proteins from different species.

1.4.2 Identification of the *L. elegans* α -kleisins

To identify the α -kleisin subunits of *L. elegans* cohesin we searched by BLASTP in the *L. elegans* RNAseq database using the Rad21/Rec8-like sequences of rice (Zhang et al. 2004) as query, and identified *in silico* four α -kleisin-like genes. The phylogenetic analysis of the different mono- and eudicot Rad21/Rec8 proteins indicated that each of the four *L. elegans* α -kleisin-like proteins were categorized into different subfamilies (Figure 10A), namely Le α -kleisin-1, Le α -kleisin-2, Le α -kleisin-3 and Le α -kleisin-4. The alignment of these four incomplete proteins revealed an overall similarity of only 8.3% to 36.8% (Table 3). However, the conserved N-terminal regions showed a higher similarity with 25.8% to 46.8% (Figure 10B).

We chose Le α -kleisin-1 for further analysis, because this protein possibly represents an ortholog of the *Arabidopsis thaliana* α -kleisin SYN4 required for cohesion along chromosome arms and at centromeres (Schubert et al. 2009). In order to determine the transcription dynamics of *Le α -kleisin-1*, cDNA derived from stems, leaves and flower buds were used to perform quantitative reverse transcription PCR (qRT-PCR, primers R2F/R2R) (Figure 10C). As shown in Figure 10D, the highest level of expression was found in flower buds. This agrees to data obtained for Rad21-1 of rice (Zhang et al. 2004).

To test the chromosomal distribution of Le α -kleisin-1, rabbit polyclonal antibodies were raised against a partial recombinant Le α -kleisin-1 protein. We cannot exclude that these antibodies recognize also other members of the α -kleisin family since the N-terminal part is conserved. Therefore, we named the antibodies 'anti-Le α -kleisin'. The molecular weight of the recombinant protein used for antibody production was ~55 kDa (Figure 10E) although the expected size is 38 kDa. Such a difference was also observed for antibodies established against α -kleisin orthologs of mouse (Lee and Hirano 2011), *C. elegans* (Birkenbihl and Subramani 1995) and budding yeast (Michaelis et al. 1997), likely due to the high polarity of the proteins. Nevertheless, the cross-reaction of anti-Le α -kleisin with antigens produced by *E. coli* confirmed its specificity (Figure 10F).



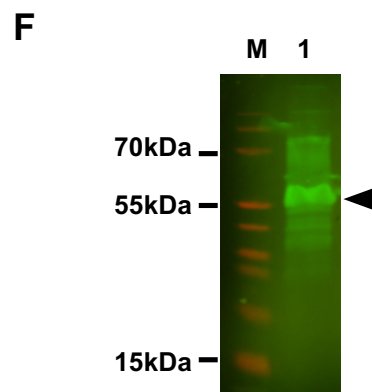
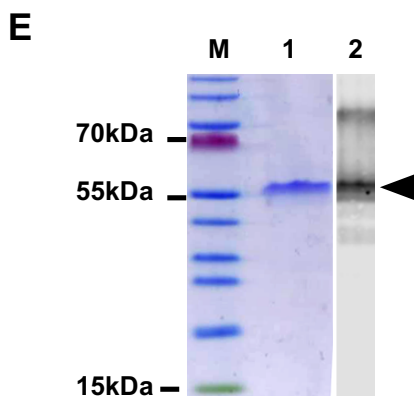
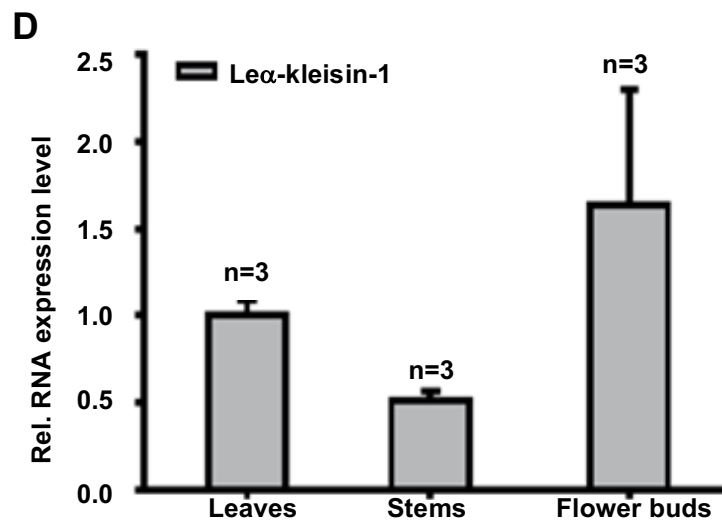
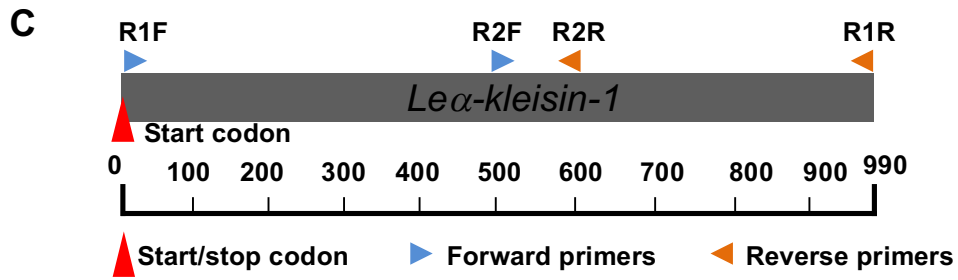


Figure 10. The α -kleisins of *L. elegans*

(A) Phylogenetic analysis of α -kleisin-like proteins from different plant species. Reference IDs for the phylogenetic analysis of the α -kleisin sequences used in this study are available in Table 2. (B) Protein structure model of four *Luzula* α -kleisin-like proteins based on in silico identification. The similarity of N-terminal conserved regions (red) among each other is indicated. (C) Gene structure model of *Leα-kleisin-1* transcripts. Positions of start/stop codon and primer sites are indicated. (D) The

total transcription level of *Le α -kleisin-1* in leaves, stems and flower buds was measured by qRT-PCR. The number of biological replicates is indicated above the standard deviation bars. (E) The purified recombinant *Le α -kleisin* protein was analyzed by comassie staining (blue gel on left) and Western blotting (black picture on right) with Anti-6X His tag antibodies. The major band observed corresponds to the *Le α -kleisin* protein (triangle). (F) The purified recombinant *Le α -kleisin* protein was analyzed by *Le α -kleisin* recombinant antibody. The major band observed corresponds to the *Le α -kleisin* protein (triangle).

Table 3 The similarity of different *Le α -kleisin* protein sequences

	<i>Leα-kleisin-1</i>	<i>Leα-kleisin-2</i>	<i>Leα-kleisin-3</i>	<i>Leα-kleisin-4</i>
<i>Leα-kleisin-1</i>	100%	15.6%	36.8%	12.1%
<i>Leα-kleisin-2</i>		100%	18.7%	8.3%
<i>Leα-kleisin-3</i>			100%	22.6%
<i>Leα-kleisin-4</i>				100%

1.4.3 Identification of SGO1 in *L. elegans*

To identify *L. elegans* SGO1 we searched by BLASTP in the *L. elegans* RNAseq database using the SGO1-like sequences of rice (Wang et al. 2011) as query, and identified *in silico* SGO1. The phylogenetic analysis of the different mono- and eudicot SGO1 proteins confirmed the correct identification of *L. elegans* SGO1-like protein (Figure 11A).

We chose *LeSGO1* for further analysis, because SGO1 could stabilize the synaptonemal complex and protects centromeric cohesion during the meiosis of rice (Wang et al., 2011). In order to determine the transcription dynamics of *LeSGO1*, cDNA derived from flower buds, young and old leaves were used to perform semi-quantitative reverse transcription PCR. As shown in Figure 11B, the highest level of expression was found in flower buds.

To test the chromosomal distribution of *LeSGO1*, mouse polyclonal antibodies were raised against a partial recombinant *LeSGO1* protein. Unfortunately, our mouse polyclonal *LeSGO1* antibodies did not cross-react with chromosomes. Therefore, I used a rabbit polyclonal *OsSGO1* (Wang et al., 2011) antibody against SGO1 from rice for the further studies.

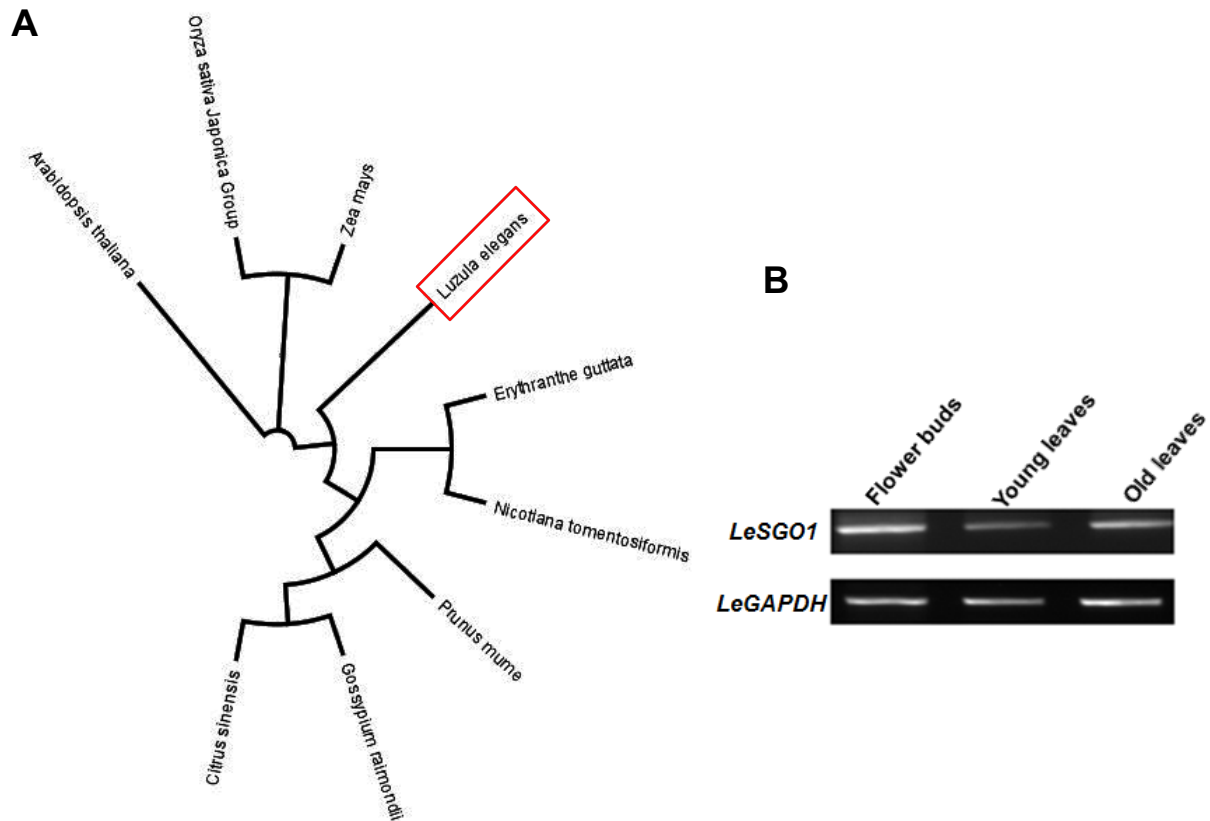


Figure 11. SGO1 of *L. elegans*.

(A) Phylogenetic analysis of SGO1-like proteins from different plant species. (B) The total transcription level of *LeSGO1* in flower buds, young and leaves was measured by RT-PCR. *LeGAPDH* was used to quantify the amount of the cDNA.

1.4.4 Prophase I is conventional in *L. elegans*

Anti- $Le\alpha$ -kleisin staining was performed on pollen mother cell chromosomes to decipher the distribution of α -kleisin in prophase I. $Le\alpha$ -kleisin signals lined up into continuous structures during leptotene/zygotene (Figure 12A, 12B). Double immunostaining with ZmZYP1 and $Le\alpha$ -kleisin antibodies showed that $Le\alpha$ -kleisin mainly localized in the ZmZYP1 positive regions during zygotene/pachytene (Figure 12C). Thus, the distribution of meiotic cohesin during prophase I seems to be as similar as reported for monocentric species (Qiao et al. 2011).

Previous immunostaining showed that the distribution of the synaptonemal complex proteins ASY1 and ZYP1 was similar to those described for species with monocentric chromosomes (Heckmann et al. 2014a). To obtain further insights we examined pachytene cells of *L. elegans* by transmission electron microscopy (in collaboration

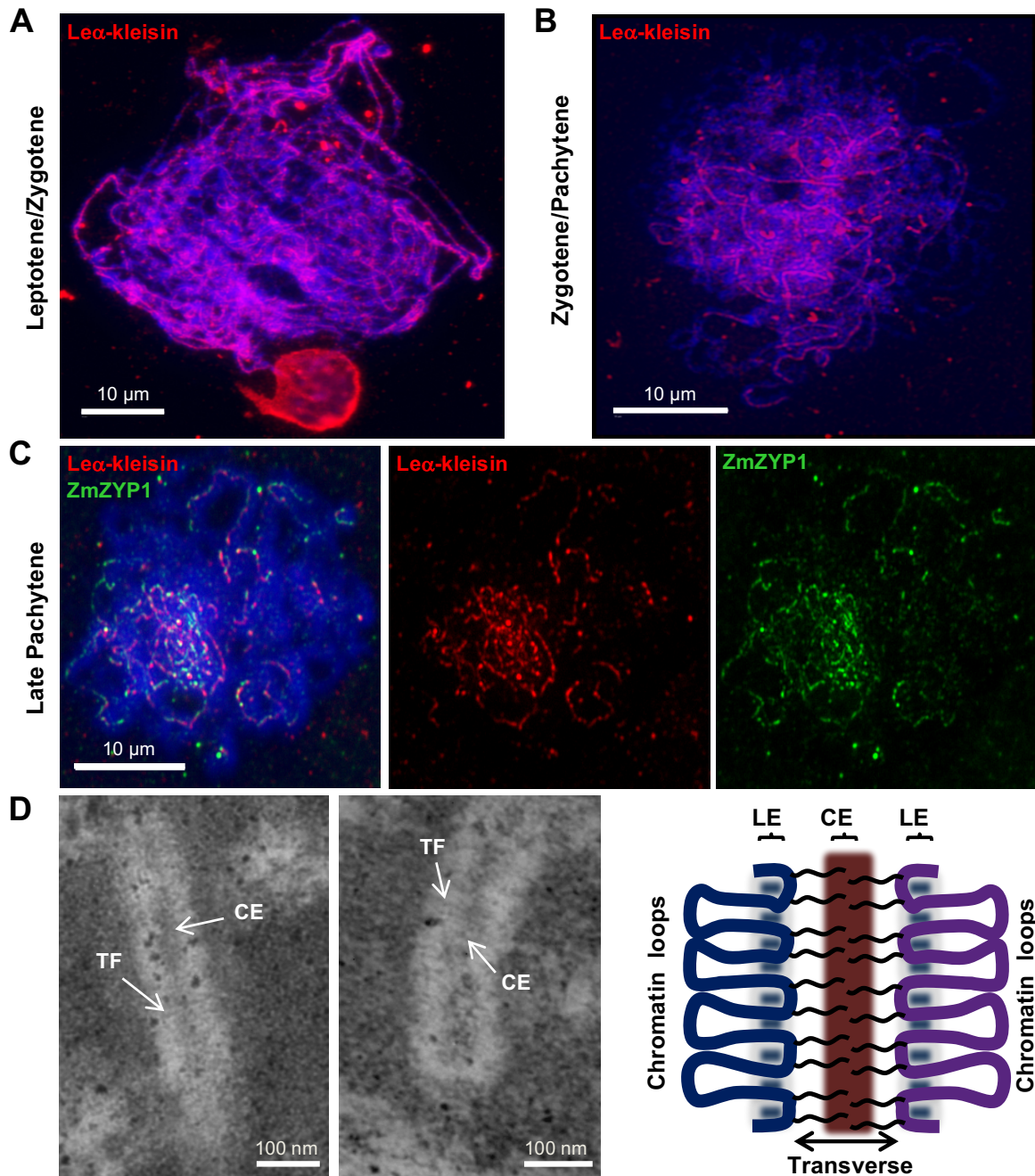


Figure 12. Prophase I is conventional in the holocentric species *L. elegans*.

(A-C) The distribution of Le α -kleisin from leptotene to late pachytene. (C) Colocalization of Le α -kleisin and ZmZYP1 at pachytene. (D) Electron micrographs of two *L. elegans* synaptonemal complexes (left), with the scheme of a synapsed homologous chromosome pair (right) in which the central element (CE), and putative transverse filaments (TF) indicated.

with Gerd Hause, Institute of Biology, Department of Genetics, Martin Luther University Halle-Wittenberg, Germany). A tripartite structure of the synaptonemal complex can be observed in *L. elegans*. We identified a $111.6 \pm 10,6$ nm (n=20) wide synaptonemal complex comprising a dense central region traversed by thin filaments

(Figure 12D). Surrounded by chromatin, the synaptonemal complex lies “zipper-like” along the central axis of the bivalent (Figure 12D). These findings indicate that the synaptonemal complex structure of holocentric species is similar to those of monocentrics.

1.4.5 $Le\alpha$ -kleisin colocalizes with the centromeres of condensed chromosomes

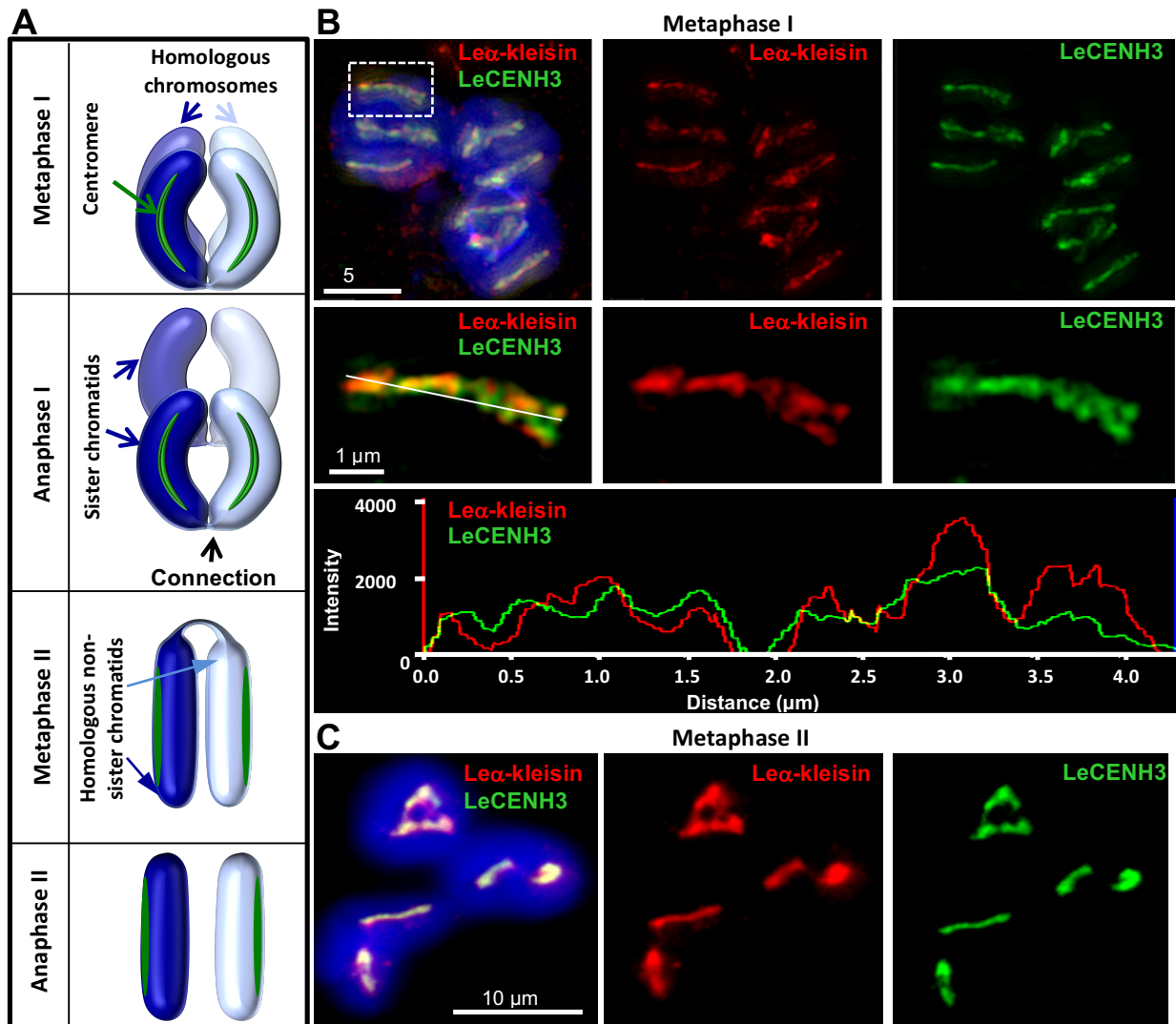


Figure 13 Distribution of $Le\alpha$ -kleisin and LeCENH3 at meiotic metaphase I and II chromosomes of *L. elegans*.

(A) Schematic model of meiosis in the holocentric species *L. elegans*. The U-shaped bivalents are aligned at metaphase I and the sister chromatids separate already during anaphase I. Homologous non-sister chromatids are connected at their termini until metaphase II. Then, they separate at anaphase II. (B) The colocalization of $Le\alpha$ -kleisin and LeCENH3 at metaphase I centromeres was identified by SIM after immunostaining (top). The middle panel shows a region of interest (rectangle) further magnified. The quantification of centromeric fluorescence intensities of $Le\alpha$ -kleisin and anti-LeCENH3 from line scans of a single optical section is indicated (below). (C) The colocalization of $Le\alpha$ -kleisin and LeCENH3 at the centromeres of a single metaphase II daughter cell.

In *L. elegans* sister chromatid cohesion becomes already resolved during metaphase I (Figure 13A). (Heckmann et al. 2014a). However, the dynamics and function of cohesin during meiosis is not yet known. Therefore, we investigated the distribution of $\text{Le}\alpha$ -kleisin by immunostaining, and found it presents only in the centromere regions of metaphase I and II chromosomes (Figure 13B, 13C). Super-resolution microscopy of metaphase I and II chromosomes labelled with anti- $\text{Le}\alpha$ -kleisin and anti-LeCENH3 revealed a close proximity of both proteins.

In addition, antibodies against rice shugoshin-specific (OsSGO1) were used as markers for cohesion. OsSGO1 stabilizes the synaptonemal complex and protects centromeric cohesion during the meiosis of rice (Wang et al., 2011). However, in *L. elegans* we found that SGO1 was exclusively located in the holocentromeres of metaphase II chromosomes (Figure 14).

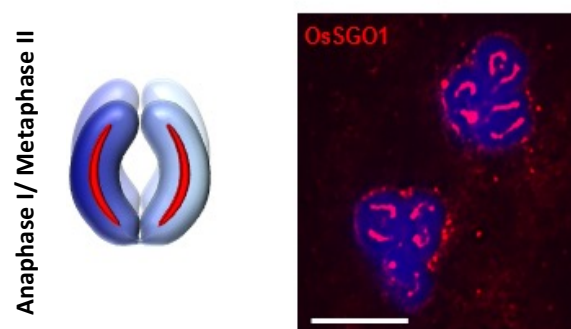


Figure 14. The distribution of anti-OsSGO1 at meiotic metaphase II chromosomes in *L. elegans*.

The distribution of anti-OsSGO1 signals (in red) in meiotic metaphase II chromosomes of *L. elegans*. Bar = 10 μm .

$\text{Le}\alpha$ -kleisin was also located at the holocentromeres of somatic *L. elegans* metaphase chromosomes, but not in regions where sister chromatids attach (Figure 15A). In monocentric metaphase chromosomes of *H. vulgare* (Figure 15B), $\text{Le}\alpha$ -kleisin signals appeared not only at the CENH3-positive regions, but also in between the sister chromatids.

In summary, the results suggest that the α -kleisins of *L. elegans* may not only realize sister chromatid cohesion, instead they colocalize with the position of the centromere. Additional experiments are required to prove the involvement of α -kleisins in the assembly of the centromeres in this species.

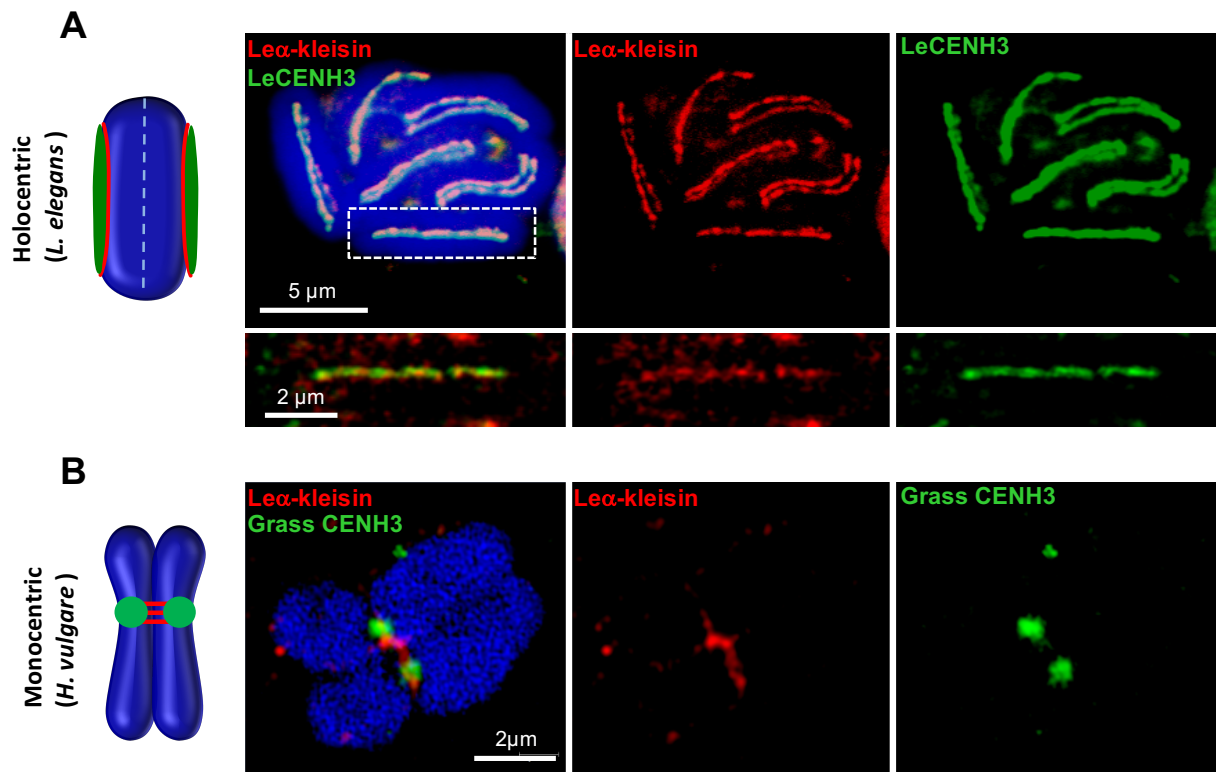


Figure 15. Distribution of Le α -kleisin and CENH3 at mitotic metaphase chromosomes of *L. elegans* (A) and *H. vulgare* (B).

(A) The holocentric species *L. elegans* shows clearly a colocalization of Le α -kleisin and LeCENH3 after immunostaining with specific antibodies. The below panels show regions of interest (rectangle) further magnified after applying SIM. (B) A monocentric *H. vulgare* chromosome acquired by SIM shows the Le α -kleisin in between of both sister centromeres, which are marked by two distinct CENH3 signals.

The schemata on the left side compare the centromere arrangement and localization of Le α -kleisin (red) and CENH3 (green) in *L. elegans* (A) and *H. vulgare* (B) chromosomes.

1.5 Discussion

1.5.1 The CENH3 of *L. elegans*

Whereas in the closely related species *L. nivea* two *CENH3* isoforms are present (Nagaki et al. 2005; Moraes et al. 2011), only one was found in *L. elegans*. But interestingly, two different *LeCENH3* splicing variants with a tissue-specific expression pattern are evident. Similarly, two pearl millet (Ishii et al. 2015) and human CENH3 (also called CENP-A) (Gerhard et al. 2004) splicing variants were proven. However, no different functions of these variants have been determined until now. By immunostaining we confirm previous findings (Heckmann et al. 2011; Heckmann et al. 2014a) that somatic *L. elegans* chromosomes contain a CENH3-positive longitudinal centromere along each sister chromatid and that holocentricity is maintained, and no fusion of sister centromeres occurs throughout meiosis.

1.5.2 α -kleisins colocalize with the centromere

In *L. elegans* four α -kleisins (*Le* α -kleisin-1-4) were identified. Based on our phylogenetic analysis they correspond to those of other plants like *A. thaliana* (*AtSYN1-4*) and *O. sativa* (*OsRad21-1-4*) as follows: *Le* α -kleisin-4/*AtSYN1/OsRad21-4*, *Le* α -kleisin-2/*AtSYN2/OsRad21-2*, *Le* α -kleisin-3/*AtSYN3/OsRad21-3* and *Le* α -kleisin-1/*AtSYN4/OsRad21-1* (da Costa-Nunes et al. 2006; Dong et al. 2001; Zhang et al. 2004; Zhang et al. 2006; Tao et al. 2007; Gong et al. 2011), in which the *Le* α -kleisin-4/*AtSYN1/OsRad21-4* α -kleisins act during meiosis.

In the holocentric nematode *C. elegans*, also four different α -kleisin proteins (*COH-1*, *COH-2*, *COH-3*, and the meiotic *REC-8* α -kleisin) were identified (Mito et al. 2003). In contrast, yeast contains only two α -kleisins, the mitotic *SCC1* and the meiosis-specific variant *REC8* (Lee and Orr-Weaver 2001). In mammals, three α -kleisins, *RAD21*, *REC8* and *RAD21L* were reported (Ishiguro et al. 2011; Nasmyth 2011). In *A. thaliana*, it was proven that the four α -kleisin proteins have different functions (reviewed in (Schubert 2009). *SYN1* mediates cohesion during meiosis (Bhatt et al. 1999; Cai et al. 2003) and in differentiated interphase nuclei (Schubert et al., 2009). *SYN2* and *SYN3*, mainly expressed in meristematic tissues, seem to be mitotic α -kleisins (Dong et al. 2001). *SYN3* is enriched in the nucleolus, therefore, its additional involvement in controlling rDNA structure and transcription and its involvement in

rRNA processing has been suggested (Jiang et al. 2007). SYN3 and SYN4 also support sister chromatid cohesion in differentiated interphase nuclei (Schubert et al., 2009). In agreement with the findings in vertebrates (Waizenegger et al. 2000) here we show that α -kleisins may mediate sister chromatid cohesion during mitosis in monocentric species as *H. vulgare*, since we observed that α -kleisin remained between the sister centromeres during metaphase. Previous studies (Suzuki et al. 2013) did not prove plant cohesins at somatic metaphase chromosomes, which may be caused by an insufficient sensitivity of the antibodies used, the image acquisition applied, or by the preparation methods employed.

We found that α -kleisin is present along each metaphase sister centromere in *L. elegans*. This is in agreement with the distribution of RAD21L in mice, where two separate signals appear at the primary constrictions during metaphase II (Herran et al. 2011). Therefore, we support the assumption of Herran et al. (2011) that the enrichment of α -kleisin at centromeres may contribute to the assembly of the inner centromere and that it may play role in promoting the bi-orientation of kinetochores (Sakuno et al. 2009).

In *L. elegans* between metaphase I and II the chromosomal termini of the homologous non-sister chromatids are connected to each other by chromatin threads. This allows to proceed an inverted sequence of meiotic sister chromatid segregation, and it was assumed that cohesins are involved in this end-to-end association (Heckmann et al. 2014b). However, here we show that α -kleisin-containing cohesin complexes obviously are not involved in maintaining these connections.

1.5.3 The meiotic prophase I is conventional in *L. elegans*

Here we report that $Le\alpha$ -kleisins localize exclusively from leptotene to pachytene along the axial and lateral elements of the synaptonemal complex. This is consistent with the finding that REC8 and HIM3, components of the chromosomes axes are required for meiotic synapsis in holocentric nematodes during leptotene, zygotene and pachytene (Zetka et al. 1999). This suggests that REC8 is a component of axial/lateral elements (Pasierbek et al. 2001). In plants, a specific and intermittent localization of SMC3 in the axial/lateral elements has been observed in tomato by electron microscopy in microsporocytes during zygotene, similar to that observed by light microscopy after the immunolabeling of SMC1, SMC3, SCC3 and REC8,

Table 4. Temporal appearance of meiotic α -kleisin subunits during the meiosis in different species.

Species		Meiotic α -kleisin	Presence during meiosis	Reference
Common name	Scientific name			
Wood rush	<i>Luzula elegans</i> Lowe	Le α -kleisin	Leptotene to anaphase II	This study
Thale cress	<i>Arabidopsis thaliana</i> (L.) Heynh.	SYN1	Leptotene to metaphase I	Cai et al. 2003
Tomato	<i>Solanum lycopersicum</i> (L.) H. Karst	REC8	Leptotene to diplotene	Qiao et al. 2011
Rice	<i>Oryza sativa</i> L.	REC8	Leptotene to diplotene	Shao et al. 2011
Nematode	<i>Caenorhabditis elegans</i> (Maupas, 1900)	REC8	Leptotene to the onset of anaphase I	de Carvalho et al. 2008
Grasshopper	<i>Eyprepocnemis plorans</i> (Charpentier, 1825)	REC8	Zygotene to metaphase I	Valdeolmillos et al. 2007; Calvente et al. 2013)
Mouse	<i>Mus musculus</i> L.	RAD21	Leptotene to the end of anaphase II	Xu et al. 2004
		REC8	Leptotene to metaphase II	Lee et al. 2003
		RAD21L	Leptotene to the end of pachytene	Lee and Hirano 2011
Rat	<i>Rattus norvegicus</i> (Berkenhout, 1769)	REC8	Leptotene to anaphase II	Eijpe et al. 2003
Human	<i>Homo sapiens</i> L.	RAD21L	Leptotene to anaphase II	Herrán et al. 2011
		REC8	Leptotene to metaphase II	Garcia-Cruz et al. 2010

although not all subunits presented the same pattern of accumulation and appearance during prophase I (Qiao et al. 2011). Also, a correlation between the progression of axial or lateral element formation and synapsis, and the localization of several cohesin subunits was observed in many different monocentric species (Calvente and Barbero 2012). Although till now, no functional analysis regarding the participation of cohesin during synaptonemal complex formation and synapsis is available in *L. elegans*, the sequential α -kleisin loading indicates a role in the correct progression of synapsis.

We report here that the synaptonemal complex of *L. elegans* is similar in structure and function as in other species (Goldstein 1987; Sym et al. 1993; Page and Hawley 2003). The measurement of the width of the central region of the synaptonemal complex is a ~ 111 nm in *L. elegans*. This is consistent with the data reported for other plants (Westergaard and von Wettstein, 1972) and of *C. elegans* (Smolikov et al. 2008). Because the $Le\alpha$ -kleisins show a similar dynamic pattern during prophase I as monocentric species (Table 4), we conclude that their function during the synaptonemal complex formation is also conserved in holocentrics.

1.6 Summary

Holocentric chromosomes occur in a number of independent eukaryotic lineages and they form holokinetic kinetochores along the entire poleward chromatid surfaces. Due to this alternative chromosome structure, the sister chromatids of *L. elegans* segregate already in anaphase I followed by the segregation of the homologues in anaphase II. However, not yet known is the localization and dynamics of cohesin and the structure of the synamptosomal complex during meiosis. We show here that the α -kleisin subunit of cohesin localizes at the centromeres of both mitotic and meiotic metaphase chromosomes, and that it thus may contribute to assemble the CENH3-containing inner centromere in *L. elegans*. This localization and the formation of a tripartite synamptosomal complex structure indicate that the prophase I behaviour of *L. elegans* is similar as in monocentric species.

1.7 Outlook

1. The localization of Le α -kleisin and the formation of a tripartite synaptonemal complex structure in prophase I indicate cohesin and SC complex of *L. elegans* are similar as reported in monocentric species. However, unclear is the conservation of meiotic recombination events in prophase I. Therefore, the antibodies specific for recombination (Spo11, Rad51 and DMC1) should be generated and used for localization study.
2. To uncover the nature of end-to-end connection of non-sister chromatids, the distribution and timing of proteins involved in crossover I (SHOC1, MLH1 and MLH3) and II (MUS81) should be determined.
3. In this thesis, we identified four incomplete Le α -kleisin proteins. Further experiments should be done to complete the whole length. The antibodies specific for each protein should be generated to predict the function of all these Le α -kleisin proteins.
4. Since we observed the different localization of Le α -kleisin compared to the monocentric plants. To verify whether the cohesin complex is conserved, immunoprecipitation using different Le α -kleisin antibodies could be performed.

2. Rye B chromosomes encode a functional Argonaute-like protein with *in vitro* slicer activities similar to its A chromosome paralog

2.1 Introduction

2.1.1 B chromosomes

In addition to the standard set of A chromosomes (As), in many eukaryotes, so called supernumerary B chromosomes (Bs) have been found causing a numerical chromosome variation. Bs occur in a wide range of taxa from fungi to plants and animals including mammals; however, the maximum number of these chromosomes are tolerated by individuals varies among different species. Despite the diversity of B chromosomes, Bs share some common features, i.e. they are dispensable and not essential for the growth and development of organisms; Bs do not pair or recombine with standard As at meiosis and do not follow Mendelian inheritance (Jones and Rees 1982). Generally, it is assumed that Bs derived from standard and/or sex chromosomes, either from the same or from a related species. The available experimental data support both scenarios suggesting that the way of how Bs form differs between different species and B chromosome types (Jones and Houben 2003).

While unbalanced numbers of As, like in the case of aneuploidy, often cause severely distorted phenotypes (Siegel and Amon 2012). In many species, the presence of Bs is associated with mild or non-obvious phenotypes if the copy number is low. This feature led to the conclusion that Bs are depleted of functional genes. Conversely, excessive numbers of Bs can cause phenotypic effects and may reduce the fertility and fitness of the host. The contributions of single Bs to these phenotypes are usually cumulative, with the severity of effects increasing with the number of Bs (reviewed in (Jones and Rees 1982; Jones 1995; Bougourd and Jones 1997; Carlson 2009)). It has been reported that in cichlid fishes (Yoshida et al. 2011), Bs are likely to play a role in sex determination, and that in the fungus *Nectria haematococca* Bs may account for antibiotic resistance and pathogenicity (Coleman et al. 2009).

2.1.2 The origin of B chromosomes

Regardless of the conceivable intra- or interspecies origin of B chromosomes, A or sex chromosome derived sequences including genic sequences are potential components of any B.

The Bs could derive from fusions or amplification of the pericentromeric region of a fragmented A chromosome(s). Evidence in favour of this hypothesis was obtained recently in rye. A multi-step model on the origin of the rye B chromosomes was proposed (Figure 16) (Martis et al. 2012). Initially, segmental or whole-genome duplication was the origin of a proto-B chromosome, followed by reductive chromosome translocations, unbalance segregation of a small translocation chromosome, and subsequent sequence insertions and gain of a drive mechanism.

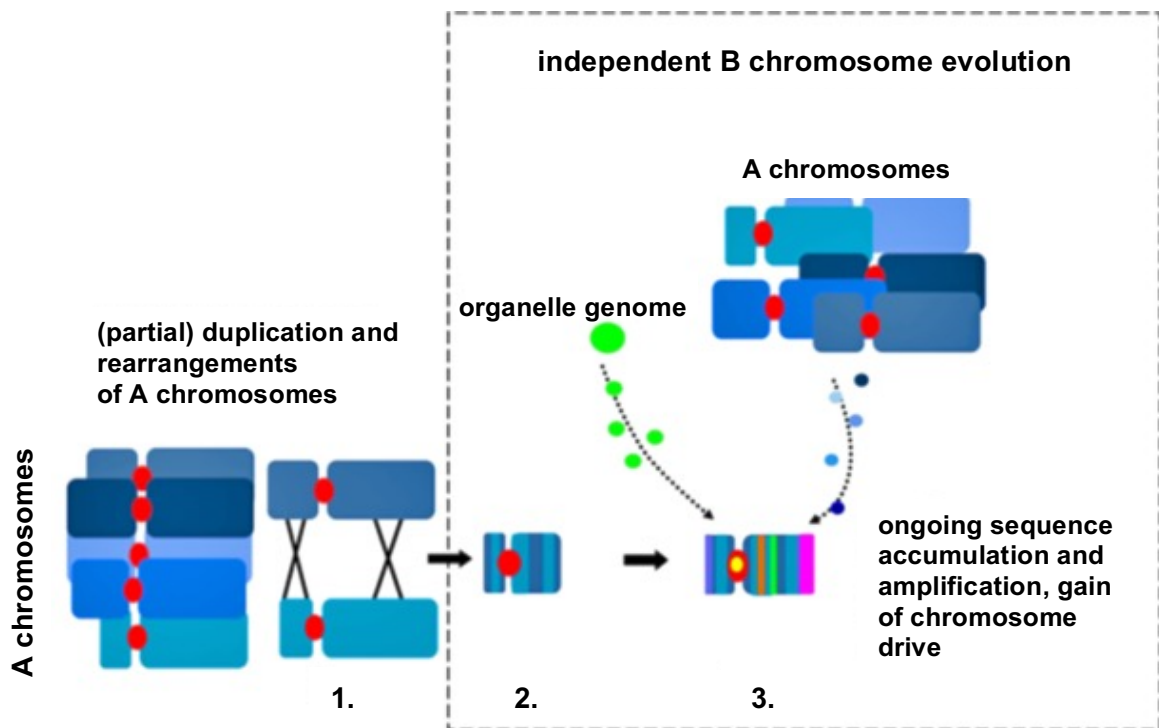


Figure 16. Model of the evolution of the B chromosome of rye (figure from Martis et al. (2012)).

(1) Translocation chromosome derived from duplicated A chromosome fragments results in (2) a decay of meiotic A–B pairing and the formation of a proto-B. (3) The accumulation of organellar and A chromosome-derived DNA fragments, amplification of B-specific repeats, erosion and inactivation of A-derived genes (Muller’s ratchet) and the gain of chromosome drive forms a B chromosome.

Sex chromosomes have previously been proposed as ancestors of B chromosomes (Hewitt 1974). For instance, analysis of B-located sequences suggest that the *Drosophila albomicans* Bs may have originated as a by-product from fused centromeric/telomeric fragments of the ancient third autosome and the ancestral sex chromosome (Zhou et al. 2012). Another example of a sex-chromosomes-derived B chromosome is the B2 chromosome of the grasshopper *Eyprepocnemis plorans*. A B-located 180 bp tandem repeat and ribosomal DNA sequences showed similarity to that of the X chromosome (López-León et al. 1994). The B chromosome of the New

Zealand frog *Leiopelma hochstetteri* also likely derived from a univalent (heteromorphic) W sex chromosome. This conclusion is based on DNA sequence comparisons (Sharbel et al. 1998) and the morphological similarities with the univalent W chromosome (Green et al. 1993).

2.1.3 B chromosome composition in general

B chromosomes have been regarded as totally heterochromatic and genetically inert for a long time. Early cytogenetic studies concerning the sequence composition of B chromosomes used available repetitive probes to find specific sequences localized on Bs. More recently, with the help of *de novo* sequencing approaches, there is a growing body of evidence that B chromosomes could also harbor pseudogenes and protein-coding genes.

One type of tandemly repeated DNA which has been frequently described for B chromosomes is ribosomal DNA (rDNA). 35S rDNA are organized as clustered tandem units and are typically visualized as secondary constriction (nucleolar organizer region or NOR) on metaphase chromosomes (e. g. through silver staining or FISH). Both inactive and active ribosomal RNA (rRNA) genes were found in B chromosomes in different species. For instance, inactive rRNA genes were reported on the B chromosomes of the daisy *Brachycome dichromosomatica* (Donald et al. 1997), the Chinese raccoon dog *Nyctereutes procyonoides* (Szczerbal and Switonski 2003) and the African cichlid fish *Haplochromis obliquoides* (Poletto et al. 2010). While active B-derived rRNA was found in the plant *Crepis capillarins* (Leach et al. 2005) and the grasshopper *Eyprepocnemis plorans* (Ruiz-Estévez et al. 2012; Ruiz-Estévez et al. 2014).

Detailed analysis of rye B-located high copy sequences revealed that Bs contain a similar proportion of repeats as A chromosomes, but differ substantially in their repeat composition (Klemme et al. 2013). The most abundant mobile elements (*Gypsy*, *Copia*) in the genome of rye are similarly distributed along As and Bs, while the ancient retroelement *Sabrina* (Shirasu et al. 2000), is less abundant on Bs than on As. In contrast, the active element *Revolver* (Tomita et al. 2008) and the predicted *Copia* retrotransposon Sc36c82, are disproportionately abundant on the B. A B-specific accumulation of *Gypsy* retrotransposons or other repeated sequences have also been reported in the fish *Alburnus alburnus* (Ziegler et al. 2003) and the fungus *Nectria haematococca* (Coleman et al. 2009).

The first autosomal gene – *C-KIT* (v-kit Hardy-Zuckerman 4 geline sarcoma viral oncogene homolog) was identified on red fox B. chromosomes, later the same gene was also observed for the Bs of Chinese and Japanese raccoon dogs (Graphodatsky et al. 2005). More recently, sequencing of flow-sorted (Martis et al. 2012) or microdissected Bs (Valente et al. 2014; Silva et al. 2014) has allowed the identification of thousands of B-located genic sequences. Gene-carrying genomic segments on B chromosomes from different vertebrate groups were reviewed in (Makunin et al. 2014). Even Bs can carry active protein coding sequences. Transcriptional activity was shown for a B-specific protein-coding sequence in different species as discussed in (Makunin et al. 2014). However, *no bona fide* B-derived protein has been demonstrated to date.

2.1.4 The DNA composition of the rye B chromosome

Employing next-generation sequencing, the DNA composition of flow-sorted rye Bs and As was determined (Martis et al. 2012) (Figure 17). Approximately 90% of the rye genome is repetitive, and 70% is represented by <60 families of high-copy repeats (Martis et al., 2012). As and Bs revealed similar contents of dispersed repeats but differences regarding sequence and abundance of tandem repeats (Klemme et al. 2013). Comparison of rye B genic sequences with different reference datasets allowed the identification of at least 4,946 putative B-located genic sequences (Martis et al. 2012).

Because Bs are dispensable, it is expected that they are prone to accumulate mutations and consequently their possible genic sequences undergo pseudogenization (Green 1990; Banaei-Moghaddam et al. 2013; Makunin et al. 2014). In rye, at least 11 subregions out of 15 B-located pseudogene-like fragments are active. Some of them had the ability to modulate the expression of their counterparts on As in a tissue and genotype dependent manner (Banaei-Moghaddam et al. 2013). However, a detail comparative analysis of A- and B-located genes regarding their completeness and functionality still is missing.

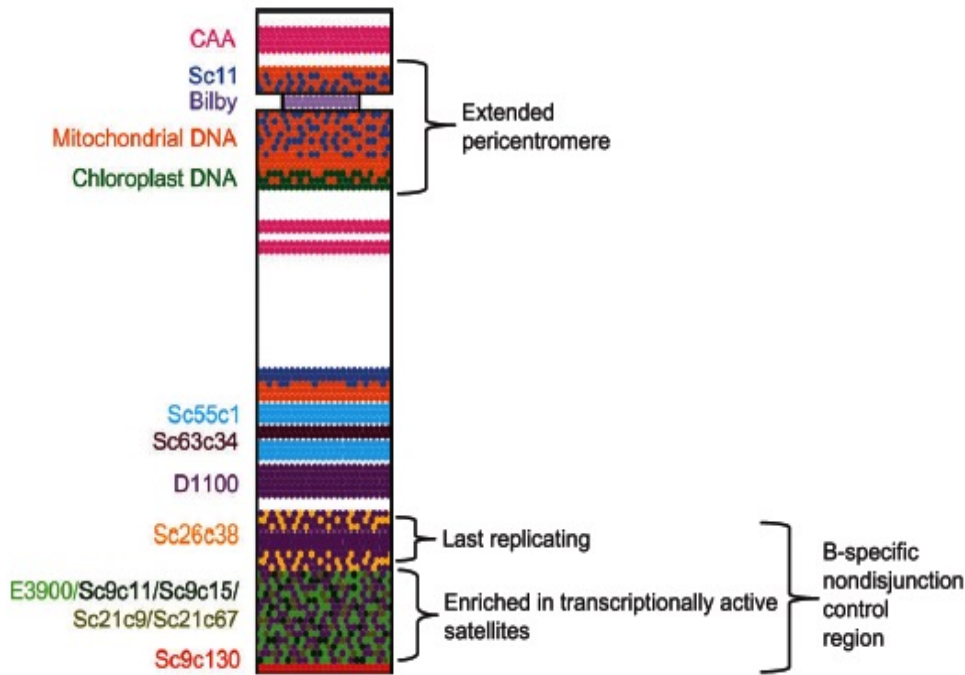


Figure 17. Model for the distribution of 15 B chromosome (B) marker sequences in rye (*S. cereale*) (figure from Klemme et al. (2013)).

Each sequence is represented by a different color. Pericentromere, late replicating, transcriptionally active, and nondisjunction control regions are indicated. The subterminal region of the long arm encompassing the nondisjunction control region is composed of mainly B-specific sequences.

2.1.5 Introduction of candidate genes

Three putative chromatin and epigenetically related rye B-derived genic sequences were selected from the transcript data of developing anthers (<http://webblast.ipk-gatersleben.de/rye/>), for further analysis in this thesis. Phylogenetic analysis revealed high similarity to the kinesin family member 4 gene (*KIF4A*), shortage in chiasmata gene (*SHOC1*) and the argonaute family member 4 gene (*AGO4B*)

The kinesins are a family of microtubule-based motor proteins that generate directional movement along microtubules and are involved in many crucial cellular processes including cell division (Vale 2003). KIF4 kinesins are key players in the processes, including chromatid motility, chromosome condensation (Zhu and Jiang 2005) as well as intracellular transport (Sekine et al. 1994).

SHOC1, is one of the ZMM proteins (including Zip1, Zip2, Zip3 and Zip4, Mer3 and MSH4-MSH5), which is involved in the class I meiotic crossovers. It has been identified in a large range of eukaryotes, including *S. cerevisiae* (Chua and Roeder 1998) and *A. thaliana* (Macaisne et al. 2008). In *Arabidopsis*, *SHOC1* has been

proposed to be required for promoting or stabilizing single strand invasion and formation of class I cross-overs during meiotic recombination processes (Macaisne et al. 2008).

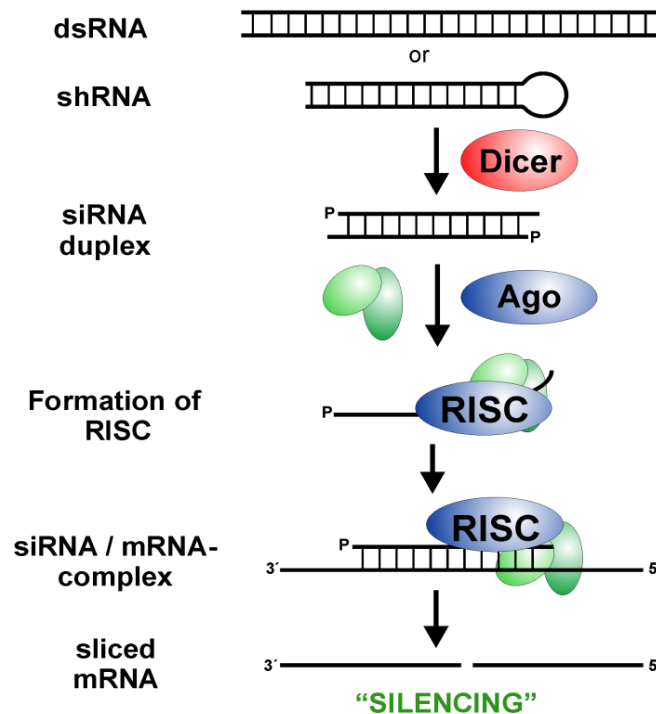


Figure 18. Mechanism of siRNA silencing (figure from <http://www.uni-konstanz.de/FuF/chemie/jhartig/>).

Dicer is an RNase III nuclease that cleaves double-stranded RNA (dsRNA) and pre-micro RNA (miRNA) into short double-stranded RNA fragments called small interfering RNA (siRNA) of about 20-25 nucleotides long, usually with a two-base overhang on the 3' ends. Dicer catalyzes the first step in the RNA interference pathway and initiates formation of the RNA-induced silencing complex (RISC), whose catalytic component argonaute is an endonuclease capable of degrading messenger RNA (mRNA) whose sequence is complementary to that of the siRNA guide strand.

AGO4 is involved in the regulation of gene expression; as a general property this protein has a 'slicer activity', i.e., is capable to catalyze sRNA-directed endonucleolytic degradation of target RNA transcripts (Zilberman et al. 2003; Qi et al. 2006) (Figure18). As its functional presence was found to be important in defense measures of the plant cell during bacterial and viral infections, AGO4 was proposed to also act as a linker of the transcriptional and post-transcriptional silencing pathways (Agorio and Vera 2007; Hamera et al. 2012; Ye et al. 2009).

2.2 Open questions and aims of the PhD work

B chromosomes of rye are unexpectedly rich in sequences with high similarity to A chromosome encoded genes (Martis et al. 2012). It was shown that some of these B-located genic sequences undergo pseudogenisation and even contribute to the transcriptome of the host genome in a tissue-type and genotype-specific manner (Banaei-Moghaddam et al. 2013). However, a detail comparative analysis of B-located genes regarding their completeness and functionality is still missing. Therefore, this work was intended to answer the question whether the B chromosome of rye carries functionally active protein-coding genes.

2.3 Materials and methods

2.3.1 Plant material and cultivation

Seeds of a rye (*Secale cereale* L.) self-fertile inbred line 7415 with and without Bs (Jimenez et al. 1994), hexaploid wheat (*Triticum aestivum* L.) “Lindström” with and without added standard rye Bs (Lindström 1965) and rye JBK lines with truncated Bs (structural variants that lack the terminal part of the long arm) (Ribeiro et al. 2004) were germinated on wet filter papers. After germination, root tips were collected to investigate the type and number of Bs in each plant individual and the seedlings were transferred to soil and cultivated for 4 weeks under short-day conditions (8 h light/16 h dark, 20°C/18°C), Then, vernalization (10 h light/14 h dark, 4°C) followed for at least 4 weeks. Finally, the plants were grown under long-day conditions (16 h light, 22°C day/16°C night), and all experimental materials from different tissues were collected during this period.

2.3.2 Probe preparation, indirect immunostaining and fluorescence in situ hybridization

Cloned *ScKIF4A*, *ScAGO4B*-specific fragments derived from rye 0B DNA and the cloned *ScSHOC1*-specific fragment derived from rye 0B anther cDNA were used as gene-specific probes (Table 5). D1100 (Sandery et al. 1990), Sc55c1 (Martis et al. 2012) and Revolver (Carchilan et al. 2009) were used as B-specific probes. All probes were labeled by nick translation with ChromaTide Texas Red-12-dUTP or Alexa Fluor 488-5-dUTP (Molecular Probes; <http://www.invitrogen.com>). The following primary and secondary antibodies were used: anti-RNA polymerase II CTD phospho (Ser2) (RNAPIISer2ph) (active) with rat monoclonal antibody (1: 200; Millipore, 04-1571) and goat anti-rat Alexa488 (1: 200; Jackson ImmunoResearch). The non-phosphorylated (inactive) enzyme was detected with mouse monoclonal antibody (1: 300; Abcam, ab817) and goat antimouse-Cy5 (1: 300; Jackson ImmunoResearch).

Fluorescence in situ hybridization and indirect immunostaining were performed as described (Ma et al. 2010; Houben et al. 2007). After dehydration in an ethanol series, the nuclei were counterstained by 4,6 - diamidino-2-phenylindole (DAPI) in Vectashield (Vector Laboratories, <http://www.vectorlabs.com>).

Table 5. List of primer sequences for PCR, RT-PCR, FISH probe preparations and *in vitro* transcription

A. List of primer sequences for (RT-) PCR and FISH probe preparations for ScKIF4A, ScSHOC1 and ScAGO4B genes

Primer Name	Primer seq (5'-3')	Tm (°C)	FISH probe length (bp)
K1F	TTGAGCAATGTGTGTATCCA	53.2	
K1R	AGTTGACTTCTCAGATGCAG	55.3	
K1F	TTGAGCAATGTGTGTATCCA	53.2	3280 bp
K2R	TCATCCCACGATTTTCCATT	53.2	
K2F	TGTCTTGTGAACAGTTAGCA	53.2	2494 bp
K3R	TCGAGCAAATCTTTCAGTCT	53.2	
K3F	GATGCTCACCAACAGTTGCT	57.3	2442 bp
K4R	CGCCGCCGTGTATTATTGAT	57.3	
K4F	AAGAAAAGGTGGTTGCGCTT	55.3	1603 bp
K5R	CGGATGCCACAGAAAACACA	57.3	
K5F	GCTGAAGTAACACGGCAGAA	57.3	
K6R	TCTTGAGCTGAGAGACCTGC	59.4	
K6F	AGGAGGCGGAGATGAAACAA	57.3	
S1F	CCATATCCTCCGCGCTATCC	61.4	
S1R	ATCGTCAACCAGCACCAACT	57.3	
S2F	AGGAGGATCTTTTGTCCGCA	57.3	
S2R	CTCCCAGCACCCAAGTTGTA	59.4	
S3F	TACAACCTGGGTGCTGGGAG	59.4	
S3R	TTACAGCAGAAAGGGAGCGA	57.3	
S4F	CTGAACAGCGGCACATAGAG	59.4	
S4R	CTTCCCCTGTGCTGCAAATA	57.3	
S5F	GACTACTTCTCTCCGGCGTC	61.4	5022 bp
S4R	CTTCCCCTGTGCTGCAAATA	57.3	
A1F	GGTGCCCATCATAGCAGAAG	59.4	2685 bp
A1R	AGAGCCTTTGTGTATCTTTGCAG	58.9	
A2F	AGTCCTGGAGGTAACAACGGT	59.8	2786 bp
A2R	GGGACTCTCTTCGATTACAGTATGAG	59.7	
A3F	TCGAGAAGTCAAGGCAGAAG	57.3	2587 bp
A3R	TAAACAGGGAAGCCATCATC	55.3	
A4F	TGGACTCAACACACTGCTTC	57.3	2704 bp
A4R	GAACATGGAGCTCCTCACTTTCTC	62.7	
A5F	GCTCTAGAGCCATGGACCCGCATGATGGGGAG	70.2	
A5R	TCCCCCGGGGAATCAGCAGAAGAACATAGAGCTC	68.3	

A6F	GCCTCTTACTATCGGGGCT	54.0	
A6R	GTCTCCTCACCTCTTCTGG	56.0	

B. List of primer sequences for *GAPDH*, *M13* and *Bilby*

Primer Name	Primer seq (5'-3')	Tm (°C)	Note
GAPDH-F	CAATGATAGCTGCACCACCAACTG		(Banaei-Moghaddam et al. 2013)
GAPDH-R	CTAGCTGCCCTTCCACCTCTCCA		
M13-F	TTGTAAAACGACGGCCAGTG	57.3	(Francki 2001)
M13-R	GGAAACAGCTATGACCATG	54.5	
Bilby-F	TTTGCGACAATGACTCAAGC		
Bilby-R	TGTAGCTCATCGTGGAGTCG		

C. List of primer sequences for *in vitro* transcription

Primer Name	Primer seq (5'-3')	Note
GFP-F	CGtaatacgaactcactatagAGAATCGAGTTAAAAGGTATTG	lowercase letters: the promoter for T7 RNA polymerase
GFP-R	ATTTgcgccgcAGAATCGAGTTAAAAGGTATTG	lowercase letters: <i>NotI</i> site

Images were collected in gray scale using an Olympus BX61 microscope (Olympus; <http://www.olympus.com>) and an ORCA-ER CCD camera (Hamamatsu; <http://www.hamamatsu.com>), then pseudocoloured and merged using Adobe Photoshop CS5 (Adobe). To achieve a lateral optical resolution of ~120 nm (super-resolution, obtained with a 488 nm laser), we applied structured illumination microscopy (SIM) using a C-Apo 63×/1.2W Korr objective of an Elyra PS.1 microscope system and the software ZEN (Carl Zeiss GmbH). Images were captured separately for each fluorochrome using the 561 nm, 488 nm and 405 nm laser lines for excitation and appropriate emission filters. SIM image stacks were used to produce 3D movies by the Imaris 8.0 (Bitplane) software.

2.3.3 Genomic DNA and RNA extraction, PCR and RT-PCR

gDNA was extracted from leaves by a DNAeasy plant mini kit (Qiagen). Total RNA was isolated from anthers by the TRIzol method (Life Technologies). RNA samples were treated with DNA-free DNase (Ambion TURBO DNase; Invitrogen) before cDNA synthesis. Absence of DNA was confirmed by PCR with *Bilby*-specific primers (Table

5). All cDNAs (20 μ l) were generated from 1 μ g DNase I - treated RNA, using the Reverse Aid H Minus First Strand cDNA Synthesis Kit (Fermentas).

25 μ l PCR or RT-PCR reaction mixtures contained: 100 ng genomic DNA or 1 μ l cDNA, 10 μ M of each forward and reverse primers (Table 5), 5 mM of each deoxynucleotide triphosphates, 2.5 μ l 10xPCR reaction buffer and 1 unit of *Taq* polymerase (Qiagen). The cycling protocol was: 94°C for 3 min, 35 cycles at (94°C for 40s, annealing temperature (Table 5) for 40 s, 1 min/kb elongation at 72°C), 72°C final elongation for 10 min. 25 cycles PCR were run with *GAPDH*-specific primers to quantify the abundance of transcripts.

qRT-PCR was performed using the SYBR Green Master (Applied Biosystems) on the 7900HT Fast Real-Time PCR System (Applied Biosystems). 10 μ l of PCR mixture contained 1 μ l of cDNA template, 5 μ l of 2 \times Power SYBR Green PCR Master Mix (Applied Biosystems), and 0.33 mM of the forward and reverse primers (Table 6) for each gene. The amplification conditions were one cycle of 10 min at 95°C, 40 cycles of two consecutive steps of 15 s at 95°C, and 60s at 60°C as a standard dissociation protocol. *GAPDH*-specific primers (Table 5) were used as endogenous control.

Table 6. List of primer sequences for quantitative RT-PCR

Primer Name	Primer seq (5'-3')
ScKIF4A-F	TCTGCCGTGTTACTTCAGCC
ScKIF4A-R	ACGCAATGGAAAATCGTGGG
ScSHOC1-F	CGAGGGATGGAGCCTCTAAG
ScSHOC1-R	AGTTCCTCCTCTGGCTTTCC
ScAGO4B-F	GTGACCAGAAGAGGGTGAGG
ScAGO4B-R	CGGAGTGCTGCCTGAGTATG

2.3.4 Sequence analysis

PCR products were purified using an Invisorb Spin DNA Extraction Kit (STRATEC Molecular, Berlin, Germany) and subsequently cloned with help of the StrataClone PCR cloning kit (Stratagene). Recombinant colonies were identified by colony PCR using a M13 primer pair (Table 5). DNA fragments were sequenced by the sequencing facility of the IPK (Gatersleben, Germany). Sequences were analyzed by Sequencher 5.2.4 (Gene Codes Corporation Inc), assembled using Seqman pro 12.0.0 (DNASTAR, Inc) and processed by EditSeq and MegAlign Lasergene 8 (DNASTAR, Inc).

Table 7. List of sequence identifiers and description of KIFs, SHOC1 and AGOs sequences used for phylogenetic tree construction

A. Accession numbers of kinesins from different species

Gene	Genbank Accession No.	Description
Kinesins	EMS55271.1	KIF4A [<i>Triticum urartu</i>]
	XP_010236916.1	KIF4 isoform X1 [<i>Brachypodium distachyon</i>]
	XP_006647875.1	KIF4A-like [<i>Oryza brachyantha</i>]
	NP_199593.2	FRA1 [<i>Arabidopsis thaliana</i>]
	XP_009108069.1	KIF4B isoform X1 [<i>Brassica rapa</i>]
	XP_012068018.1	KIF4B [<i>Jatropha curcas</i>]
	NP_567768.1	kinesin 2 [<i>Arabidopsis thaliana</i>]
	XP_009143182.1	kinesin-2 [<i>Brassica rapa</i>]
	NP_568811.1	kinesin 3 [<i>Arabidopsis thaliana</i>]
	XP_009119997.1	kinesin-3 [<i>Brassica rapa</i>]
	XP_002265300.1	kinesin-1-like [<i>Vitis vinifera</i>]
	XP_006360099.1	kinesin-1-like [<i>Solanum tuberosum</i>]
	NP_192428.2	kinesin 5 [<i>Arabidopsis thaliana</i>]
	XP_009114495.1	kinesin-5 [<i>Brassica rapa</i>]
	NP_188285.1	kinesin 13A [<i>Arabidopsis thaliana</i>]
	XP_010551072.1	kinesin-13A [<i>Tarenaya hassleriana</i>]
	XP_008656143.1	kinesin-13A-like [<i>Zea mays</i>]
	XP_006615478.1	kinesin-like protein KIF18A-like [<i>Apis dorsata</i>]
	XP_003396433.2	kinesin-like protein KIF18A [<i>Bombus terrestris</i>]
	XP_003693634.1	kinesin-like protein KIF18A [<i>Apis florea</i>]
	XP_008210888.1	kinesin-like protein KIF18A isoform X2 [<i>Nasonia vitripennis</i>]
	KIZ05185.1	kinesin-like protein KIF6 [<i>Monoraphidium neglectum</i>]
XP_002899294.1	kinesin-like protein KIF6 [<i>Phytophthora infestans</i> T30-4]	
CCA23637.1	kinesin-like protein KIF6 putative [<i>Albugo laibachii</i> Nc14]	

B. Accession numbers of SHOC1 from different species

SHOC1	gb EEE57462.1	[<i>Oryza sativa Japonica</i> Group]
	XP_010236836.1	[<i>Brachypodium distachyon</i>]
	EEC73682.1	[<i>Oryza sativa Indica</i> Group]
	XP_008645986.1	[<i>Zea mays</i>]
	ACI22656.1	[<i>Arabidopsis thaliana</i>]
	XP_007038687.1	[<i>Theobroma cacao</i>]

C. Accession numbers of AGOs from different species

AGOs	NP_565633.1	argonaute 4 [<i>Arabidopsis thaliana</i>]
	AGO99012.1	argonaute 4, partial [<i>Triticum aestivum</i>]
	EMT11809.1	argonaute 4B [<i>Aegilops tauschii</i>]
	XP_004960963.1	argonaute 4B [<i>Setaria italica</i>]
	XP_006652094.1	argonaute 4B-like [<i>Oryza brachyantha</i>]
	EMS68540.1	argonaute 4A [<i>Triticum urartu</i>]
	XP_010230772.1	argonaute 4A [<i>Brachypodium distachyon</i>]
	XP_004967701.1	argonaute 4A-like [<i>Setaria italica</i>]
	XP_006644052.1	argonaute 4A-like [<i>Oryza brachyantha</i>]
	EMT20780.1	argonaute 4A [<i>Aegilops tauschii</i>]
	EMS52406.1	argonaute 4B [<i>Triticum urartu</i>]
	NP_849784.1	argonaute 1 [<i>Arabidopsis thaliana</i>]
	XP_009107358.1	argonaute 1 [<i>Brassica rapa</i>]
	XP_010549027.1	argonaute 1 [<i>Tarenaya hassleriana</i>]
	NP_174414.1	argonaute 3 [<i>Arabidopsis thaliana</i>]
	AGS47790.1	argonaute 3 [<i>Salvia miltiorrhiza</i>]
	NP_001274720.1	argonaute 3 [<i>Solanum lycopersicum</i>]
	NP_850110.1	argonaute 5 [<i>Arabidopsis thaliana</i>]
	XP_010473185.1	argonaute 5-like [<i>Camelina sativa</i>]
	XP_009103628.1	argonaute 5 [<i>Brassica rapa</i>]
	XP_011037293.1	argonaute 5-like [<i>Populus euphratica</i>]
	XP_010651834.1	argonaute 5 [<i>Vitis vinifera</i>]
	XP_009608773.1	argonaute 5 [<i>Nicotiana tomentosiformis</i>]
	NP_180853.2	argonaute 6 [<i>Arabidopsis thaliana</i>]
	XP_010413926.1	argonaute 6 [<i>Camelina sativa</i>]
	XP_009132895.1	argonaute 6 [<i>Brassica rapa</i>]
	XP_010556972.1	argonaute 6 [<i>Tarenaya hassleriana</i>]
	XP_011007758.1	argonaute 16 [<i>Populus euphratica</i>]
	XP_010657243.1	argonaute 16 [<i>Vitis vinifera</i>]
	XP_008229810.1	argonaute 16 [<i>Prunus mume</i>]
	XP_009769203.1	argonaute 16 [<i>Nicotiana sylvestris</i>]
	NP_177103.1	argonaute 7 (protein ZIPPY) [<i>Arabidopsis thaliana</i>]
	XP_010415589.1	argonaute 7-like [<i>Camelina sativa</i>]
XP_009105000.1	argonaute 7 [<i>Brassica rapa</i>]	
XP_012067710.1	argonaute 7 [<i>Jatropha curcas</i>]	
XP_010551411.1	argonaute 7 [<i>Tarenaya hassleriana</i>]	
XP_009758122.1	argonaute 7 [<i>Nicotiana sylvestris</i>]	

2.3.5 Molecular phylogenetic analyses

Reference IDs for the phylogenetic analysis of kinesins (KIFs), shortage in chiasmata 1 (SHOC1) and argonautes (AGOs) sequences used in this study are available in Table 7. After aligning the sequences with ClustalW, phylogenetic trees were calculated using the boot-strapped neighbor-joining algorithm in MEGA 6.06 (<http://www.megasoftware.net/>) with 1000 trials.

2.3.6 Genotyping of ScKIF4A and ScSHOC1 fragments by CAPS

Primers K7F and K6R (Table 5) were used to amplify A- and B- derived ScKIF4A fragments. Primers S2F and S1R (Table 5) were used to amplify A- and B- derived ScSHOC1 fragments. Then, the PCR products were checked for non-specific amplification on a 1% agarose gel. The *Bam*HI enzyme for ScKIF4A and the *Nsi*I enzyme for ScSHOC1 were used for genotyping. 20 µl of the restriction enzyme digestion reaction included: 10 µl PCR reaction mixture, 2 µl 10×buffer and 10 units of *Bam*HI or *Nsi*I (Thermo Scientific). The reaction was incubated for 5 hours at 37°C. The digestion products were checked after 2% agarose gel electrophoresis.

2.3.7 *In vitro* transcription

To generate plasmids for *in vitro* transcription of A- and B-derived ScAGO4B-like transcripts, the complete open reading frames were amplified by A5F and A5R primers (Table 5) using rye anther 0B and 4B cDNAs, then inserted via *Xba*I/*Sma*I restriction sites into a modified pSP64-poly(A) vector (Promega) that contained an additional *Swa*I restriction site downstream of the poly(A) sequence. Transcription and further treatment of the transcript were performed using standard procedures. Firefly luciferase RNA was generated by SP6 RNA polymerase (Thermo Scientific) from the *Xho*I-linearized plasmid pSP-luc(+) (Promega). The mRNAs encoding the AGO4-like proteins were synthesized in the presence of the monomethylated cap analog m⁷GP₃G (Jena Biosciences, Jena) from *Swa*I-linearized plasmids using SP6 RNA polymerase.

To generate a target for the GFP-specific siRNA, a 432 bp sequence was amplified by PCR from plasmid pGFP-C1 using primers GFP-F and GFP-R (Table 5). Transcription of the GFP target RNA was performed from this PCR fragment by T7 polymerase in the presence of 0.5 µCi/µl [α -³²P]CTP using standard conditions.

2.3.8 siRNAs

The sequences of the 24 nt variant of GFP-specific siRNA were 5'-aaguucauccaugccauguguaau-3' (guide strand) and 5'-uacacauggcauggaugaacuuua-3' (passenger strand). To produce siRNA duplexes, the single-stranded RNA oligonucleotides (Biomers, Ulm) were heated for 1 min at 90°C in annealing buffer (30 mM HEPES-KOH, pH 7.4, 100 mM potassium acetate, 2 mM magnesium acetate) and hybridized for 60 min at 37°C.

2.3.9 Cell culture and preparation of cytoplasmic BY-2 cell extract

Nicotiana tabacum BY-2 cells were cultured as described (Gursinsky et al. 2009) at 23°C in Murashige-Skoog liquid medium. Evacuolated BY-2 protoplasts for the preparation of cytoplasmic extract (BYL) were obtained by percoll gradient centrifugation (Komoda et al. 2004; Gursinsky et al. 2009).

2.3.10 Target cleavage assay

In vitro translation of *AGO4B*-like mRNAs was performed in 50% (v/v) BYL at previously described conditions (Schuck et al. 2013). 1.5 µg of the mRNA were translated in a 20 µl reaction for 60 min at 25°C in the presence of 50 nM siRNA. Then, the same amount of siRNA was added again and the reaction continued for 90 min. Afterwards, 2 µg of firefly luciferase (competitor) mRNA and the ³²P-labeled GFP target RNA (50 fmol) were added and the cleavage reaction was carried out for 15 min at 25°C. Total RNA was isolated from the reaction by treatment with 20 µg Proteinase K in the presence of 0.5% SDS for 30 min at 37°C, followed by extraction with chloroform and ethanol precipitation. ³²P-labeled products were separated on 5% Tris-borate polyacrylamide gels containing 8 M urea and visualized by phosphor-imaging.

2.3.11 Accession Number

Sequence data of *ScKIF4A*, *ScSHOC1* and *ScAGO4B* from this article can be found in the GenBank data libraries. The accession numbers for each sequences are listed in the Table 8.

Table 8. Accession numbers of ScKIF4A, ScSHOC1 and ScAGO4B genes

Sequence content	Gene	Genbank No.	Notes
A – located gDNA	<i>ScKIF4A</i>	KT750012	Complete
	<i>ScSHOC1</i>	KT750013	Complete
	<i>ScAGO4B</i>	KT750014	Complete
B – located gDNA	<i>ScKIF4A</i>	KT946783	Partial (variant 1)
	<i>ScKIF4A</i>	KT946784	Partial (variant 2)
A – derived mRNA	<i>ScKIF4A</i>	KT956052	Complete
	<i>ScSHOC1</i>	KT750017	Complete
	<i>ScAGO4B</i>	KT750015	Complete
B – derived mRNA	<i>ScKIF4A</i>	KT750020	Partial (variant 1)
	<i>ScKIF4A</i>	KT750021	Partial (variant 2)
	<i>ScSHOC1</i>	KT750018	Complete
	<i>ScAGO4B</i>	KT750016	Complete
B-located contig cI	<i>ScKIF4A</i>	KT713602	Partial
B-located contig cII		KT713603	Partial
B-located contig cIII		KT713604	Partial
B-located contig cIV		KT713605	Partial
B-located contig cV		KT713606	Partial
B-located contig cI	<i>ScSHOC1</i>	KT713607	Partial
B-located contig cII		KT713608	Partial
B-located contig cIII		KT713609	Partial
B-located contig cIV		KT713610	Partial
B-located contig cV		KT713611	Partial
B-located contig cVI		KT713612	Partial
B-located contig cVII		KT713613	Partial
B-located contig cVIII		KT713614	Partial
B-located contig cI	<i>ScAGO4B</i>	KT713615	Partial
B-located contig cII		KT713616	Partial
B-located contig cIII		KT713617	Partial
B-located contig cIV		KT713618	Partial
B-located contig cV		KT713619	Partial

2.4 Results

At the beginning of my PhD study, we knew from our comparative transcriptome analysis results that rye B chromosomes contribute to the transcriptome. However, a detail comparative analysis of A- and B-located genes regarding their completeness and functionality still was still missing. Therefore, based on our RNAseq data set (<http://webblast.ipk-gatersleben.de/rye/>), three putative chromatin and epigenetically related genes (*ScKIF4A*, *ScSHOC1* and *ScAGO4B*) were selected from the transcript data of developing rye anthers for completeness and functionality analysis. The workflow below represents the questions we asked and how we answered the questions in this study (Figure 19).

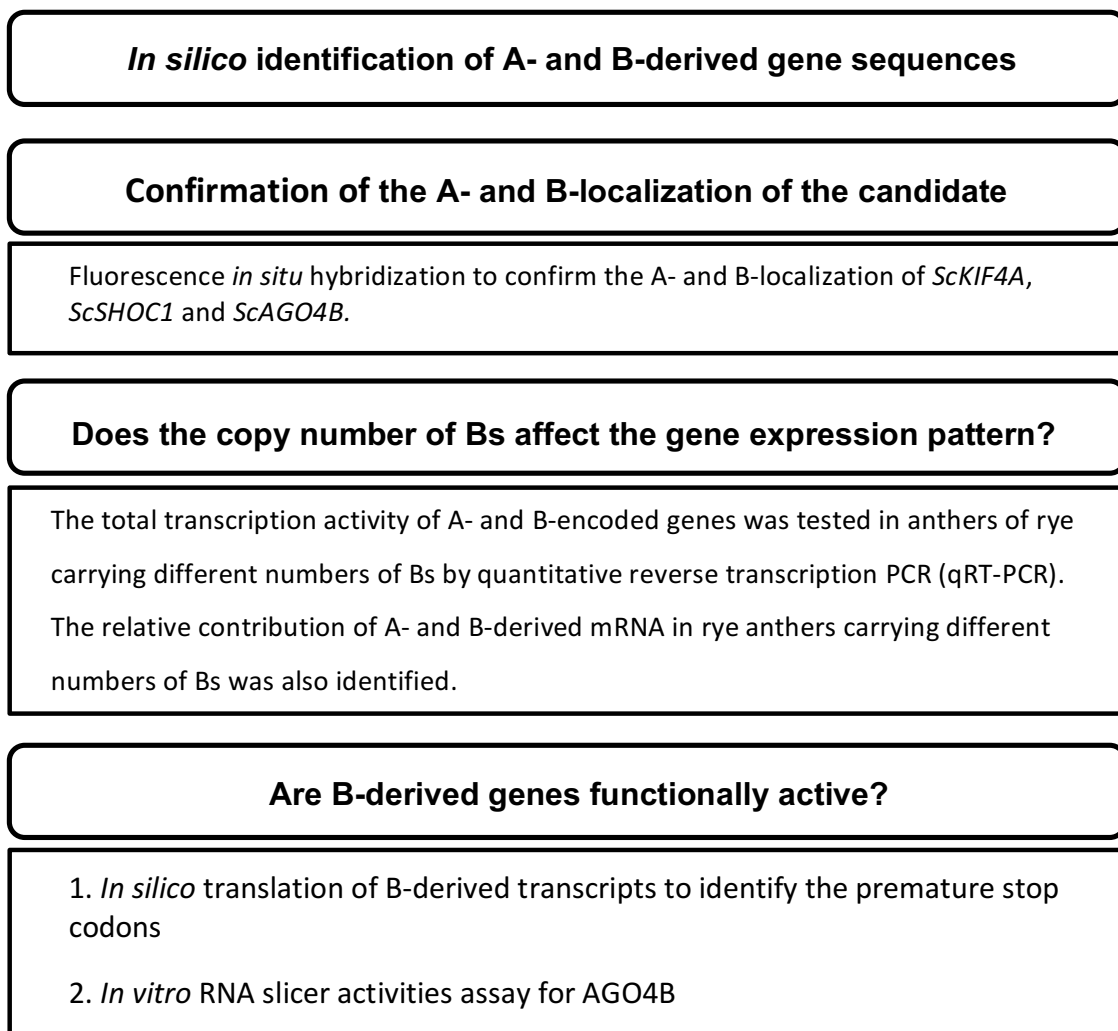


Figure 19. A workflow diagram describing the steps of the study

The questions asked in each step are indicated in bold. The methods we used to answer the questions are listed below the questions.

2.4.1 Active RNAPII enzymes are closely associated to rye B chromatin

Most eukaryotic genes are transcribed by RNA polymerase II (RNAPII). Therefore, the co-localization of transcripts and RNAPII are a sensitive prove for active transcription (Sims et al. 2004; Komarnitsky et al. 2000). We combined immunostaining with FISH to test the potential transcriptional activities of rye B chromosomes. Immunolabeling visualized active RNAPII enzymes phosphorylated at serine 2 (RNAPIISer2ph) in interphase nuclei of rye and wheat containing two Bs. To identify the Bs in both species, a subsequent FISH was performed, applying the sub-terminal B-specific repeat D1100 (Sandery et al. 1990) and the rye-specific repeat *Revolver* (Carchilan et al. 2009) as markers, respectively. By super-resolution microscopy (SIM) the close association of active RNAPII and B chromatin was proven in both species, and its distribution did not differ between A and B chromatin. Whereas heterochromatic regions (strongly stained by DAPI) of rye were devoid of active RNAPII, the D1100 repeats and *revolver*-positive chromatin were intermingled by RNAPIISer2ph-specific immunosignals (Figures 20A, 20B). It is obviously that the distribution of active RNAPII enzymes indicating transcriptional activity is similar at A and B euchromatin in interphase nuclei.

In addition, we applied in the same experiment antibodies against inactive RNAPII which is not phosphorylated. Interestingly, this enzyme modification is similarly distributed within the interphase nuclei around the rye and wheat B chromatins as found for the active RNAPII (Figures 20A, 20B). In rye with 2Bs, even an accumulation of inactive RNAPII at B chromatin was proven (Figure 20A). Obviously, RNAPII molecules seem to be present permanently within euchromatin, where they can become activated when transcription is required.

2.4.2 The B chromosome-located genes *ScKIF4A*, *ScSHOC1* and *ScAGO4B* are transcribed

Based on our RNA-seq data set (<http://webblast.ipk-gatersleben.de/rye/>), three putative chromatin and epigenetical related rye B-derived genic sequences were selected from the generative transcript data for further analysis. A phylogenetic analysis revealed a high similarity to the kinesin family member 4 gene (*KIF4A*), shortage in chiasmata gene (*SHOC1*) and Argonaute family member 4 gene (*AGO4B*) (Figure 21A-C). KIF4 kinesins are key players in several crucial cellular processes,

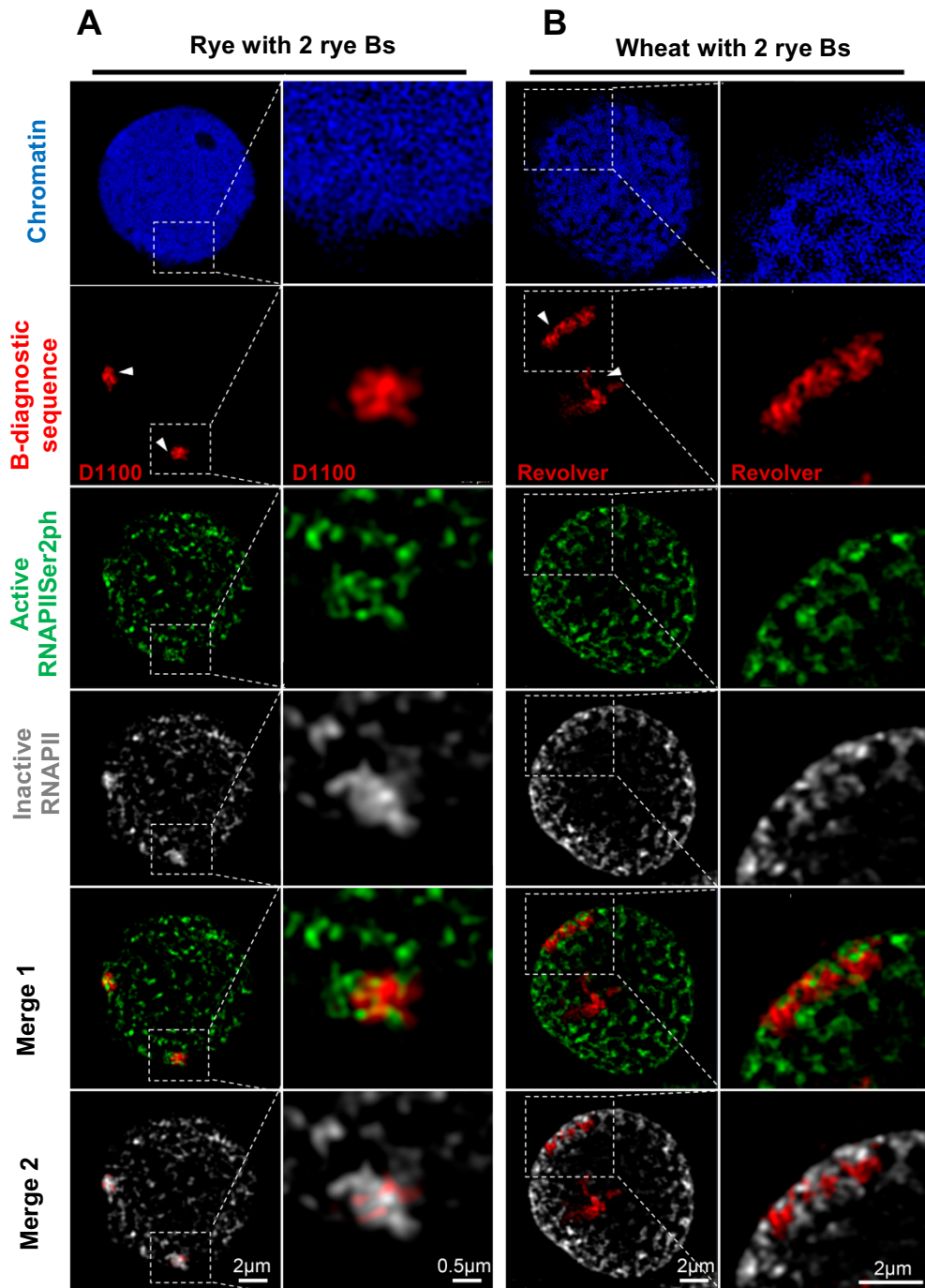
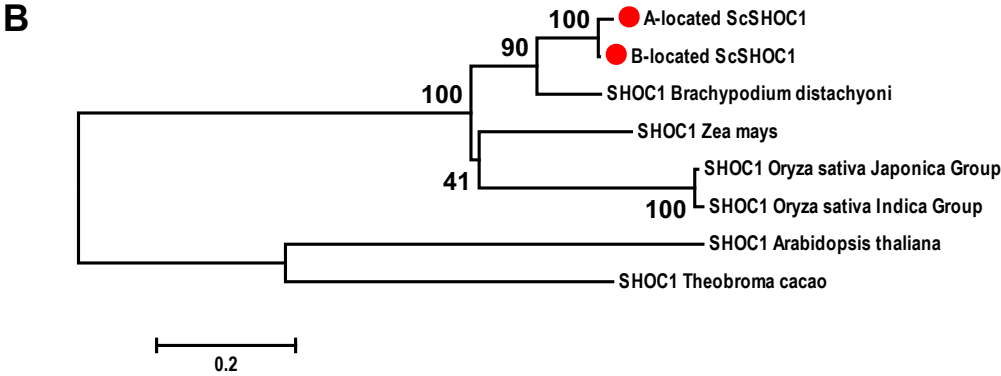
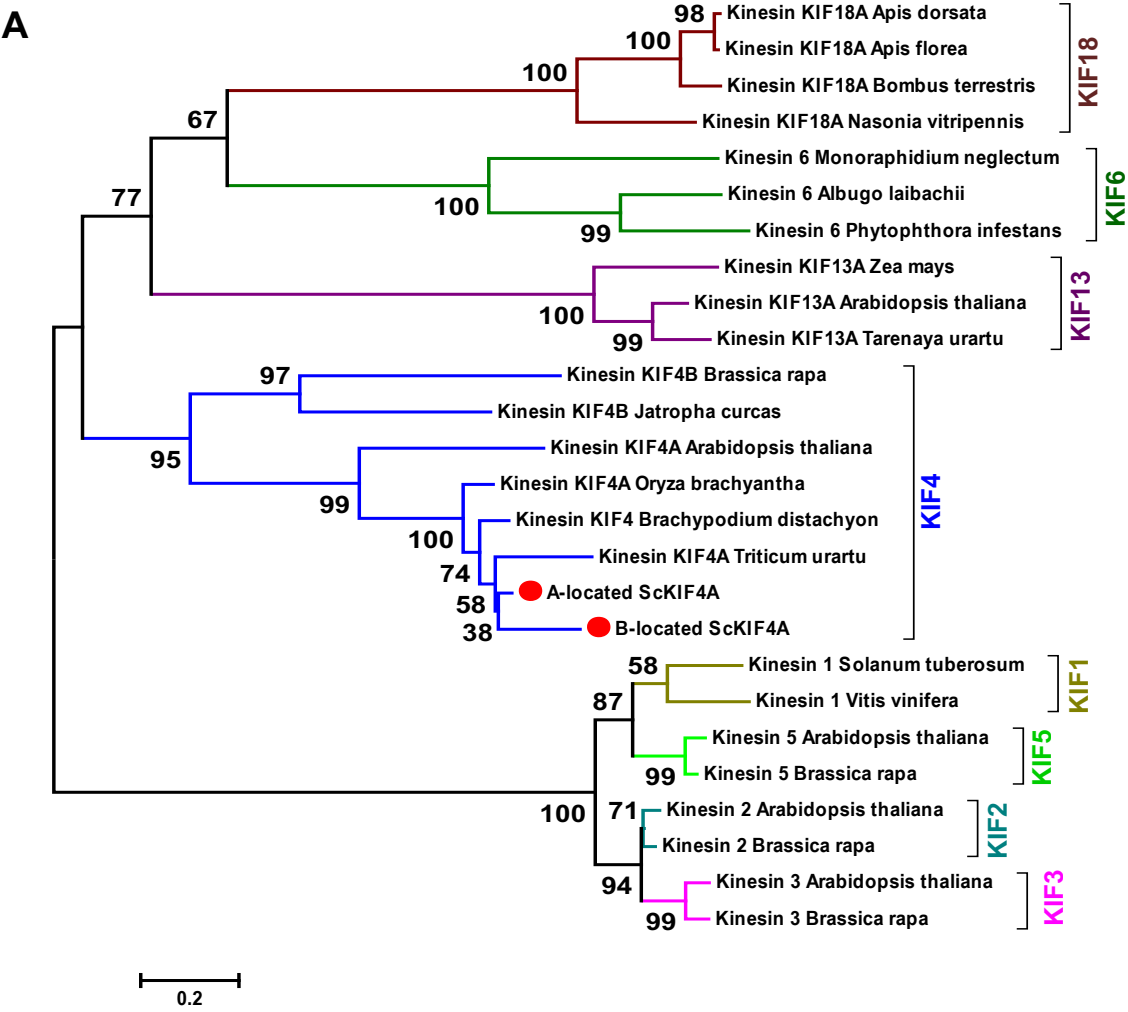


Figure 20. The distribution of active and inactive RNAPII in rye and wheat nuclei with 2Bs was identified by SIM.

Immunostaining of RNAPIISer2ph (active) and FISH with the B-specific repeat D1100 or Revolver to identify rye B chromatin show the presence of active RNAPII at rye B chromatin (arrow heads, merge 1). Inactive RNAPII also colocalizes with B chromatin, and in rye it is even amplified (merge 2). The right panels show the regions of interest (rectangle) magnified.

including chromatid motility, chromosome condensation (Zhu and Jiang 2005) as well as intracellular transport (Sekine et al. 1994). SHOC1 is required for promoting or

stabilizing single strand invasion and formation of class I cross-overs during meiotic recombination processes (Macaisne et al. 2008). AGO4 is involved in the regulation of gene expression (see below and Discussion). As a general property this protein has a ‘slicer activity’, i.e., it is capable to catalyze sRNA-directed endonucleolytic degradation of targeted RNA transcripts (Zilberman et al. 2003; Qi et al. 2006).



C

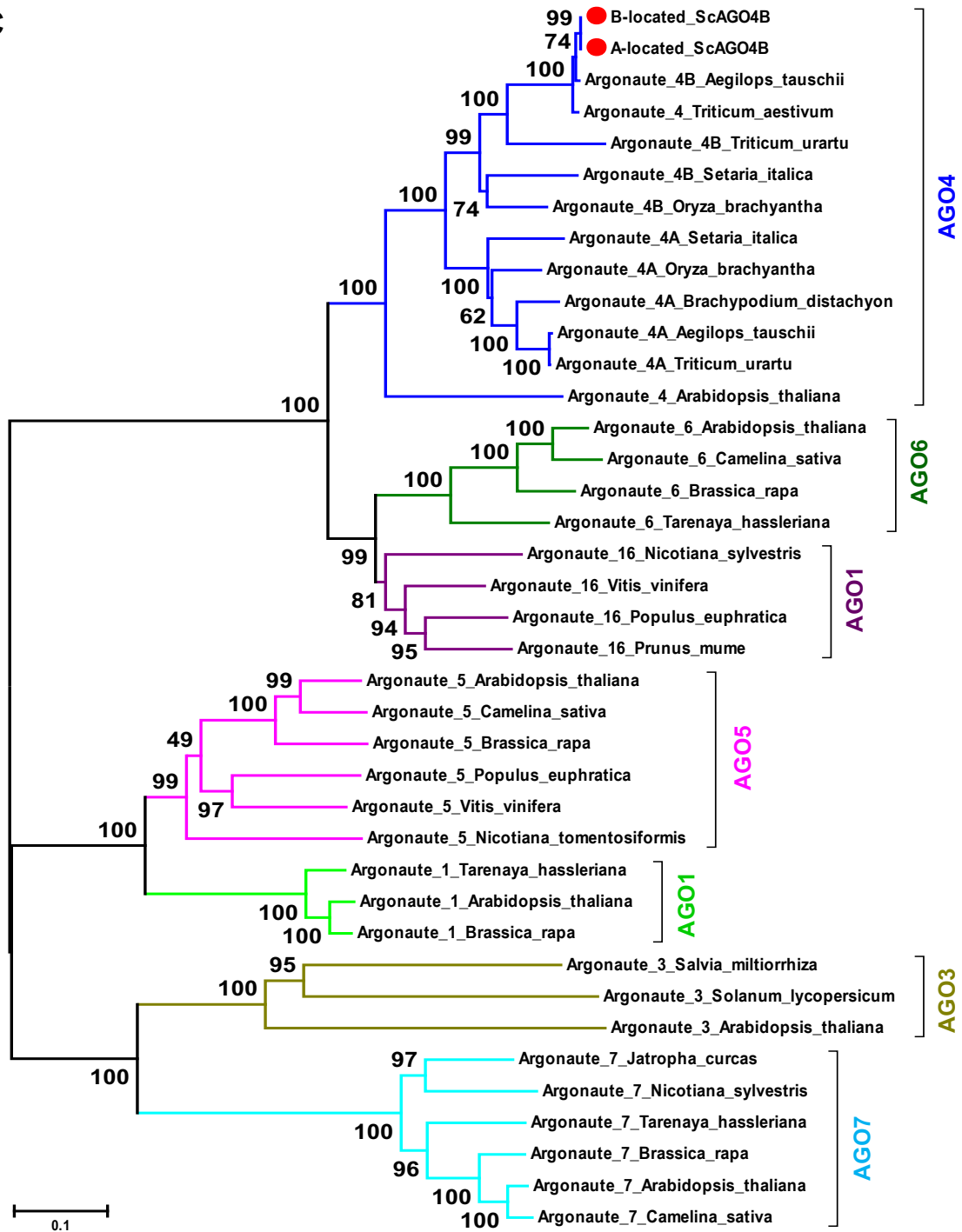


Figure 21. Phylogenetic analysis of Kinesin KIF (A), Shortage in chiasmata SHOC1 (B) and Argonaute AGO (C).

Sequence comparison performed for Kinesin KIF (A), Shortage in chiasmata SHOC1 (B) and Argonaute AGO (C) from different species. After aligning the sequences with Clustal W, phylogenetic trees were calculated using the boot-strapped neighbor-joining algorithm in MEGA 6.06 with 1000 trials (<http://www.megasoftware.net/>). Bootstrap values are indicated as percentages of the 1000 trials at their respective node. For convenience rye A- and B-derived sequences are indicated with red circles before the name.

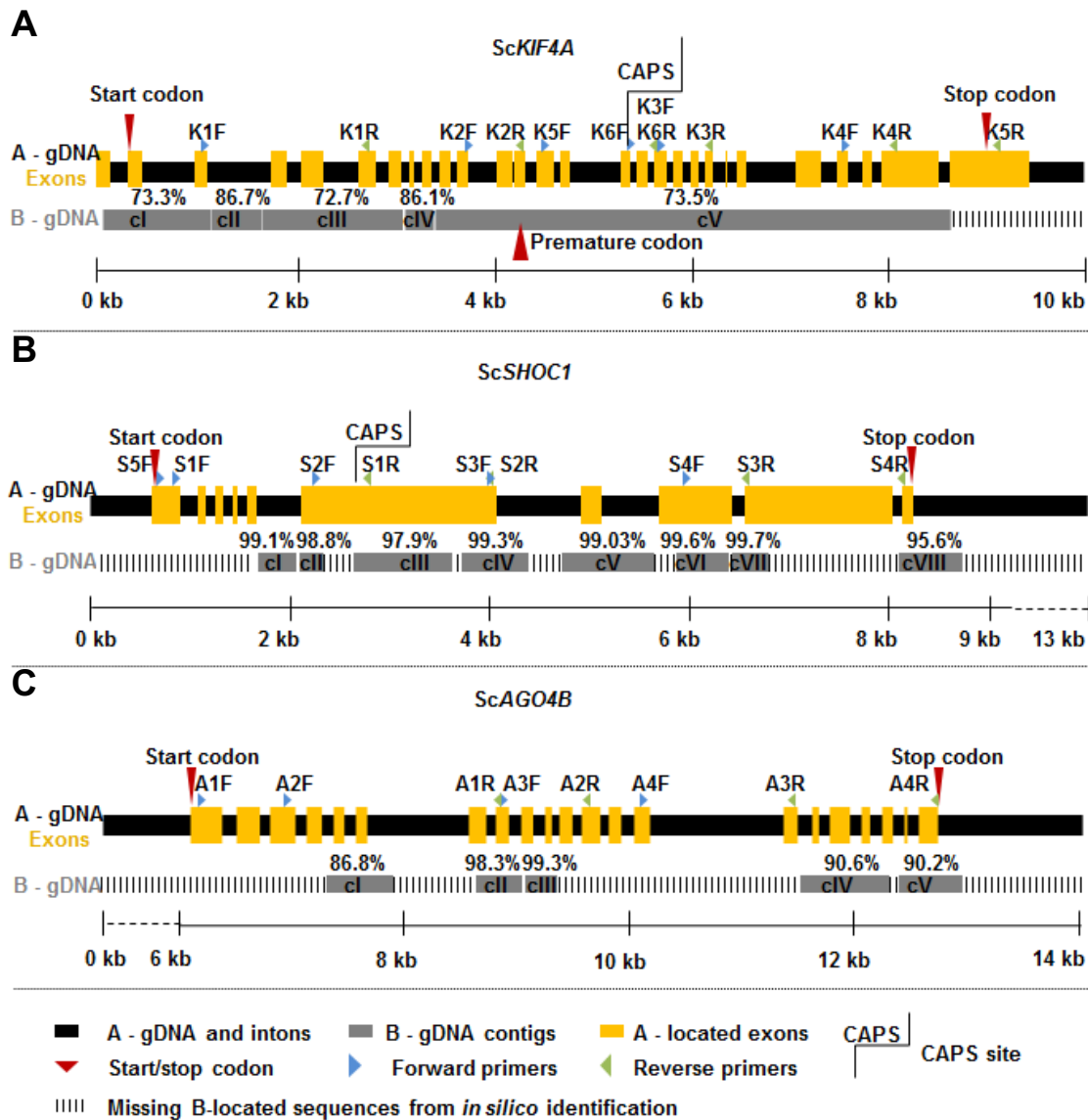


Figure 22. Gene structure model for three selected genes based on *in silico* identification.

The black and orange boxes correspond to the A- located introns and individual exons, respectively. Grey boxes with numbers represent the B-located genomic contigs. The regions of missing B-located genomic sequences are indicated in black vertical lines. The similarity (%) between A-located sequences and B-located counterparts, positions of start/stop codon, primer sites and CAPS markers are indicated.

The corresponding A- and B-located genomic sequences of each of the transcripts were identified by BLAST analysis of a database containing rye genomic 0B and sequences of flow sorted Bs described in the European Nucleotide Archive (accession no.ERP001061, PRJEB12520). The gene structure with putative intronic and exonic regions was predicted by FGENESH (<http://linux1.softberry.com/berry.phtml>) based on the A-located genes (Figure 22). All

GenBank accession numbers corresponding to the different nucleotide sequences are available in Table 8. Primers were designed for both, A- and B- located sequences in the putative exonic regions based on the gene models (Figure 22; Table 5).

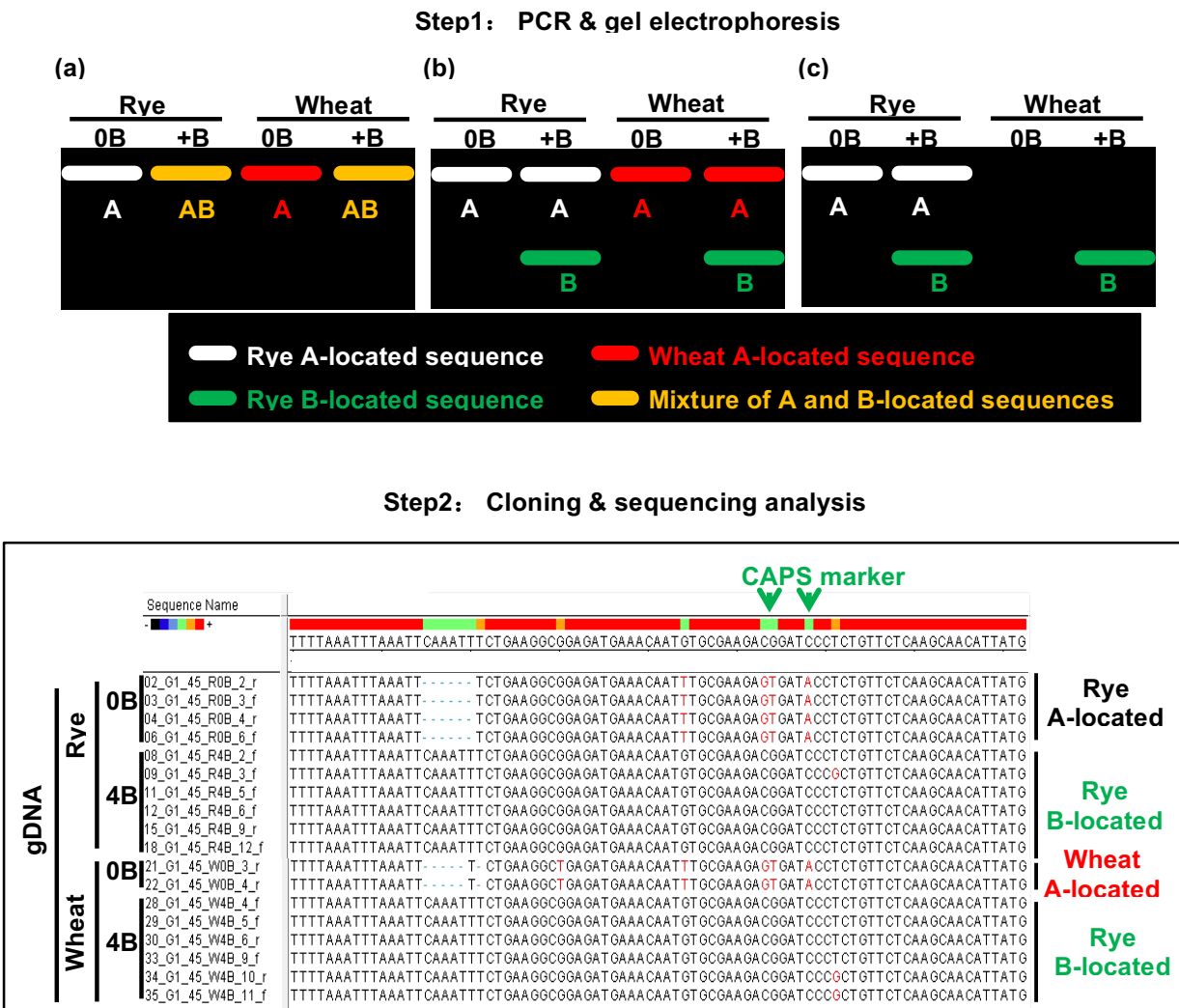


Figure 23. Workflow representation of how to distinguish A- and B- located sequences.

Three criteria are categorized according to PCR and gel electrophoresis (Step 1), B-located sequences for category (b) and (c) are able to be distinguished due to fragment size differences from A-located counterparts. For category (a), B-located sequences are able to be distinguished only after sequencing analysis (Step 2).

Alignments of informative sequenced *ScKIF4A* clones derived from gDNA of rye and wheat with Bs (+B) as well as without Bs (0B) (Step 2). A- and B-located *ScKIF4A* sequences are able to be distinguished by polymorphic sites (CAPS marker position used to distinguish A- and B- located *ScKIF4A* are indicated).

Next, the *in silico* identified sequences were sequence confirmed after PCR and RT-PCR using genomic DNA, another cDNA of rye and wheat with Bs (+B) as well as without Bs (0B) as templates. To distinguish between A- and B-derived sequences, the following criteria were used (Figure 23): (i) the same amplicon size exists, but B-specific SNPs are detectable after sequencing, (ii) additional differently-sized amplicons are formed in wheat and rye with Bs and (iii) amplicons are only formed in wheat carrying additional Bs with the same size as the additionally differently-sized amplicons which are formed in rye with Bs.

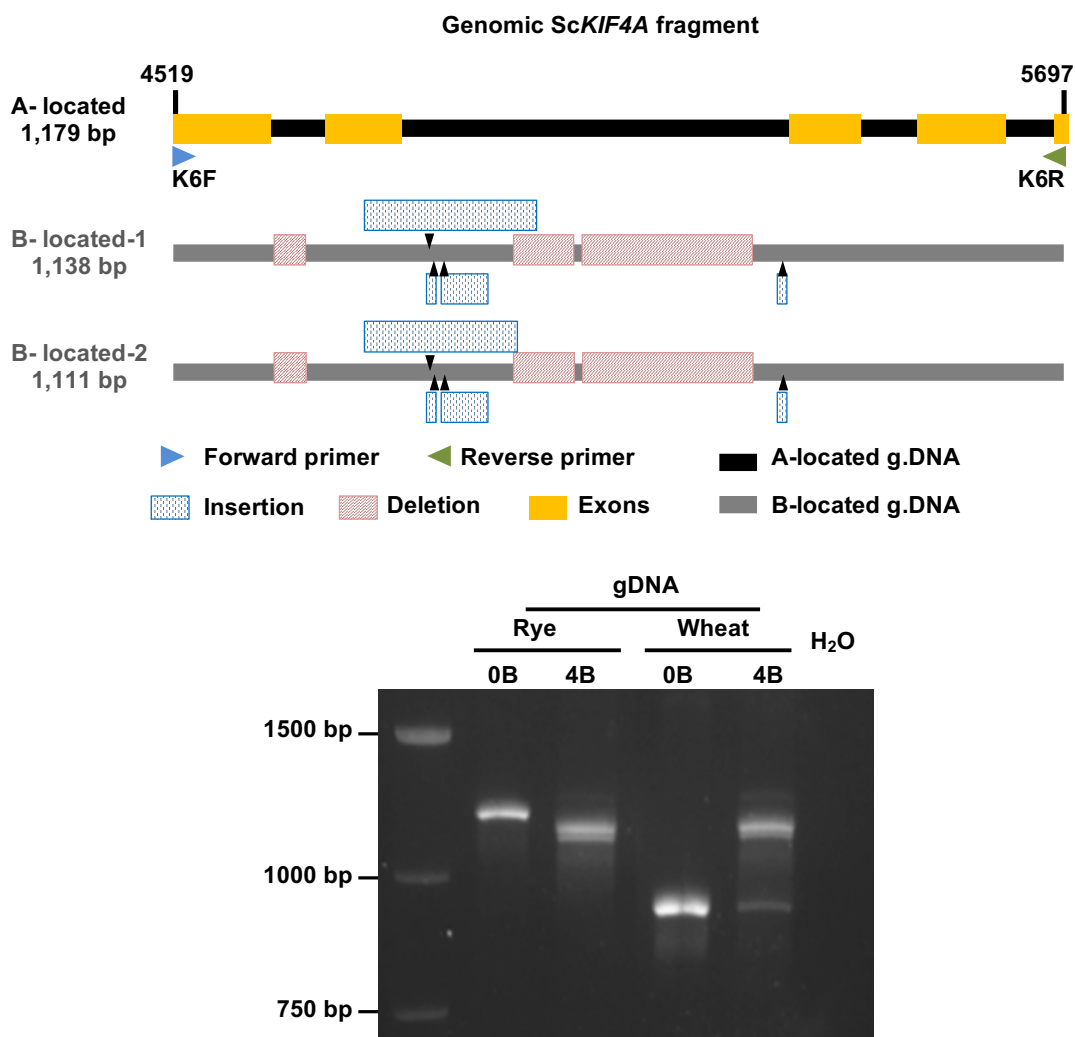


Figure 24. B-located *ScKIF4A*-like fragments where subjected to structural modifications.

PCR performed on genomic DNA of rye and wheat without and with B chromosomes. Schemata show the polymorphic sites between two types of rye B-located *ScKIF4A*-like fragments and their A-located counterpart according to the sequencing results.

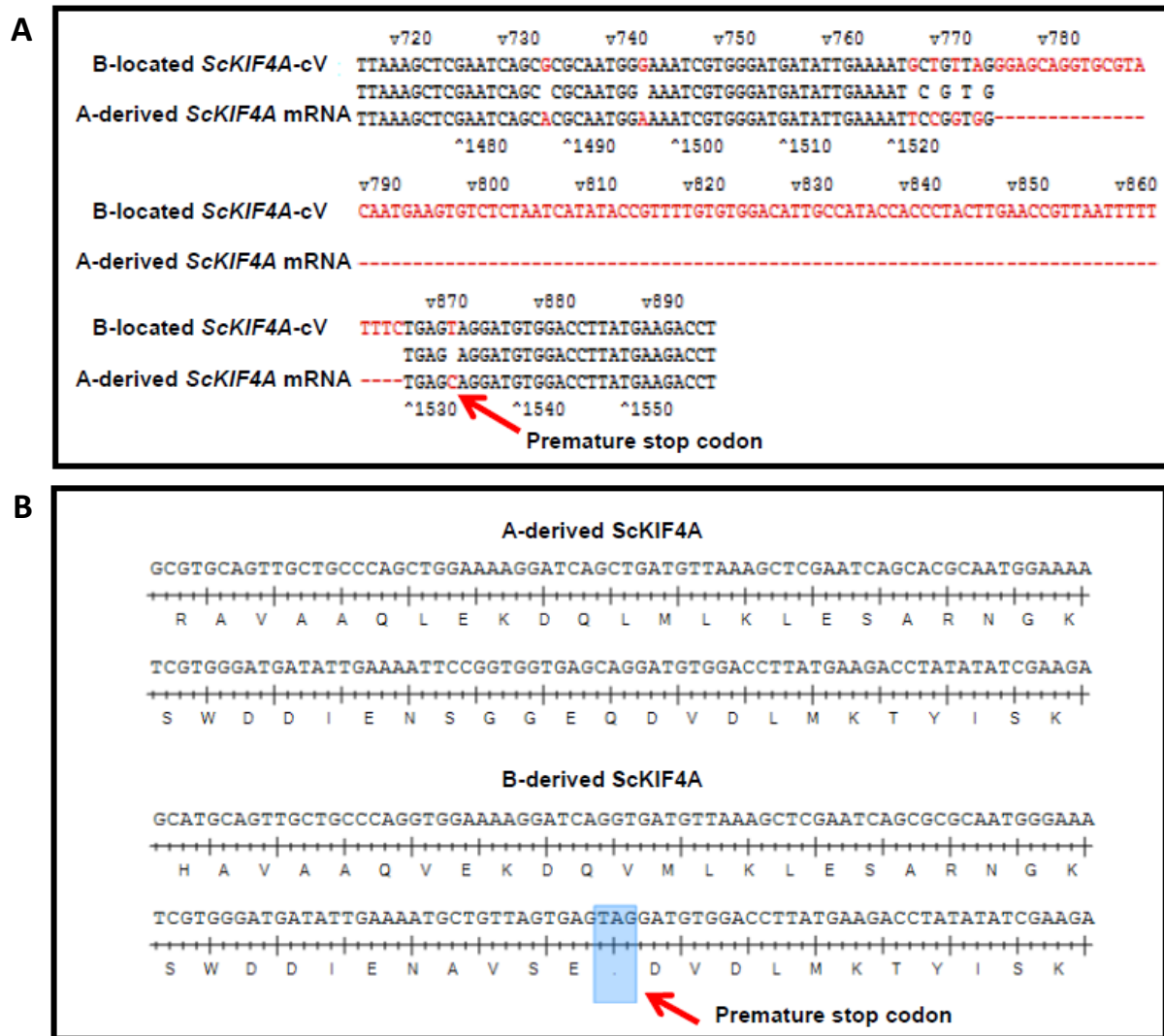


Figure 25. A premature stop codon was *in silico* identified in rye B-derived KIF4A-like gene.

Comparison of A- and B-derived *ScKIF4A* gene (A) and protein sequences (B). The arrows indicate the position of the premature stop codon.

Different states of pseudogenization were observed after comparison between A- and B-located genomic contig sequences was performed (Figure 22). The A- and B chromosome-located *ScKIF4A* sequences revealed an overall 78.5% similarity over the entire length of 10 kb (Figure 22A). However, a 1.1 kb long subregion of *ScKIF4A* showed only 53.6% similarity, a 224 bp deletion and a 201 bp long insertion as well as some SNPs were observed exclusively in the B-located sequence (Figure 24). Notably, at least two variants of the B-located *ScKIF4A* were found, which are characterized by a few polymorphic sites (Figure 23, 24). The ~13 kb long A-located *ScSHOC1* sequence exhibited 98.6% (Figure 22B) and the ~8 kb long A-located *ScAGO4B* 93% similarity to the corresponding B-located sequences at the genomic

level (Figure 22C). Hence, we conclude that the B-located genic sequences undergo pseudogenization.

To test whether the B chromosome-originated transcripts are potentially functional, *in silico* translation (<http://web.expasy.org/translate/>) was performed based on the B-derived mRNAs which were identified by searching the RNA-seq reads and B-located genomic contigs or by sequencing of RT-PCR products. The predicted amino acid sequences were analyzed to identify potential stop codons. One of the nucleotide changes (C>T) was found in the B chromosome-located *ScKIF4A* genomic contig cV (position 872) and resulted in a premature stop codon (Figure 22A; Figure 25). B chromosomes-encoded *ScSHOC1* and *ScAGO4B* genes did not reveal any premature stop codon.

2.4.3 Amplification increased the copy number of the B chromosome-located genic sequences

To verify the A and B chromosome-localization of the candidate genes, FISH was performed on rye mitotic and meiotic metaphase cells containing Bs. After FISH with a *ScKIF4A*-specific probe, all mitotic Bs displayed a strong hybridization signal at the long chromosome arm near the D1100-positive region, but outside the non-disjunction control region. In contrast, two pairs of A chromosomes showed only weak *ScKIF4A* hybridization signals (Figure 26A). Similarly, *ScSHOC1* gave strong hybridization signals on all Bs, but only faint signals were observed on two A chromosome pairs at metaphase I of meiosis (Figure 26B). *ScAGO4B* also displayed a comparable situation, i.e., the meiotic Bs showed very intense *ScAGO4B* signals at an interstitial position while a single A chromosome pair displayed a rather weak hybridization signal (Figure 26C). The stronger hybridization signals on the Bs suggest the amplification of the B-encoded *ScKIF4A*, *ScSHOC1* and *ScAGO4B* sequences.

2.4.4 The number of Bs affects the gene expression pattern

The total transcription activity of A- and B-encoded genes was tested in anthers of rye carrying different numbers of Bs. This was done by quantitative reverse transcription PCR (qRT-PCR) using primers which did not discriminate between A- and B-derived transcripts. To further determine the relative contribution of A- and B-

derived mRNAs in rye anthers carrying different numbers of Bs, the A- or B-origin of the transcript was identified.

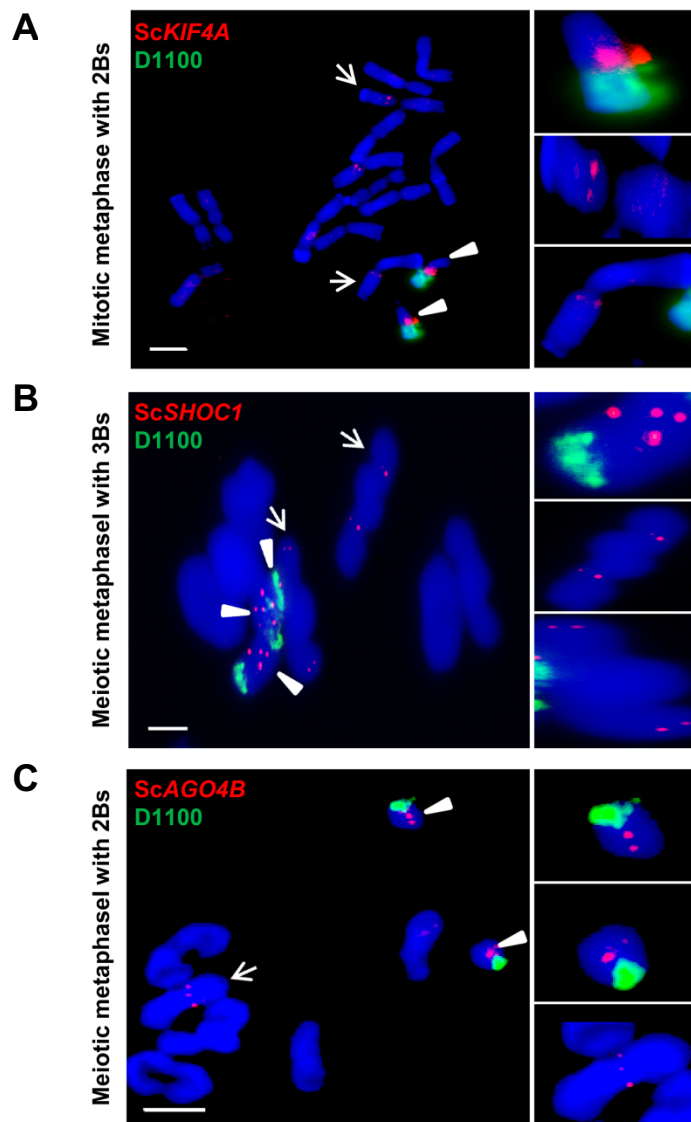


Figure 26. Chromosomal locations of *ScKIF4A*, *ScSHOC1* and *ScAGO4B* as revealed by FISH.

Mitotic metaphase or meiotic metaphase I cells of rye with Bs after FISH with labeled *ScKIF4A* (A), *ScSHOC1* (B) and *ScAGO4B* (C) (in red). FISH with the B-specific D1100 repeat (in green) allowed the identification of Bs. Chromosomes are stained by DAPI (in blue). Note signals from Bs are indicated by arrow heads, A-localized FISH signals are indicated by arrows. The inset shows the signals on further enlarged A and B chromosomes. Bar = 5 μm.

An increased expression of total *ScKIF4A* was found in +2B plants, while reduced and more similar expression patterns were revealed in plants with either 0B, 1B, 3Bs or 4Bs (Figure 27A). To determine the relative contribution of A- and B-derived *ScKIF4A* transcripts, cDNA of rye anthers with different number of Bs were used to

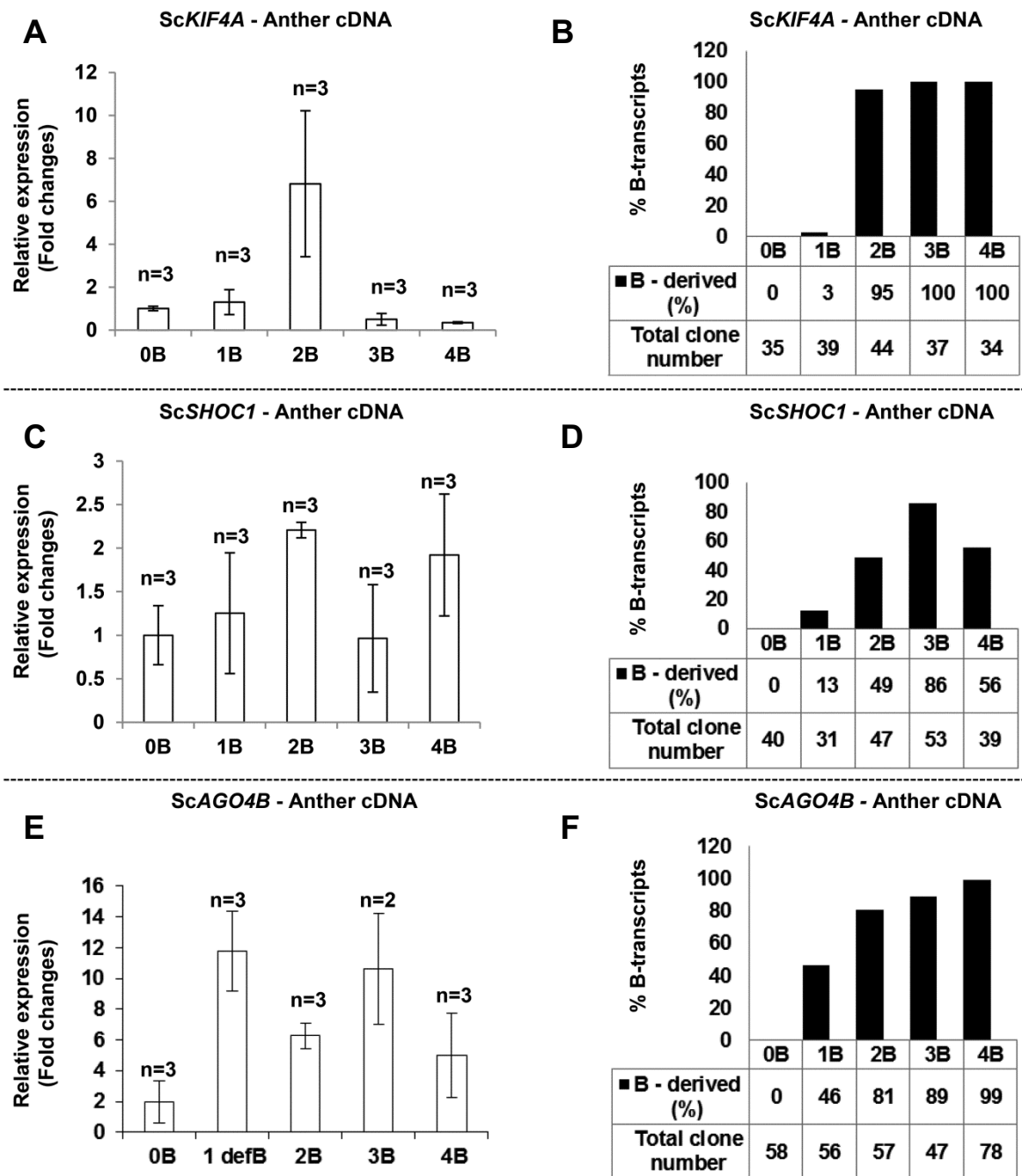


Figure 27. Quantitative analysis of *ScKIF4A*, *ScAGO4B* and *ScSHOC1* transcripts in presence and absence of Bs.

The total transcription of *ScKIF4A* (A), *ScSHOC1* (C) and *ScAGO4B* (E) was measured by qRT-PCR in rye anther cDNA containing different numbers of B chromosomes. The number of biological replicates is indicated above the bars. Error bars represent standard deviation. The contribution of B-derived *ScKIF4A* (B), *ScSHOC1* (D) and *ScAGO4B* (F) transcripts from rye anther cDNA with different numbers of Bs was measured by colony PCR followed by CAPS analysis or nested PCR.

perform RT-PCR with the primers K7F and K6R. A cleaved amplified polymorphic sequences (CAPS) analysis was followed after PCR of the cloned RT-PCR products

using the primer pair K7F/K6R (see Supplemental Figure 28A, 28B). Interestingly, in plants carrying more than 2Bs, all *ScKIF4A* transcripts derived exclusively from the B chromosomes (Figure 27B, Figure 28A).

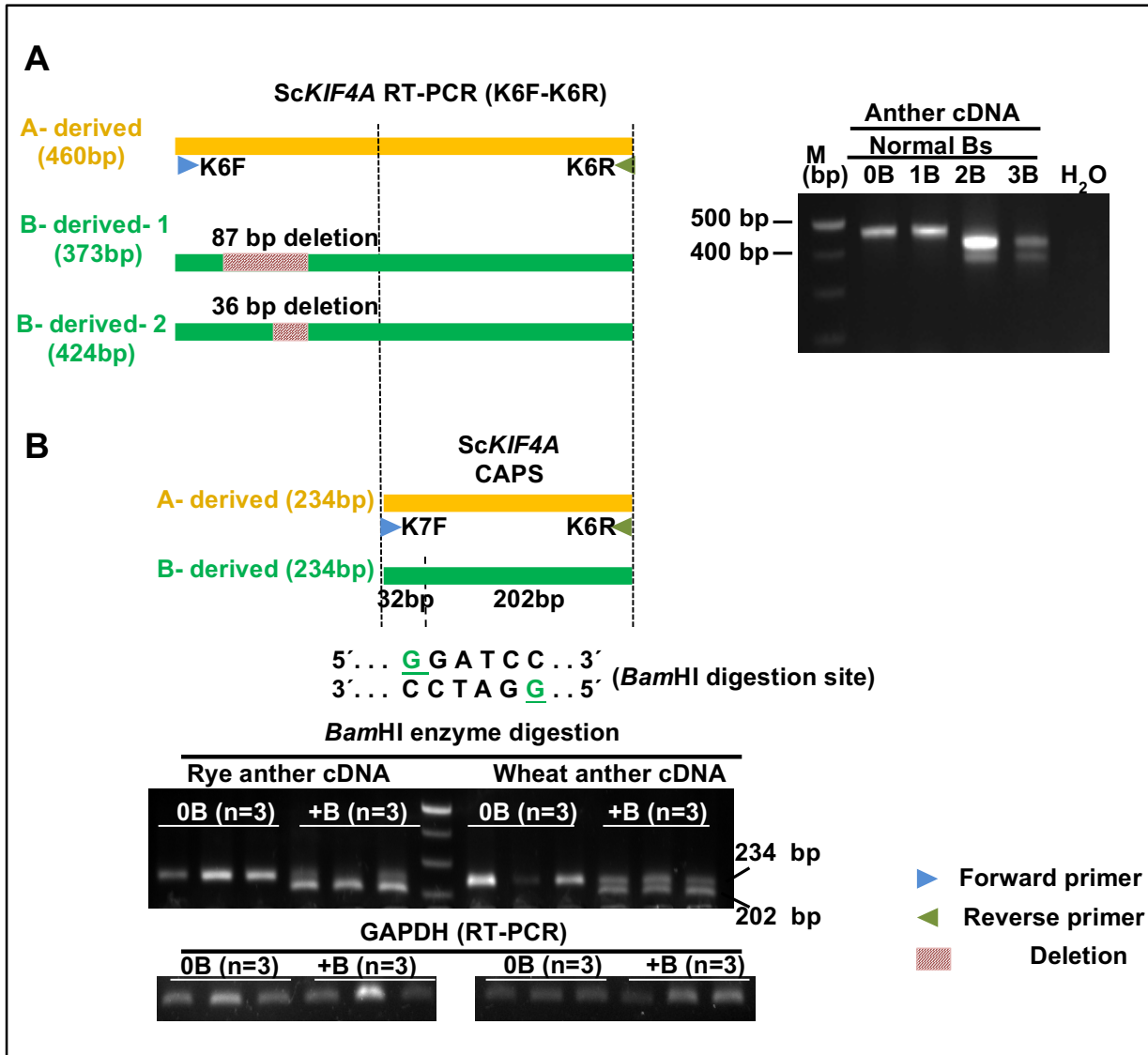
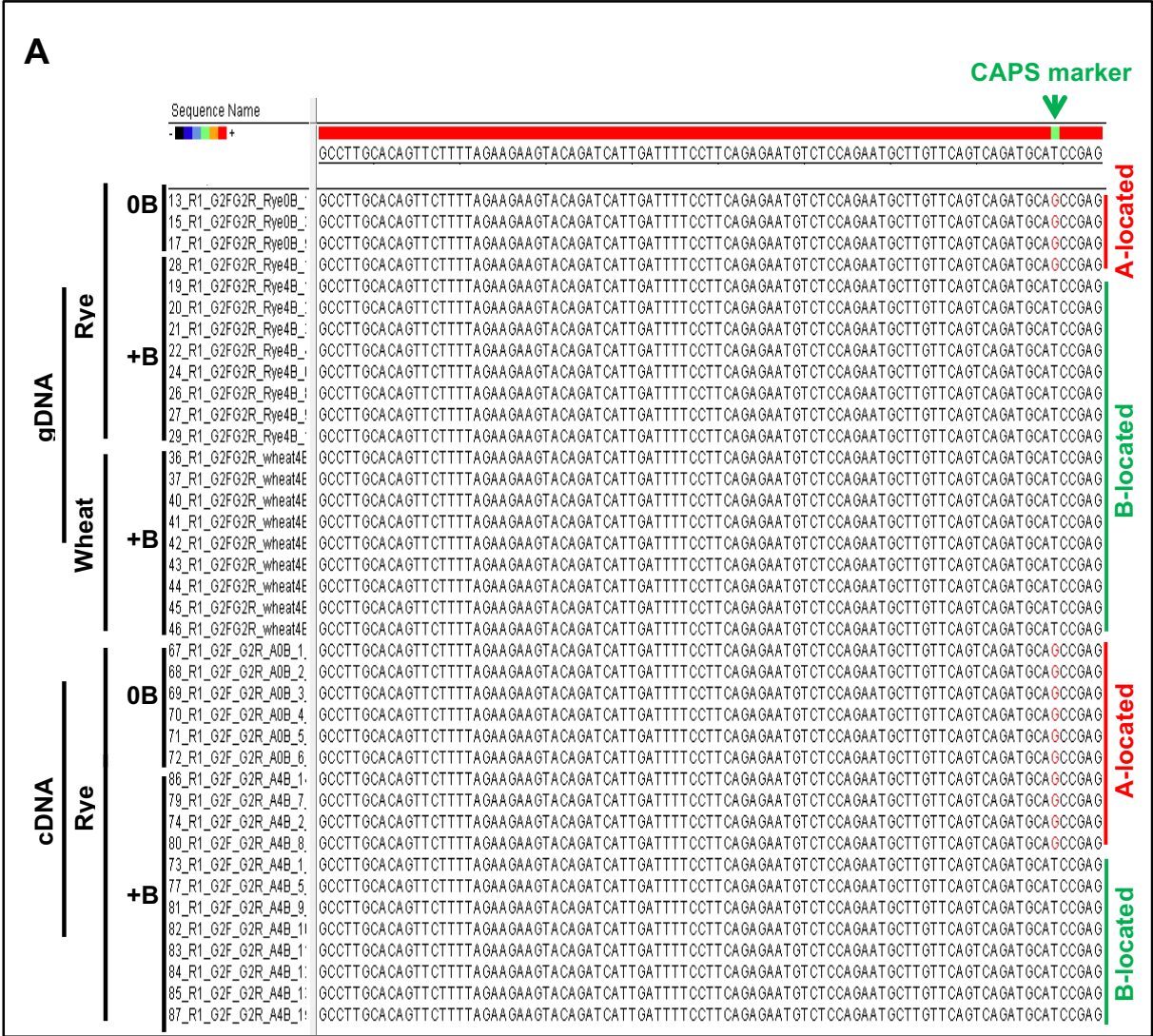


Figure 28. CAPS analysis for A- and B-derived *ScKIF4A* transcripts.

(A) Schemata represent the sequence comparison between two rye B- derived *ScKIF4A* fragments and their A- derived counterpart. RT-PCR (primers K6F and K6R) was performed using anther cDNAs from rye with and without Bs. A major contribution of the B chromosome is found in 2 and 3B plants.

(B) Schemata represent the CAPS site position for B-located *ScKIF4A* transcripts. Two SNP sites between rye B-located *ScKIF4A*-like fragments and its A-located counterpart were found at A-located genomic position 5358 (T to G) and 5362 (A to C) (Figure 23). RT-PCR (primers K7F and K6R) using rye and wheat cDNA from anthers of 0B and +B carriers was performed following by CAPS analysis with *Bam*HI enzyme. Extra bands are only found in rye and wheat possessing Bs. Three biological replicates were used for each experiment. *GAPDH*-specific primers were used to quantify the amount of cDNA.

ScSHOC1 revealed a similar dynamic expression pattern. An increased expression was found in +2B and +4B plants (Figure 27C). To determine the relative contribution of B-derived ScSHOC1 transcripts, cDNA of rye anthers with different number of Bs were used to perform RT-PCR with the primer pair S2F/S2R. A CAPS analysis of the cloned RT-PCR products was subsequently performed to determine the relative contribution of A- and B-derived using the primer pairs S2F/S1R (Figure 29). The analysis revealed that the amounts of B-derived ScSHOC1 transcripts increased almost linear from 1B to 3B but were reduced in plants with 4Bs (Figure 27D). In 3B plants 86% of ScSHOC1 transcripts were encoded by Bs.



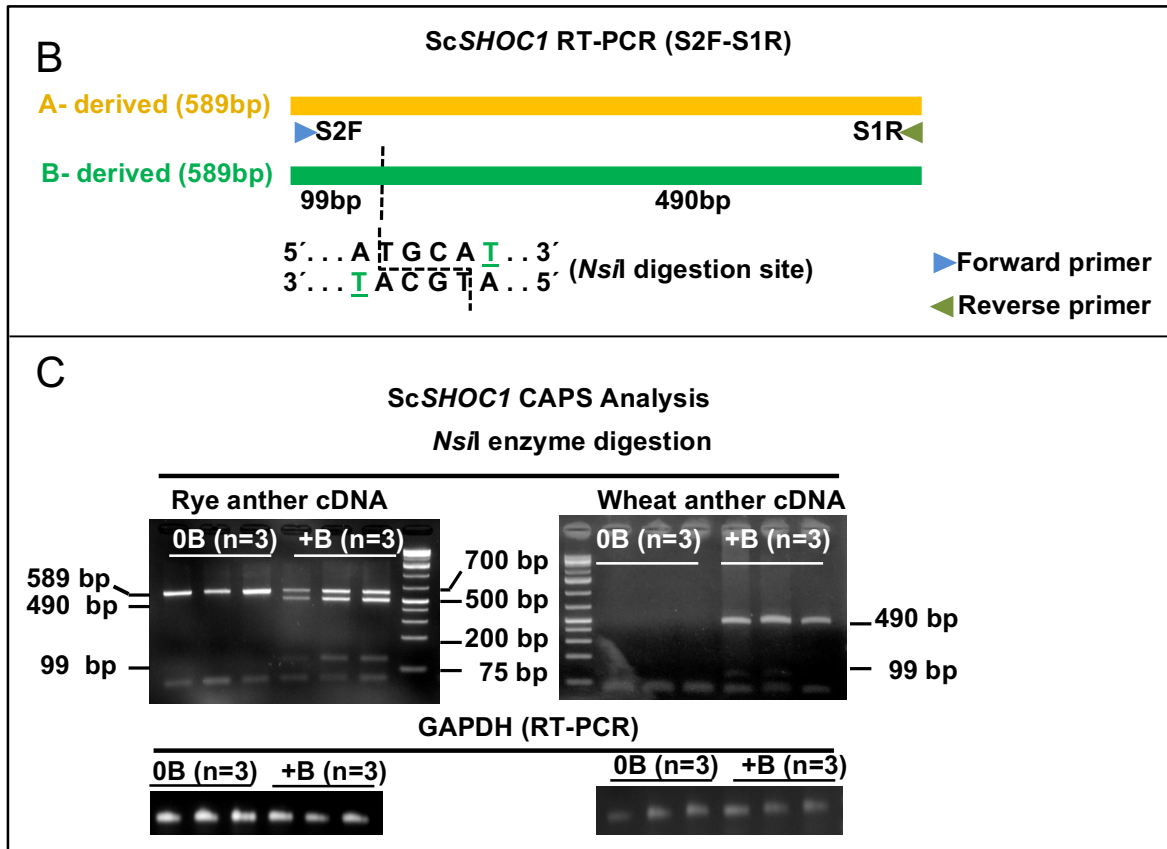


Figure 29. CAPS analysis for A- and B-derived ScSHOC1 transcripts.

Sequencing (A) and schemata (B) represent one SNP site between rye B-located ScSHOC1-like fragment and its A-located counterpart. This SNP site locates in the exonic region at A-located genomic position 2,686 (G to T). RT-PCR using rye and wheat cDNA from anthers of 0B and +B carriers was performed following by CAPS analysis with *NsiI* enzyme. Extra bands are only found in rye and wheat possessing Bs (C). Three biological replicates were used for each experiment. *GAPDH*-specific primers were used to quantify the amount of cDNA.

The expression of *ScAGO4B* varied in the presence of different numbers of B chromosomes in a zig-zag like pattern (Figure 27E). The full length *ScAGO4B* transcripts were cloned using the primer pair A5F/A5R. To distinguish between A- and B-originated transcripts a subsequent nested PCR flanking the polymorphic region between A- and B-transcripts was performed (Figure 30). The PCR results revealed that with an increasing number of Bs, the amount of B-derived transcripts increased (Figure 27F). Interestingly, in plants with four additional B chromosomes, 99% of transcripts derived from Bs.

Altogether, we concluded that the total transcriptional activity of *ScKIF4A*, *ScSHOC1* and *ScAGO4B* varies by the presence of different B chromosome numbers, while the

B-derived transcript portion increases gradually and in general with increasing numbers of Bs.

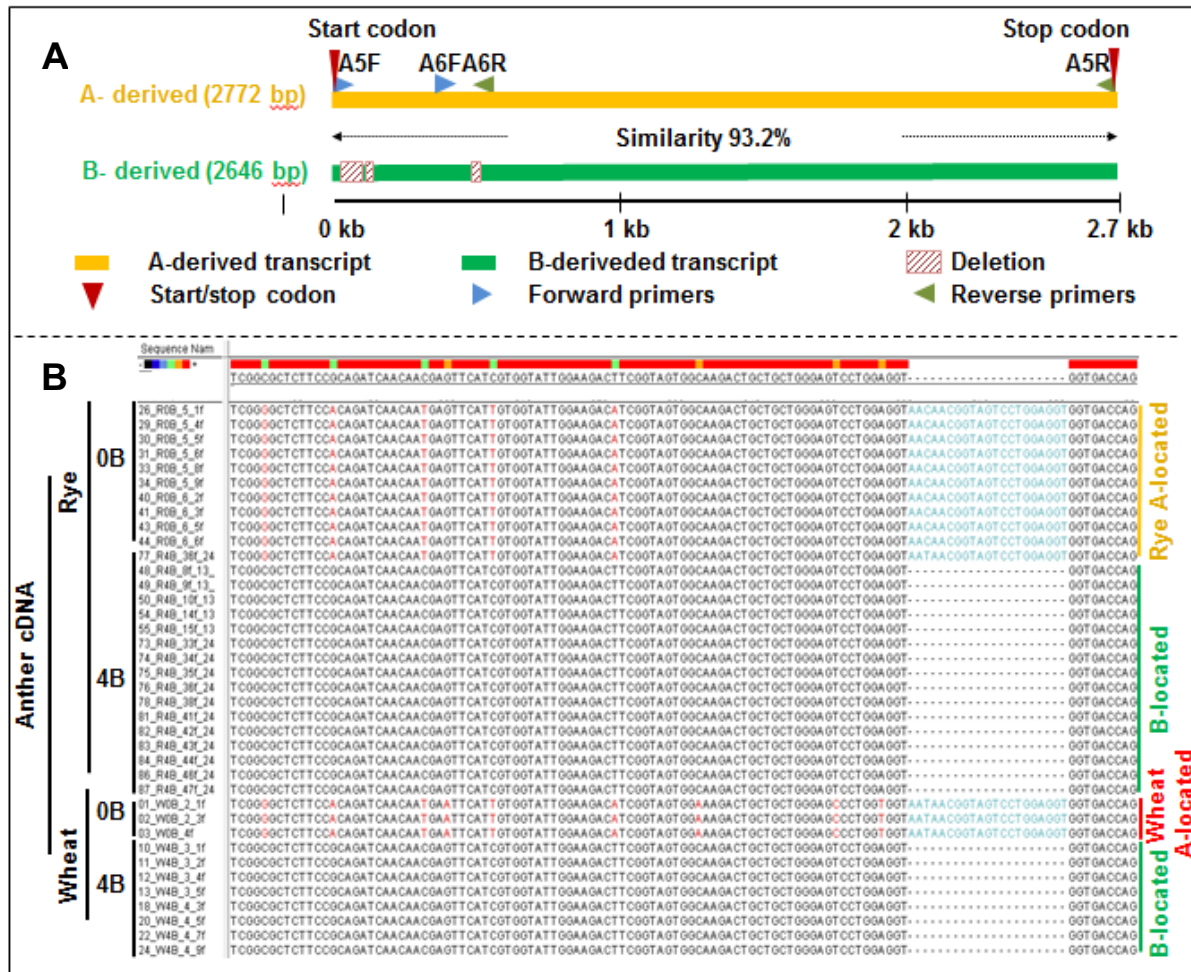


Figure 30. Gene structure model of A- and B-derived ScAGO4B transcripts.

(A) Schemata represent the sequence comparison between A- and B-derived ScAGO4B transcripts. Percentage of similarity, position of sequence polymorphisms, primers and start/stop codons are indicated.

(B) Alignments of informative sequenced ScAGO4B clones derived from anther cDNA of rye and wheat with Bs (+B) as well as without Bs (0B). A- and B-derived ScAGO4B sequences could be distinguished by polymorphic sites.

2.4.5 A and B chromosome-encoded ScAGO4B-like proteins show similar *in vitro* RNA slicer activities

The protein sequences that were deduced from the identified A- and B-located ScAGO4B transcripts showed significant homologies to the *Arabidopsis thaliana* (At) AGO4 gene (Figure 21C). The A and B chromosome-derived ScAGO4B transcripts revealed a similarity of 93.2% over the entire length. Three deletions (78 bp, 27 bp

and 21 bp length) and 61 SNPs were observed in the B-derived transcripts (Figure 30). This caused a 42 amino acids deletion (Figure 31), 38 silent mutations and 23 missense mutations. To test whether these mutations in the B-derived ScAGO4B lead to protein changes, we predicted the conserved domains of the ScAGO4B protein using the NCBI protein annotation resource Conserved Domain Database online tool (CDD) (<http://www.ncbi.nlm.nih.gov/Structure/cdd/cdd.shtml>). We found that all mutations were located outside of the conserved domains known to be important for the slicer activity of AtAGO4 (Irvine et al. 2006) and are concentrated in the N-terminal, non-conserved region of the protein (Figure 31).

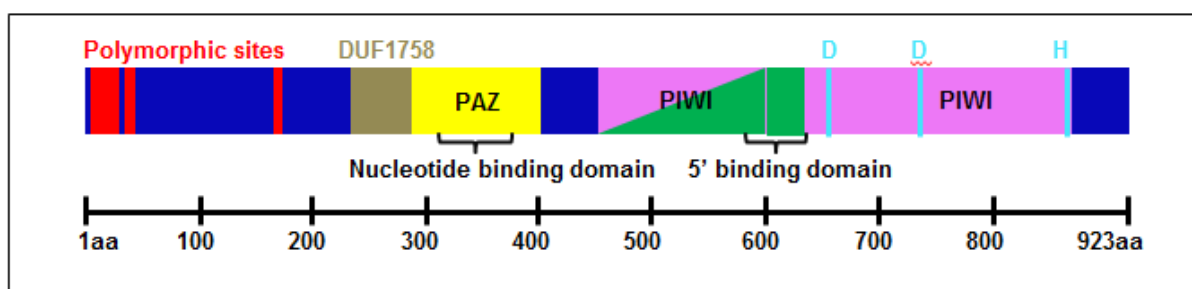


Figure 31. Domain structure of ScAGO4B protein.

Argonaute proteins are classified by the PAZ and PIWI domains. The PAZ domain contains a nucleic acid binding interface. A 5'RNA binding site exists and an active site (DDH) reside in the PIWI domain. The polymorphic sites of B-located ScAGO4B are indicated.

AGO4 has an endonuclease activity ('slicer' activity), which is directed by a bound, single-stranded sRNA guide strand. The slicer activity accordingly cleaves target RNA molecules that are complementary to the sRNA guide strand (Qi et al. 2006; Carbonell and Carrington 2015). To evaluate the functionality of the proteins that are encoded by the A- and B-derived ScAGO4B-like genes, respectively, each of them was tested for its slicer activity. For this, we applied in cooperation with Prof. Dr. Sven-Erik Behrens's laboratory (Institute of Biochemistry and Biotechnology, Section Microbial Biotechnology, Faculty of Life Sciences, Martin Luther University Halle-Wittenberg, 06120 Halle/Saale, Germany) a cell-free extract (BYL) of tobacco (*Nicotiana tabacum*) BY-2 protoplasts, which enables the reconstitution of functional AGO-containing RNA-induced silencing complexes (AGO/RISC) *in vitro* (Iki et al. 2010; Schuck et al. 2013). That is, the A- and B-chromosome derived cDNAs of the ScAGO4B genes were transcribed *in vitro* to generate the corresponding mRNAs. The mRNAs were then translated *in vitro* in the BYL to yield the respective AGO4

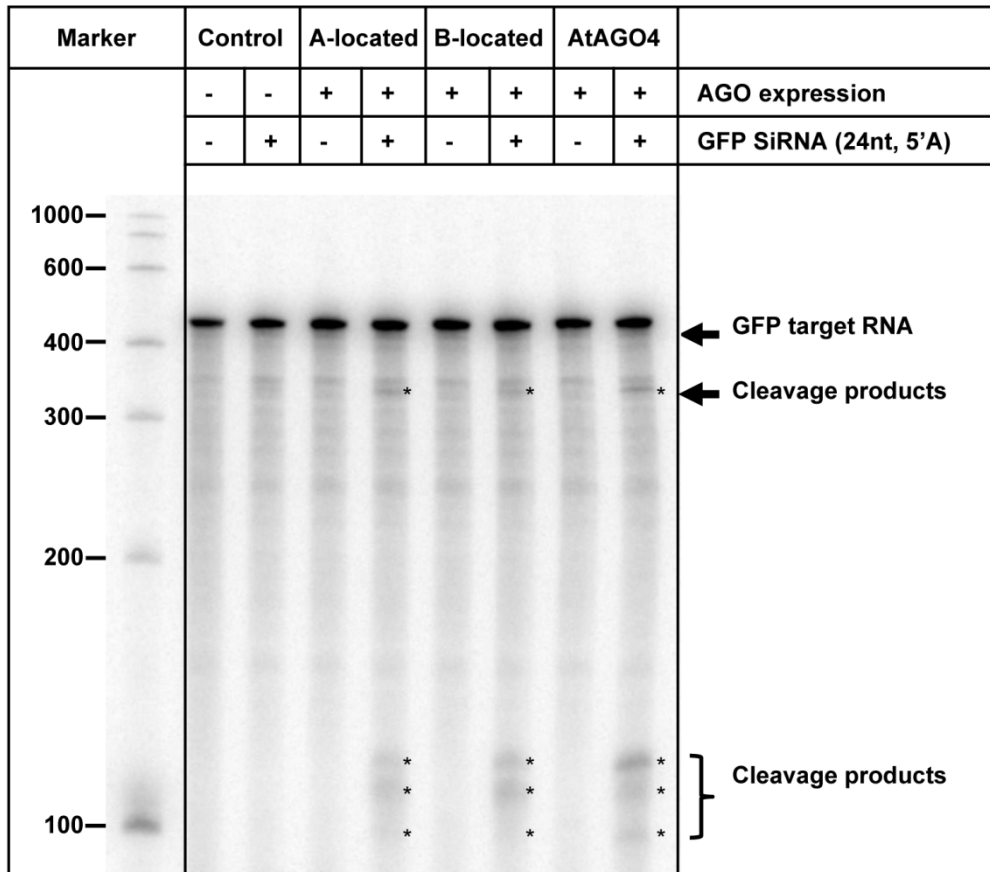


Figure 32. Rye A- and B-derived AGO4B-like proteins show similar *in vitro* slicer activity.

The mRNAs encoding the A and B-derived AGO4-like proteins were translated in *N. tabacum* BY-2 lysate (BYL) in the absence or presence of an exogenous, 24 nt siRNA targeting the mRNA of green fluorescent protein (GFP). Subsequently, a ^{32}P -labeled GFP mRNA fragment was added as an AGO4/RISC target and cleavage products analyzed by denaturing PAGE and autoradiography. As negative and positive controls, the reactions were performed the absence of additionally expressed (*in vitro* translated) AGO and with the mRNA encoding the *Arabidopsis thaliana* AGO4, respectively.

protein variants and, by adding a small interfering RNA (siRNA) to the translation reaction, the respective AGO4 variants were *in statu nascendi* loaded ('programmed') with this RNA. Since the AtAGO4 was known to associate preferentially with 24 nt long siRNAs containing a 5'-terminal adenosine nucleotide (Qi et al. 2006; Mi et al. 2008), we applied this type of siRNA. Most importantly, the guide strand of the chosen siRNA was complementary to the mRNA of the green fluorescent protein (GFP). Thus programmed, functional AGO4/RISC was accordingly expected to show an endonucleolytic activity on this RNA. In fact, when we added a ^{32}P -labeled GFP target RNA to *in vitro* BYL reactions, which contained the respective *in vitro* translated AGO4 variants, specific cleavage of this RNA was observed (Figure 32). Importantly, all reactions, irrespectively whether they used the two rye AGO4B-like

proteins or the AtAGO4, showed the same pattern of cleavage products, i.e., a larger 5' product, which was clearly visible and a 3' product (ca. 100 nt) that was less evidently to detect. Additional fragments with sizes of just above 100 nt were suspected to result from further processing of the 5' cleavage product. Specific cleavage products were not detected when the reactions were performed in the absence of the GFP-specific siRNA or when *AGO4* mRNA translation was omitted. Hence, we conclude that the AGO4B-like proteins, regardless of whether they were encoded by the A or B chromosomes of rye, are able to form active RISC. Thus, each protein shows a slicer activity that is comparable and homologous to the activity of the AtAGO4 containing RISC.

2.5 Discussion

2.5.1 B chromosomes of rye are transcriptionally active

The detection of active RNAPII in the proximity of B chromatin, the RNA-seq analysis based identification of B chromosome transcripts in different tissues, and the characterization of B-located genes undergoing pseudogenization are in accordance with previous data on the transcription of B-located coding and non-coding sequences (Carchilan et al. 2009; Banaei-Moghaddam et al. 2015; Banaei-Moghaddam et al. 2013).

With increasing numbers of B chromosomes, the amount of *ScKIF4A*, *ScSHOC1* and *ScAGO4B* transcripts encoded by As and Bs changed differently. *ScKIF4A* transcripts decreased with increasing numbers of Bs, with the exception that a significant increase was observed by presence of 2Bs. For *ScAGO4B*, already the presence of 1B highly increased the activity and continued to decrease till 4Bs in a zig-zag-like pattern. This pattern could reflect the already described odd-even effect for B chromosome containing organisms. Strong effects associated with odd numbers of Bs were already shown in different species (Jones and Rees 1982). In the case of *ScSHOC1*, the presence of Bs did not change the expression level significantly. A certain higher expression appeared in the presence of 2Bs, but the increase was less pronounced than found for the other two genes that were analysed.

In general, the quantitative analyses of the relative contribution of A- and B-originated transcripts showed that the amount of B-originated transcripts increased with increasing B chromosome number, while the amount of A-originated transcripts decreased. However, there were two exceptions: the B-derived *ScSHOC1* transcripts decreased in 4Bs after increasing from 1B to 3Bs and, in comparison to 0B, the total expression of *ScAGO4B* increased 6-fold in the presence of one deficient B. As 54% of transcripts are A-originated, this indirectly implies that there should also be an increase in the A-originated expression. Similarly, expression changes caused by aneuploidy have often genome-wide impacts, and the spectrum of expression changes is often complex (Birchler 2014). In maize, the compensation for the majority of genes on aneuploid chromosomes occurs at the RNA level (Guo et al. 1996). In plants, *de novo* formed genes show a high epigenetic variation among different individuals which is reflected in their expression patterns. It seems that newly formed genes are especially prone to epigenetic variation (Silveira et al. 2013). However, it is

not yet known whether this is also true for B-located coding sequences. Another possibility would be that the promoter regions of B-located sequences may have a higher affinity to transcription factors or RNAPII causing the suppression of A-located genes in competition for regulatory factors.

2.5.2 Rye B chromosomes undergo pseudogenization

Our comparison of A-located parental genes with their B-located counterparts showed that the mutation rate is different among the analyzed candidates. A high degree of polymorphisms may indicate the location of such genic fragments on Bs already at the onset of B chromosome evolution. Alternatively, according to the gene-balance hypothesis (Birchler et al. 2014), the activity of such genes may interfere with their A-counterparts. As a result, the rapid inactivation of the B genes after gene duplication and B chromosome insertion may have occurred. A subsequent integration of duplicated genes after proto-B formation might explain the presence of fragments with less polymorphisms.

Among the selected genes, the B-derived *ScKIF4A* gene shows the best evidence of pseudogenisation, as a premature stop codon was found for one B-encoded copy. However, the existence of functional active B-located *ScKIF4A* variants cannot be excluded as different B-located *ScKIF4A* variants were found. Besides being derived from ancestral founder A chromosomes, B-located genic sequences could also originate from hitchhiking of genomic fragments from As via transposable elements, as demonstrated for non-collinear *Triticeae* genes (Wicker et al. 2011). To address the exact mechanism underlying particular gene insertions, it will be necessary to analyze flanking regions of the respective B-located genic sequences.

Despite degeneration, a pseudogene can still be functional by regulating its parental gene (Pennisi 2012), for example, via encoded endo-siRNAs and thus, regulate the expression of their parental genes (Johnsson et al. 2014). Likely, as B-specific transcripts would be aberrant due to less selective pressure, they may serve as a substrate for RNA-directed RNA polymerases producing double strand RNAs (dsRNAs). These dsRNAs may then be processed to small regulatory RNAs. Alternatively, pseudogene transcripts may function as indirect post-transcriptional regulators by acting as miRNA 'sponges'. Due to high similarity between parental and pseudogene transcripts, both could compete for miRNA leading to the degradation of the parental gene transcripts (Muro et al. 2011). Further, it has been shown that

some pseudogene transcripts may be translated and then, produce short functional peptides or truncated proteins (Johnsson et al. 2014). Comparative profiling of small RNAs from individuals with and without Bs could address the question whether B-derived regulatory siRNA acting as regulators are indeed formed.

Could any duplicated gene be located on B chromosomes? Dosage sensitive genes are less likely part of an evolving B, as duplication of a B chromosome-donor fragment containing such genes could result in a detrimental phenotype. In contrast, dosage insensitive genes like structural genes having no regulatory roles for transcription or translation (Bellott et al. 2014) could be B-hosted, lost or undergo pseudogenization. Duplicated genes are often associated with detrimental effects and thus, may be removed by natural selection. As most of the mutations are degenerative, it is more likely that a duplicated gene undergoes inactivation rather than to acquire new functions. Nevertheless, there is evidence for the beneficial role of duplicated genes, especially under stress conditions (Tang and Amon 2013). Under certain circumstances the selective retention of duplicated genes may occur, i.e., when their redundancy protects corresponding parental genes from immediate detrimental mutations, or when over-dominance between their products exists. In the second case duplicated genes could convert to new genes by achieving beneficial mutations (Katju and Bergthorsson 2013). Thus, B-located duplicated genes may accelerate the evolution of Bs. The potential function of the here discovered active genes on rye Bs, the mechanism of its regulation, especially in response to the presence of a different number of Bs, remains to be answered.

In line with previous findings on the B-specific amplification of coding sequences in Lake Victoria cichlid fishes (Yoshida et al. 2011; Valente et al. 2014) and different canidae species (Becker et al. 2011; Graphodatsky et al. 2005; Trifonov et al. 2013) also the B-coding sequences of rye displayed an increase in copy number. In analogy to homogeneously stained regions and double minute chromosomes which exist in addition to the normal chromosome complement in vertebrates, and chromosome aberrations that are characterized by the amplification of sequences, we propose in agreement with (Makunin et al. 2014) that the mechanisms involved in the sequence amplification on Bs, may be common for these genomic elements.

The *in vitro* analysis of the A-and B-encoded ScAGO4B protein variants revealed that both operate a slicer activity, similar as that observed for *A. thaliana* AGO4. These

data demonstrated unambiguously the presence of a functional *ScAGO4B* gene on rye Bs and that these Bs carry both functional protein coding genes as well as pseudogene copies.

What may be the functional consequences of an additional AGO4 gene being expressed *via* the B chromosome in rye? In concert with Pol IVA and Pol IVB, the RNA-dependent RNA polymerases RDR2 and RDR5, the Dicer-like protein DCL3, and DNA methyl transferases, AGO4 is indicated to function in RNA-directed DNA methylation (RdDM), e. g., by controlling the maintenance of epigenetically silent states at repeated loci, transposons and heterochromatin (reviewed in (Zhang et al. 2015; Vaucheret 2008)). Transcripts of Pol IV are copied into double-stranded RNAs (dsRNAs) by RDR2, and these dsRNAs are then processed by DCL3 into 24-nt siRNAs, which are preferentially bound by AGO4. The AGO4-bound siRNAs then may guide the targeting of nascent scaffold transcripts from RNA polymerase V by sequence complementarity and recruit DNA methyltransferase activity to mediate *de novo* methylation (reviewed in (Zhang et al. 2015)). As its functional presence was found to be important in defense response of the plant cell during bacterial and viral infections, AGO4 was proposed to act also as a linker of the transcriptional and post-transcriptional silencing pathways (Agorio and Vera 2007; Hamera et al. 2012; Ye et al. 2009). Additional AGO4 pseudogenes on B chromosomes thus may be important to ensure the silencing of certain sequence elements such as transposons.

In short, this report suggests that B encoded genes may provide an additional level of gene control and complexity in combination with their related A-located genes. Hence, physiological effects, associated with the presence of Bs, may be explained by the activity of B-located (pseudo)genes.

2.6 Summary

B chromosomes (Bs) are supernumerary, dispensable parts of the nuclear genome, which appear in many different species of eukaryotes. So far, Bs were considered to be genetically inert elements without any functional genes. Detailed analysis of three key player genes from that set with chromatin related functions (*ScKIF4A*, *ScSHOC1* and *ScAGO4B*) were subjected to detailed experimental analyses. They showed high sequence homologies between the A- and B-located genes, but the copy-number of these genes was increased in the B's. The total transcriptional activity of *ScKIF4A*, *ScSHOC1* and *ScAGO4B* varied by the presence of different B numbers. Functionality of a B-encoded protein gene was demonstrated by an *in vitro* analysis of A- and B-encoded *ScAGO4B* proteins, which revealed a similar RNA-mediated slicer activity.

2.7 Outlook

1. Our RNA-seq analysis identified many B-encoded genes with different functions. Since we showed three genes showing a different degree of pseudogenization, an interesting question will be whether the pseudogenization process in terms of different classes of genes proceeds differently. A detailed examination of the pseudogenization process could be determined in different classes of genes.

2. We found that the copy numbers of genic sequences are increased on B chromosomes. It is unknown whether all genic sequences are amplified on B chromosomes and what the mechanism behind is. A detailed examination of candidate genes could be performed by FISH.

3. Since we confirmed the functional activity of the B-located ScAGO4B gene *in vitro*, further confirmation could be done *in vivo*. Like generating a specific antibody for B-derived ScAGO4B, mutating the A-derived ScAGO4B gene based on polymorphic sites (large deletion for example) by CRISPR-cas9 could be possible.

3. References

- Agorio, A., and Vera, P.** (2007). ARGONAUTE4 is required for resistance to *Pseudomonas syringae* in *Arabidopsis*. *The Plant Cell* **19**, 3778-3790.
- Albertson, D.G., and Thomson, J.N.** (1993). Segregation of holocentric chromosomes at meiosis in the nematode, *Caenorhabditis elegans*. *Chromosome Research* **1**, 15-26.
- Anderson, D.E., Losada, A., Erickson, H.P., and Hirano, T.** (2002). Condensin and cohesin display different arm conformations with characteristic hinge angles. *The Journal of Cell Biology* **156**, 419-424.
- Banaei-Moghaddam, A.M., Meier, K., Karimi-Ashtiyani, R., and Houben, A.** (2013). Formation and expression of pseudogenes on the B chromosome of rye. *The Plant Cell* **25**, 2536-2544.
- Banaei-Moghaddam, A.M., Martis, M.M., Macas, J., Gundlach, H., Himmelbach, A., Altschmied, L., Mayer, K.F., and Houben, A.** (2015). Genes on B chromosomes: Old questions revisited with new tools. *Biochimica et Biophysica Acta (BBA)-Gene Regulatory Mechanisms* **1849**, 64-70.
- Becker, S.E., Thomas, R., Trifonov, V.A., Wayne, R.K., Graphodatsky, A.S., and Breen, M.** (2011). Anchoring the dog to its relatives reveals new evolutionary breakpoints across 11 species of the Canidae and provides new clues for the role of B chromosomes. *Chromosome Research* **19**, 685-708.
- Bellott, D.W., Hughes, J.F., Skaletsky, H., Brown, L.G., Pyntikova, T., Cho, T.J., Koutseva, N., Zaghlul, S., Graves, T., Rock, S., Kremitzki, C., Fulton, R.S., Dugan, S., Ding, Y., Morton, D., Khan, Z., Lewis, L., Buhay, C., Wang, Q.Y., Watt, J., Holder, M., Lee, S., Nazareth, L., Rozen, S., Muzny, D.M., Warren, W.C., Gibbs, R.A., Wilson, R.K., and Page, D.C.** (2014). Mammalian Y chromosomes retain widely expressed dosage-sensitive regulators. *Nature* **508**, 494-499.
- Bhatt, A. M., Lister, C., Page, T., Fransz, P., Findlay, K., Jones, G. H., ... and Dean, C.** (1999). The DIF1 gene of *Arabidopsis* is required for meiotic chromosome segregation and belongs to the REC8/RAD21 cohesin gene family. *The Plant Journal* **19**, 463-472.
- Birchler, J.A.** (2014). Facts and artifacts in studies of gene expression in aneuploids and sex chromosomes. *Chromosoma* **123**, 459-469.
- Birkenbihl, R.P., and Subramani, S.** (1995). The rad21 gene product of *Schizosaccharomyces pombe* is a nuclear, cell cycle-regulated phosphoprotein. *Journal of Biological Chemistry* **270**, 7703-7711.
- Blower, M.D., Sullivan, B.A., and Karpen, G.H.** (2002). Conserved organization of centromeric chromatin in flies and humans. *Developmental Cell* **2**, 319-330.

- Bougourd, S.M., and Jones, R.N.** (1997). B chromosomes: a physiological enigma. *The New Phytologist* **137**, 43-54.
- Cabral, G., Marques, A., Schubert, V., Pedrosa-Harand, A., and Schlögelhofer, P.** (2014). Chiasmatic and achiasmatic inverted meiosis of plants with holocentric chromosomes. *Nature Communications* **5**, 5070.
- Cai, X., Dong, F., Edelman, R.E., and Makaroff, C.** (2003). The *Arabidopsis* SYN1 cohesin protein is required for sister chromatid arm cohesion and homologous chromosome pairing. *Journal of Cell Science* **116**, 2999-3007.
- Calvente, A., and Barbero, J.L.** (2012). Cohesins and Cohesin-Regulators in Meiosis. INTECH Open Access Publisher.
- Carbonell, A., and Carrington, J.C.** (2015). Antiviral roles of plant ARGONAUTES. *Current Opinion in Plant Biology* **27**, 111-117.
- Carchilan, M., Kumke, K., Mikolajewski, S., and Houben, A.** (2009). Rye B chromosomes are weakly transcribed and might alter the transcriptional activity of A chromosome sequences. *Chromosoma* **118**, 607-616.
- Carlson, W.** (2009). The B chromosome of maize. In *Handbook of Maize* J.L. Bennetzen and S. Hake, eds (New York: Springer), pp.459-480.
- Chua, P.R., and Roeder, G.S.** (1998). Zip2, a meiosis-specific protein required for the initiation of chromosome synapsis. *Cell* **93**, 349-359.
- Coleman, J.J., Rounsley, S.D., Rodriguez-Carres, M., Kuo, A., Wasmann, C.C., Grimwood, J., Schmutz, J., Taga, M., White, G.J., Zhou, S., Schwartz, D.C., Freitag, M., Ma, L.J., Danchin, E.G., Henrissat, B., Coutinho, P.M., Nelson, D.R., Straney, D., Napoli, C.A., Barker, B.M., Gribskov, M., Rep, M., Kroken, S., Molnar, I., Rensing, C., Kennell, J.C., Zamora, J., Farman, M.L., Selker, E.U., Salamov, A., Shapiro, H., Pangilinan, J., Lindquist, E., Lamers, C., Grigoriev, I.V., Geiser, D.M., Covert, S.F., Temporini, E., and Vanetten, H.D.** (2009). The genome of *Nectria haematococca*: contribution of supernumerary chromosomes to gene expansion. *PLoS Genet* **5**, e1000618.
- da Costa-Nunes, J. A., Bhatt, A. M., O'Shea, S., West, C. E., Bray, C. M., Grossniklaus, U., & Dickinson, H. G.** (2006). Characterization of the three *Arabidopsis thaliana* RAD21 cohesins reveals differential responses to ionizing radiation. *Journal of Experimental Botany* **57**, 971-983.
- de Carvalho, C.E., Zaaier, S., Smolikov, S., Gu, Y., Schumacher, J.M., and Colaiácovo, M.P.** (2008). LAB-1 antagonizes the Aurora B kinase in *C. elegans*. *Genes & Development* **22**, 2869-2885.
- Dernburg, A.F.** (2001). Here, there, and everywhere kinetochore function on holocentric chromosomes. *The Journal of Cell Biology* **153**, F33-F38.

- Donald, T.M., Houben, A., Leach, C.R., and Timmis, J.N.** (1997). Ribosomal RNA genes specific to the B chromosomes in *Brachycome dichromosomatica* are not transcribed in leaf tissue. *Genome* **40**, 674-681.
- Dong, F., Cai, X., and Makaroff, C.** (2001). Cloning and characterization of two *Arabidopsis* genes that belong to the RAD21/REC8 family of chromosome cohesin proteins. *Gene* **271**, 99-108.
- Francki, M.G.** (2001). Identification of *Bilby*, a diverged centromeric Ty1-*copia* retrotransposon family from cereal rye (*Secale cereale* L.). *Genome* **44**, 266-274.
- Gerhard, D. S., Wagner, L., Feingold, E. A., Shenmen, C. M., Grouse, L. H., Schuler, G., ... and Guyer, M.** (2004). The status, quality, and expansion of the NIH full-length cDNA project. *Genome Research* **14**, 2121-2127.
- Goldstein, P.** (1987). Multiple synaptonemal complexes (polycomplexes): origin, structure and function. *Cell Biology International Reports* **11**, 759-796.
- Golubovskaya, I.N., Hamant, O., Timofejeva, L., Wang, C.J.R., Braun, D., Meeley, R., and Cande, W.Z.** (2006). Alleles of *afd1* dissect REC8 functions during meiotic prophase I. *Journal of Cell Science* **119**, 3306-3315.
- Golubovskaya, I.N., Wang, C.J.R., and Timofejeva, L., and Cande, W.Z.** (2011). Maize meiotic mutants with improper or non-homologous synapsis due to problems in pairing or synaptonemal complex formation. *Journal of Experimental Botany*, erq292.
- Gong, C., Li, T., Li, Q., Yan, L., and Wang, T.** (2011). Rice OsRAD21-2 is expressed in actively dividing tissues and its ectopic expression in yeast results in aberrant cell division and growth. *J Integr Plant Biol* **53**, 14-24.
- Graphodatsky, A.S., Kukekova, A.V., Yudkin, D.V., Trifonov, V.A., Vorobieva, N.V., Beklemisheva, V.R., Perelman, P.L., Graphodatskaya, D.A., Trut, L.N., and Yang, F.** (2005). The proto-oncogene C-KIT maps to canid B-chromosomes. *Chromosome Research* **13**, 113-122.
- Green, D.M.** (1990). Muller's Ratchet and the evolution of supernumerary chromosomes. *Genome* **33**, 818-824.
- Green, D.M., Zeyl, C.W., and Sharbel, T.F.** (1993). The evolution of hypervariable sex and supernumerary (B) chromosomes in the relict New Zealand frog, *Leiopelma hochstetteri*. *Journal of Evolutionary Biology* **6**, 417-441.
- Guo, M., Davis, D., and Birchler, J.A.** (1996). Dosage effects on gene expression in a maize ploidy series. *Genetics* **142**, 1349-1355.
- Haering, C.H., and Nasmyth, K.** (2003). Building and breaking bridges between sister chromatids. *BioEssays* **25**, 1178-1191.
- Hakansson, A.** (1958). Holocentric chromosomes in *Eleocharis*. *Hereditas* **44**, 531-540.

- Hamera, S., Song, X., Su, L., Chen, X., and Fang, R.** (2012). Cucumber mosaic virus suppressor 2b binds to AGO4-related small RNAs and impairs AGO4 activities. *The Plant Journal* **69**, 104-115.
- Hartsuiker, E., Vaessen, E., Carr, A., and Kohli, J.** (2001). Fission yeast Rad50 stimulates sister chromatid recombination and links cohesion with repair. *The EMBO Journal* **20**, 6660-6671.
- Heckmann, S., Schroeder-Reiter, E., Kumke, K., Ma, L., Nagaki, K., Murata, M., Wanner, G., and Houben, A.** (2011). Holocentric chromosomes of *Luzula elegans* are characterized by a longitudinal centromere groove, chromosome bending, and a terminal nucleolus organizer region. *Cytogenet Genome Res* **134**, 220-228.
- Heckmann, S., Jankowska, M., Schubert, V., Kumke, K., Ma, W., and Houben, A.** (2014a). Alternative meiotic chromatid segregation in the holocentric plant *Luzula elegans*. *Nature Communications* **5**, 4979.
- Heckmann, S., Schubert, V., and Houben, A.** (2014b). Holocentric plant meiosis: first sisters, then homologues. *Cell Cycle* **13**, 3623-3624.
- Henderson, K.A., and Keeney, S.** (2005). Synaptonemal complex formation: where does it start? *BioEssays* **27**, 995-998.
- Henikoff, S., and Dalal, Y.** (2005). Centromeric chromatin: what makes it unique? *Current Opinion in Genetics & Development* **15**, 177-184.
- Hewitt, G.M.** (1974). The integration of supernumerary chromosomes into the Orthopteran genome. In: *Cold Spring Harbor symposia on quantitative biology*. Cold Spring Harbor Laboratory Press, pp 183-194.
- Herran, Y., Gutierrez-Caballero, C., Sanchez-Martin, M., Hernandez, T., Viera, A., Barbero, J.L., Alava, E., Rooij, D.G., Suja, J.A., Liano, E., and Pendas, A.M.** (2011). The cohesin subunit RAD21L functions in meiotic synapsis and exhibits sexual dimorphism in fertility. *The EMBO Journal* **30**, 3091-3105.
- Houben, A., Schroeder-Reiter, E., Nagaki, K., Nasuda, S., Wanner, G., Murata, M., and Endo, T.R.** (2007). CENH3 interacts with the centromeric retrotransposon cereba and GC-rich satellites and locates to centromeric substructures in barley. *Chromosoma* **116**, 275-283.
- Iki, T., Yoshikawa, M., Nishikiori, M., Jaudal, M.C., Matsumoto-Yokoyama, E., Mitsuhashi, I., Meshi, T., and Ishikawa, M.** (2010). *In vitro* assembly of plant RNA-induced silencing complexes facilitated by molecular chaperone HSP90. *Molecular Cell* **39**, 282-291.
- Ishiguro, K., Kim, J., Fujiyama-Nakamura, S., Kato, S., and Watanabe, Y.** (2011). A new meiosis-specific cohesin complex implicated in the cohesin code for homologous pairing. *EMBO Reports* **12**, 267-275.

- Ishii, T., Sunamura, N., Matsumoto, A., Eltayeb, A. E., and Tsujimoto, H. (2015).** Preferential recruitment of the maternal centromere-specific histone H3 (CENH3) in oat (*Avena sativa* L.)× pearl millet (*Pennisetum glaucum* L.) hybrid embryos. *Chromosome Research* **23**, 709-718.
- Irvine, D.V., Zaratiegui, M., Tolia, N.H., Goto, D.B., Chitwood, D.H., Vaughn, M.W., Joshua-Tor, L., and Martienssen, R.A. (2006).** Argonaute slicing is required for heterochromatic silencing and spreading. *Science* **313**, 1134-1137.
- Jiang, L., Xiam M., Strittmatter, L.I., and Makaroff, C.A. (2007).** The *Arabidopsis* cohesin protein SYN3 localizes to the nucleolus and is essential for gametogenesis. *The Plant Journal* **50**, 1020-1034.
- Jimenez, M., Romera, E., Puertas, M., and Jones, R. (1994).** B-chromosomes in inbred lines of rye (*Secale cereale* L.). *Genetica* **92**, 149-154.
- Johnsson, P., Morris, K.V., and Grander, D. (2014).** Pseudogenes: a novel source of trans-acting antisense RNAs. *Methods Mol Biol* **1167**, 213-226.
- Jones, N., and Houben, A. (2003).** B chromosomes in plants: escapees from the A chromosome genome? *Trends Plant Sci* **8**, 417-423.
- Jones, R.N. (1995).** Tansley review no 85. B chromosomes in plants. *The New Phytologist* **131**, 411-434.
- Jones, R.N., and Rees, H. (1982).** B chromosomes, 1 st ed. (London, New York: Academic Press).
- Kaitna, S., Pasierbek, P., Jantsch, M., Loidl, J., and Glotzer, M. (2002).** The aurora B kinase AIR-2 regulates kinetochores during mitosis and is required for separation of homologous chromosomes during meiosis. *Current Biology* **12**, 798-812.
- Kalitsis, P., and Choo, K.A. (2012).** The evolutionary life cycle of the resilient centromere. *Chromosoma* **121**, 327-340.
- Katju, V., and Bergthorsson, U. (2013).** Copy-number changes in evolution: rates, fitness effects and adaptive significance. *Frontiers in Genetics* **4**, 273.
- Kitajima, T.S., Kawashima, S.A., and Watanabe, Y. (2004).** The conserved kinetochore protein shugoshin protects centromeric cohesion during meiosis. *Nature* **427**, 510-517.
- Klein, F., Mahr, P., Galova, M., Buonomo, S.B., Michaelis, C., Nairz, K., and Nasmyth, K. (1999).** A central role for cohesins in sister chromatid cohesion, formation of axial elements, and recombination during yeast meiosis. *Cell* **98**, 91-103.
- Klemme, S., Banaei-Moghaddam, A.M., Macas, J., Wicker, T., Novak, P., and Houben, A. (2013).** High-copy sequences reveal distinct evolution of the rye B chromosome. *The New Phytologist* **199**, 550-558.

- Komarnitsky, P., Cho, E.J., and Buratowski, S.** (2000). Different phosphorylated forms of RNA polymerase II and associated mRNA processing factors during transcription. *Genes & Development* **14**, 2452-2460.
- Kudo, N.R., Wassmann, K., Anger, M., Schuh, M., Wirth, K.G., Xu, H., Helmhart, W., Kudo, H., Mckay, M., and Maro, B.** (2006). Resolution of chiasmata in oocytes requires separase-mediated proteolysis. *Cell* **126**, 135-146.
- Kudo, N.R., Anger, M., Peters, A.H., Stemmann, O., Theussl, H.C., Helmhart, W., Kudo, H., Heyting, C., and Nasmyth, K.** (2009). Role of cleavage by separase of the Rec8 kleisin subunit of cohesin during mammalian meiosis I. *Journal of Cell Science* **122**, 2686-2698.
- Leach, C.R., Houben, A., Field, B., Pistrick, K., Demidov, D., and Timmis, J.N.** (2005). Molecular evidence for transcription of genes on a B chromosome in *Crepis capillaris*. *Genetics* **171**, 269-278.
- Lee, J., and Hirano, T.** (2011). RAD21L, a novel cohesin subunit implicated in linking homologous chromosomes in mammalian meiosis. *The Journal of Cell Biology* **192**, 263-276.
- Lee, J.Y., and Orr-Weaver, T.L.** (2001). The molecular basis of sister-chromatid cohesion. *Annual Review of Cell and Developmental Biology* **17**, 753-777.
- Lermontova, I., Schubert, V., Fuchs, J., Klätte, S., Macas, J., and Schubert, I.** (2006). Loading of *Arabidopsis* centromeric histone CENH3 occurs mainly during G2 and requires the presence of the histone fold domain. *The Plant Cell* **18**, 2443-2451.
- Lermontova, I., Koroleva, O., Rutten, T., Fuchs, J., Schubert, V., Moraes, I., Koszegi, D., and Schubert, I.** (2011). Knockdown of CENH3 in *Arabidopsis* reduces mitotic divisions and causes sterility by disturbed meiotic chromosome segregation. *The Plant Journal* **68**, 40-50.
- Lindström, J.** (1965). Transfer to wheat of accessory chromosomes from rye. *Hereditas* **54**, 149-155.
- Llano, E., Gómez, R., Gutiérrez-Caballero, C., Herrán, Y., Sánchez-Martín, M., Vázquez-Quiñones, L., Hernández, T., de Álava, E., Cuadrado, A., and Barbero, J.L.** (2008). Shugoshin-2 is essential for the completion of meiosis but not for mitotic cell division in mice. *Genes & Development* **22**, 2400-2413.
- López-León, M., Neves, N., Schwarzacher, T., Heslop-Harrison, J.P., Hewitt, G., and Camacho, J.** (1994). Possible origin of a B chromosome deduced from its DNA composition using double FISH technique. *Chromosome Research* **2**, 87-92.
- Losada, A., Hirano, M., and Hirano, T.** (2002). Cohesin release is required for sister chromatid resolution, but not for condensin-mediated compaction, at the onset of mitosis. *Genes & Development* **16**, 3004-3016.

- Ma, L., Vu, G.T., Schubert, V., Watanabe, K., Stein, N., Houben, A., and Schubert, I.** (2010). Synteny between *Brachypodium distachyon* and *Hordeum vulgare* as revealed by FISH. *Chromosome Research* **18**, 841-850.
- Macaisne, N., Novatchkova, M., Peirera, L., Vezon, D., Jolivet, S., Froger, N., Chelysheva, L., Grelon, M., and Mercier, R.** (2008). SHOC1, an XPF endonuclease-related protein, is essential for the formation of class I meiotic crossovers. *Current Biology* **18**, 1432-1437.
- Makunin, A.I., Dementyeva, P.V., Graphodatsky, A.S., Volobouev, V.T., Kukekova, A.V., Malheiros, N., and de Castro, D.** (2014). Genes on B chromosomes of vertebrates. *Molecular Cytogenetics* **7**, 99.
- Malheiros, N., and de Castro, D.** (1947). Chromosome number and behaviour in *Luzula purpurea* Link. *Nature* **160**, 156.
- Marques, A., Ribeiro, T., Neumann, P., Macas, J., Novák, P., Schubert, V., and Brandt, R.** (2015). Holocentromeres in *Rhynchospora* are associated with genome-wide centromere-specific repeat arrays interspersed among euchromatin. *Proceedings of the National Academy of Sciences* **112**, 13633-13638.
- Martis, M.M., Klemme, S., Banaei-Moghaddam, A.M., Blattner, F.R., Macas, J., Schmutzer, T., Scholz, U., Gundlach, H., Wicker, T., Simkova, H., Novak, P., Neumann, P., Kubalaková, M., Bauer, E., Haseneyer, G., Fuchs, J., Dolezel, J., Stein, N., Mayer, K.F., and Houben, A.** (2012). Selfish supernumerary chromosome reveals its origin as a mosaic of host genome and organellar sequences. *Proceedings of the National Academy of Sciences of the United States of America* **109**, 13343-13346.
- Mi, S., Cai, T., Hu, Y., Chen, Y., Hodges, E., Ni, F., Wu, L., Li, S., Zhou, H., and Long, C.** (2008). Sorting of small RNAs into *Arabidopsis* argonaute complexes is directed by the 5' terminal nucleotide. *Cell* **133**, 116-127.
- Michaelis, C., Ciosk, R., and Nasmyth, K.** (1997). Cohesins: chromosomal proteins that prevent premature separation of sister chromatids. *Cell* **91**, 35-45.
- Mito, Y., Sugimoto, A., and Yamamoto, M.** (2003). Distinct developmental function of two *Caenorhabditis elegans* homologs of the cohesin subunit Scc1/Rad21. *Molecular Biology of the Cell* **14**, 2399-2409.
- Moraes, I.C., Lermontova, I., and Schubert, I.** (2011). Recognition of *A. thaliana* centromeres by heterologous CENH3 requires high similarity to the endogenous protein. *Plant Molecular Biology* **75**, 253-261.
- Muro, E.M., Mah, N., and Andrade-Navarro, M.A.** (2011). Functional evidence of post-transcriptional regulation by pseudogenes. *Biochimie* **93**, 1916-1921.

- Nabeshima, K., Villeneuve, A.M., and Colaiácovo, M.P.** (2005). Crossing over is coupled to late meiotic prophase bivalent differentiation through asymmetric disassembly of the SC. *The Journal of Cell Biology* **168**, 683-689.
- Nagaki, K., Kashihara, K., and Murata, M.** (2005). Visualization of diffuse centromeres with centromere-specific histone H3 in the holocentric plant *Luzula nivea*. *Plant Cell* **17**, 1886-1893.
- Nasmyth, K.** (2011). Cohesin: a catenase with separate entry and exit gates? *Nature Cell Biology* **13**, 1170-1177.
- Page, S.L., and Hawley, R.S.** (2003). Chromosome choreography: the meiotic ballet. *Science* **301**, 785-789.
- Palmer, D.K., O'Day, K., Wener, M.H., Andrews, B.S., and Margolis, R.L.** (1987). A 17-kD centromere protein (CENP-A) copurifies with nucleosome core particles and with histones. *The Journal of Cell Biology* **104**, 805-815.
- Pasierbek, P., Jantsch, M., Melcher, M., Schleiffer, A., Schweizer, D., and Loidl, J.** (2001). A *Caenorhabditis elegans* cohesion protein with functions in meiotic chromosome pairing and disjunction. *Genes & Development* **15**, 1349-1360.
- Pazy, B., and Plitmann, U.** (1995). Chromosome divergence in the genus *Cuscuta* and its systematic implications. *Caryologia* **48**, 173-180.
- Pennisi, E.** (2012). ENCODE project writes eulogy for junk DNA. *Science* **337**, 1159-1161.
- Poletto, A.B., Ferreira, I.A., and Martins, C.** (2010). The B chromosomes of the African cichlid fish *Haplochromis obliquidens* harbour 18S rRNA gene copies. *BMC Genetics* **11**, 1.
- Qi, Y., He, X., Wang, X.J., Kohany, O., Jurka, J., and Hannon, G.J.** (2006). Distinct catalytic and non-catalytic roles of ARGONAUTE4 in RNA-directed DNA methylation. *Nature* **443**, 1008-1012.
- Qiao, H., Lohmiller, L.D., and Anderson, L.K.** (2011). Cohesin proteins load sequentially during prophase I in tomato primary microsporocytes. *Chromosome Research* **19**, 193-207.
- Ribeiro, T., Pires, B., Delgado, M., Viegas, W., Jones, N., and Morais-Cecílio, L.** (2004). Evidence for 'cross-talk' between A and B chromosomes of rye. *Proceedings of the Royal Society of London B: Biological Sciences* **271**, S482-S484.
- Ruiz-Estévez, M., Lopez-Leon, M.D., Cabrero, J., and Camacho, J.P.M.** (2012). B-chromosome ribosomal DNA is functional in the grasshopper *Eyrepocnemis plorans*. *PLoS ONE* **7**, e36600.
- Ruiz-Estevez, M., Badisco, L., Broeck, J.V., Perfectti, F., Lopez-Leon, M.D., Cabrero, J., and Camacho, J.P.** (2014). B chromosomes showing active ribosomal RNA genes

- contribute insignificant amounts of rRNA in the grasshopper *Eyprepocnemis plorans*. *Molecular Genetics and Genomics* **289**, 1209-1216.
- Sandery, M.J., Forster, J.W., Blunden, R., and Jones, R.N.** (1990). Identification of a family of repeated sequences on the rye B-chromosome. *Genome* **33**, 908-913.
- Sanei, M., Pickering, R., Kumke, K., Nasuda, S., and Houben, A.** (2011). Loss of centromeric histone H3 (CENH3) from centromeres precedes uniparental chromosome elimination in interspecific barley hybrids. *Proceedings of the National Academy of Sciences* **108**, E498-E505.
- Sakuno, T., Tada, K., and Watanabe, Y.** (2009). Kinetochore geometry defined by cohesion within the centromere. *Nature* **458**, 852-851
- Schägger, H., and Von, Jagow G.** (1987). Tricine-sodium dodecyl sulfate-polyacrylamide gel electrophoresis for the separation of proteins in the range from 1 to 100 kDa. *Analytical Biochemistry* **166**, 368-379.
- Schubert, I., Dolezel, J., Houben, A., Scherthan, H., and Wanner, G.** (1993). Refined examination of plant metaphase chromosome structure at different levels made feasible by new isolation methods. *Chromosoma* **102**, 96-101.
- Schubert, V.** (2009). SMC proteins and their multiple functions in higher plants. *Cytogenet Genome Res* **124**, 202-214.
- Schubert, V., Weissleder, A., Ali, H., Fuchs, J., Lermontova, I., Meister, A., and Schubert, I.** (2009). Cohesin gene defects may impair sister chromatid alignment and genome stability in *Arabidopsis thaliana*. *Chromosoma* **118**, 591-605.
- Schuck, J., Gursinsky, T., Pantaleo, V., Burgyán, J., and Behrens, S.E.** (2013) AGO/RISC-mediated antiviral RNA silencing in a plant *in vitro* system. *Nucleic Acids Research* **41**, 5090-5103.
- Sekine, Y., Okada, Y., Noda, Y., Kondo, S., Aizawa, H., Takemura, R., and Hirokawa, N.** (1994). A novel microtubule-based motor protein (KIF4) for organelle transports, whose expression is regulated developmentally. *The Journal of Cell Biology* **127**, 187-201.
- Sharbel, T.F., Green, D.M., and Houben, A.** (1998). B-chromosome origin in the endemic New Zealand frog *Leiopelma hochstetteri* through sex chromosome devolution. *Genome* **41**, 14-22.
- Sheikh, S.A., Kondo, K., and Hoshi, Y.** (1995). Study on diffused centromeric nature of *Drosera* chromosomes. *Cytologia* **60**, 43-47.
- Shirasu, K., Schulman, A.H., Lahaye, T., and Schulze-Lefert, P.** (2000). A contiguous 66-kb barley DNA sequence provides evidence for reversible genome expansion. *Genome Research* **10**, 908-915.

- Siegel, J.J., and Amon, A.** (2012). New insights into the troubles of aneuploidy. *Annual Review of Cell and Developmental Biology* **28**, 189-214.
- Silva, D.M., Pansonato-Alves, J.C., Utsunomia, R., Araya-Jaime, C., Ruiz-Ruano, F.J., Daniel, S.N., Hashimoto, D.T., Oliveira, C., Camacho, J.P., Porto-Foresti, F., and Foresti, F.** (2014). Delimiting the origin of a B chromosome by FISH mapping, chromosome painting and DNA sequence analysis in *Astyanax paranae* (Teleostei, Characiformes). *PLoS One* **9**, e94896.
- Silveira, A.B., Trontin, C., Cortijo, S., Barau, J., Del-Bem, L.E.V., Loudet, O., Colot, V., and Vincentz, M.** (2013). Extensive natural epigenetic variation at a de novo originated gene. *PLoS Genetics* **9**, e1003437.
- Sims, R.J., Mandal, S.S., and Reinberg, D.** (2004). Recent highlights of RNA-polymerase-II-mediated transcription. *Current Opinion in Cell Biology* **16**, 263-271.
- Smolikov, S., Schild-Prufert, K., and Colaiácovo, M.P.** (2008). CRA-1 uncovers a double-strand break-dependent pathway promoting the assembly of central region proteins on chromosome axes during *C. elegans* meiosis. *PLoS Genet* **4**, e1000088
- Spurr, A.R.** (1969). A low-viscosity epoxy resin embedding medium for electron microscopy. *Journal of Ultrastructure Research* **26**, 31-43.
- Sumara, I., Vorlaufer, E., Stukenberg, P.T., Kelm, O., Redemann, N., Nigg, E.A., and Peters, J.M.** (2002). The dissociation of cohesin from chromosomes in prophase is regulated by Polo-like kinase. *Molecular Cell* **9**, 515-525.
- Suzuki, G., Nishiuchi, C., Tsuru, A., Kako, E., Li, J., Yamamoto, M., and Mukai, Y.** (2013). Cellular localization of mitotic RAD21 with repetitive amino acid motifs in *Allium cepa*. *Gene* **514**, 75-81.
- Sym, M., Engebrecht, J., and Roeder, G.S.** (1993). ZIP1 is a synaptonemal complex protein required for meiotic chromosome synapsis. *Cell* **72**, 365-378.
- Szczerbal, I., and Switonski, M.** (2003). B chromosomes of the Chinese raccoon dog (*Nyctereutes procyonoides procyonoides* Gray) contain inactive NOR-like sequences. *Caryologia* **56**, 213-216.
- Tanaka, N., and Tanaka, N.** (1977). Chromosome studies in *Chionographis* (Liliaceae). *Cytologia* **42**, 753-763.
- Tang, Y.C., and Amon, A.** (2013). Gene copy-number alterations: a cost-benefit analysis. *Cell* **152**, 394-405.
- Tao, J., Zhang, L., Chong, K., and Wang, T.** (2007). OsRAD21-3, an orthologue of yeast RAD21, is required for pollen development in *Oryza sativa*. *The Plant Journal* **51**, 919-930.
- Tomita, M., Shinohara, K., and Morimoto, M.** (2008). *Revolver* is a new class of transposon-like gene composing the Triticeae genome. *DNA Research* **15**, 49-62.

- Trifonov, V.A., Demytyeva, P.V., Larkin, D.M., O'Brien, P.C.M., Perelman, P.L., Yang, F., Ferguson-Smith, M.A., and Graphodatsky, A.S.** (2013). Transcription of a protein-coding gene on B chromosomes of the Siberian roe deer (*Capreolus pygargus*). *BMC Biology* **11**, 90.
- Vale, R.D.** (2003). The molecular motor toolbox for intracellular transport. *Cell* **112**, 467-480.
- Valente, G.T., Conte, M.A., Fantinatti, B.E., Cabral-de-Mello, D.C., Carvalho, R.F., Vicari, M.R., Kocher, T.D., and Martins, C.** (2014). Origin and evolution of B chromosomes in the cichlid fish *Astatotilapia latifasciata* based on integrated genomic analyses. *Molecular Biology and Evolution*, msu148.
- Vaucheret, H.** (2008). Plant argonautes. *Trends in Plant Science* **13**, 350-358.
- Waizenegger, I. C., Hauf, S., Meinke, A., & Peters, J. M.** (2000). Two distinct pathways remove mammalian cohesin from chromosome arms in prophase and from centromeres in anaphase. *Cell* **103**, 399-410.
- Wang, M., Tang, D., Wang, K., Shen, Y., Qin, B., Miao, C., Li, M., and Cheng, Z.** (2011). OsSGO1 maintains synaptonemal complex stabilization in addition to protecting centromeric cohesion during rice meiosis. *The Plant Journal* **67**, 583-594.
- Weisshart, K., Fuchs, J. and Schubert, V.** (2016). Structured illumination microscopy (SIM) and photoactivated localization microscopy (PALM) to analyze the abundance and distribution of RNA polymerase II molecules on flow-sorted *Arabidopsis* nuclei. *Bio-protocol* **6**, e1725.
- Westergaard, M., and D, von. Wettstein.** (1972). The synaptonemal complex. *Annual Review of Genetics* **60**, 533-554.
- Wicker, T., Mayer, K.F., Gundlach, H., Martis, M., Steuernagel, B., Scholz, U., Simkova, H., Kubalaková, M., Choulet, F., Taudien, S., Platzer, M., Feuillet, C., Fahima, T., Budak, H., Dolezel, J., Keller, B., and Stein, N.** (2011). Frequent gene movement and pseudogene evolution is common to the large and complex genomes of wheat, barley, and their relatives. *The Plant Cell* **23**, 1706-1718.
- Ye, J., Qu, J., Zhang, J.F., Geng, Y.F., and Fang, R.X.** (2009). A critical domain of the cucumber mosaic virus 2b protein for RNA silencing suppressor activity. *FEBS Letters* **583**, 101-106.
- Yoshida, K., Terai, Y., Mizoiri, S., Aibara, M., Nishihara, H., Watanabe, M., Kuroiwa, A., Hirai, H., Hirai, Y., Matsuda, Y., and Okada, N.** (2011). B chromosomes have a functional effect on female sex determination in lake victoria cichlid fishes. *PLoS Genetics* **7**, e1002203.
- Zhang, L.R., Tao, J.Y., and Wang, T.** (2004). Molecular characterization of OsRAD21-1, a rice homologue of yeast RAD21 essential for mitotic chromosome cohesion. *Journal of Experimental Botany* **55**, 1149-1152.

- Zhang, L., Tao, J., Wang, S., Chong, K., and Wang, T.** (2006). The rice OsRad21-4, an orthologue of yeast Rec8 protein, is required for efficient meiosis. *Plant Molecular Biology* **60**, 533-554.
- Zhang, H., Xia, R., Meyers, B.C., and Walbot, V.** (2015). Evolution, functions, and mysteries of plant ARGONAUTE proteins. *Current Opinion in Plant Biology* **27**, 84-90.
- Zetka, M.C., Kawasaki, I., Strome, S., and Müller, F.** (1999). Synapsis and chiasma formation in *Caenorhabditis elegans* require HIM-3, a meiotic chromosome core component that functions in chromosome segregation. *Genes & Development* **13**, 2258-2270.
- Zhou, Q., Zhu, H.M., Huang, Q.F., Zhao, L., Zhang, G.J., Roy, S.W., Vicoso, B., Xuan, Z.L., Ruan, J., and Zhang, Y.** (2012). Deciphering neo-sex and B chromosome evolution by the draft genome of *Drosophila albomicans*. *BMC Genomics* **13**, 109.
- Zhu, C., and Jiang, W.** (2005). Cell cycle-dependent translocation of PRC1 on the spindle by Kif4 is essential for midzone formation and cytokinesis. *Proceedings of the National Academy of Sciences of the United States of America* **102**, 343-348.
- Ziegler, C., Lamatsch, D., Steinlein, C., Engel, W., Scharl, M., and Schmid, M.** (2003). The giant B chromosome of the cyprinid fish *Alburnus alburnus* harbours a retrotransposon-derived repetitive DNA sequence. *Chromosome Research* **11**, 23-35.
- Zilberman, D., Cao, X., and Jacobsen, S.E.** (2003). ARGONAUTE4 control of locus-specific siRNA accumulation and DNA and histone methylation. *Science* **299**, 716-719.

List of publications related to this thesis

Wei Ma, Tobias Sebastian Gabriel, Mihaela Maria Martis, *et al.* Rye B chromosomes encode a functional Argonaute-like protein with *in vitro* slicer activities similar to its A chromosome paralog (Submitted).

Wei Ma, Veit Schubert, Mihaela Maria Martis, *et al.* The distribution of α -kleisin during meiosis in holocentromeric plant *Luzula elegans*. Chromosome Research (Accepted).

Heckmann S, Jankowska M, Schubert V, Kumke K, **Ma W**, Houben A. Alternative meiotic chromatid segregation in the holocentric plant *Luzula elegans*. Nature Communication. 5 (2014) 4979.

Wanner G, Schroeder-Reiter E, **Ma W**, Houben A, Schubert V. The ultrastructure of mono- and holocentric plant centromeres: an immunological investigation by structured illumination microscopy and scanning electron microscopy. Chromosoma 124 (2015) 503-517.

Curriculum Vitae

Person details

Name Wei Ma
Sex Male
Nationality Chinese
Present address Hans-Stubbe Straße 3, 06466, Gatersleben, Germany
Date of birth Pingluo, Ningxia province, China

Contact information

Phone +49(0)394825477(office)/+49(0)1703066381(mobile)
E-Mail ma@ipk-gatersleben.de

Education

Since October 2012 PhD student at the **Leibniz Institute of Plant Genetics and Crop Plant Research (IPK)**, Gatersleben, Germany. Department of Breeding Research, group of Chromosome Structure and Function (Dr. habil. Andreas Houben)

September 2009-July 2012 Msc at the **Norwest Agriculture and Forestry University (NWFU)**, Yangling, Shaanxi province, China. College of Animal Science and Technology, majoring Genetics (Prof. Dr. Hong Chen). Title of the thesis: Molecular cloning, SNP detection of bovine *TMEM18* gene and their associations with growth traits.

27.05.2016, Gatersleben

Wei Ma

Stays in another research center

March 2015 (2 weeks) **Institute of Genetics and Developmental Biology, Chinese Academy of Sciences (CAS)**, Beijing, China. research group of Prof. Dr. Zhukuan Cheng.

Oral presentations (only talks presented by Wei Ma)

Wei Ma. Title: Role of Rad21 during inverted meiosis in holocentric species *L. elegans* (18.03.2015). In the group of Prof. Dr. Zhukuan Cheng. Institute of Genetics and Developmental Biology, Chinese Academy of Sciences (CAS), Beijing, China.

Wei Ma. Title: Role of Rad21 during inverted meiosis in holocentric species *L. elegans* (03.06.2015). Plant Science student Conference, Martin Luther University Halle-Wittenberg, Halle, Germany.

Poster presentations

Ma W., Houben, A. Characterization of Syn1- and Shugoshin of the holocentric species *Luzula elegans*(28.05-31.05.2013), Plant science student conference, Halle, Germany.

Ma W., Banaei-Moghaddam A M., Houben, A. Title: Characterization of rye A and B chromosome-located genes (07.04-09.04.2014) 3rd B-chromosome conference, Gatersleben, Germany.

Ma W., Jankowska, M., Shubert, V., Scholz, U., Conrad U., Houben, A. Unraveling an alternative meiosis (17.05.2014) IPK institute day, Gatersleben, Germany.

Ma W., Banaei-Moghaddam A M., Houben, A. Title: Characterization of rye A and B chromosome-located genes (02.06-05.06.2014) Plant science student conference, Gatersleben, Germany.

Ma W., Banaei-Moghaddam A M., Houben, A. Title: Characterization of rye A and B chromosome-located genes (23.09-24.09.2014). Symposium Plant molecular cytogenetics in genomic and postgenomic era, Katowice, Poland.

Jankowska, M., **Ma W.**, Heckmann, S., Houben, A. Title: *Luzula elegans* - a holocentric species with an inverted sequence of meiotic events (14.11-19.11.2013) EMBO conference series-MEIOSIS, Dresden, Germany.

Jankowska, M., **Ma W.**, Heckmann, S., Houben, A. Title: Inverted meiosis in the holocentric plant *Luzula elegans* (02.04-03.04.2014) SPP1384 Meiosis meeting, Heidelberg, Germany.

Jankowska, M., **Ma W.**, Heckmann, S., Kumke, K., Shubert, V., Houben, A. Title: Alternative meiotic chromatid segregation in the holocentric plant *Luzula elegans* (23.09-24.09.2014) Symposium Plant molecular cytogenetics in genomic and postgenomic era, Katowice, Poland.

Jankowska, M., **Ma W.**, Houben, A. Title: Inverted meiosis in the holocentric plant *Luzula elegans* (12.10-13.10.2015) SPP1384 Meiosis meeting, Dresden, Germany.

Attended Conferences

28.05-31.05.2013 Plant science student conference, Halle, Germany.

14.11-19.11.2013 EMBO conference series-MEIOSIS, Dresden, Germany.

02.04-03.04.2014 DFG Priority Programme SPP1384 – Mechanisms of Genome Haploidization - Annual Meeting, Heidelberg, Germany.

07.04-09.04.2014 3rd B-chromosome conference, Gatersleben, Germany.

02.06-05.06.2014 Plant science student conference, Gatersleben, Germany.

23.09-24.09.2014 Symposium Plant molecular cytogenetics in genomic and postgenomic era, Katowice, Poland.

12.10-13.10.2015 DFG Priority Programme SPP1384 – Mechanisms of Genome Haploidization - Annual Meeting, Dresden, Germany.

02.06-05.06.2015 Plant Science student Conference, Martin Luther University Halle-Wittenberg, Halle, Germany.

Eidesstattliche Erklärung / Declaration under Oath

Hiermit erkläre ich, Wei Ma, an Eides statt, dass ich die Arbeit selbstständig und ohne fremde Hilfe verfasst, keine anderen als die von mir angegebenen Quellen und Hilfsmittel benutzt und die den benutzten Werken wörtlich oder inhaltlich entnommenen Stellen als solche kenntlich gemacht habe.

I declare under penalty of perjury that this thesis is my own work entirely and has been written without any help from other people. I used only the sources mentioned and included all the citations correctly both in word or content.

Gatersleben, 27.05.2016

Wei Ma

Erklärung über bestehende Vorstrafen und anhängige Ermittlungsverfahren / Declaration concerning Criminal Record and Pending Investigations

Hiermit erkläre ich, Wei Ma, dass ich weder vorbestraft bin noch dass gegen mich Ermittlungsverfahren anhängig sind.

I hereby declare that I have no criminal record and that no preliminary investigations are pending against me.

Gatersleben, 27.05.2016

Wei Ma